UNIVERSITY OF VERONA

DEPARTMENT OF BIOTECHNOLOGY

GRADUATE SCHOOL OF NATURAL SCIENCES AND ENGINEERING

DOCTORAL PROGRAM IN BIOTECHNOLOGY

CYCLE: *XXXIV*

TITLE OF THE DOCTORAL THESIS

Targeting macrophages with Astaxanthin-loaded microparticles: a strategy to attenuate radiation-induced fibrosis

S.S.D. (Disciplinary Sector) ING-IND/34

Coordinator: Prof. Matteo Ballottari

Tutor: Prof. Gianni Zoccatelli

Co-tutor: Prof. Roberto Chignola

Doctoral Student: Eleonora Binatti

Targeting macrophages with Astaxanthin-loaded microparticles: a strategy to attenuate radiation-induced fibrosis

Eleonora Binatti
PhD thesis
Verona, 6 December 2021
ISBN 12324-5678-910

University of Verona Research Office – National and International PhD programmes ph: 045.802.8608 – fax 045.802.8411 – Via Giardino Giusti 2 – 37129 Verona

Sommario del progetto di ricerca

La fibrosi indotta da radiazioni (RIF) è uno degli effetti avversi più comuni della radioterapia (incidenza complessiva tra il 10-20%) e provoca una moltitudine di sintomi che possono avere un impatto significativo sulla qualità della vita dei pazienti oncologici. È un complesso processo multifattoriale che causa un accumulo eccessivo di collagene e di altri componenti della matrice extracellulare in molti organi, tra cui polmoni, pelle, intestino tenue, seno, fegato e reni, compromettendone le loro funzioni.

La RIF è innescata dal danno cellulare indotto dalla radiazione diretta e da meccanismi indiretti che, a loro volta, comportano la generazione di specie reattive dell'ossigeno e dell'azoto (ROS e RNS, rispettivamente) attraverso la radiolisi dell'acqua e l'attivazione dell'ossido nitrico sintasi. Centrale per l'insorgenza della patologia è il ruolo dei leucociti residenti nei tessuti, come i macrofagi che, in risposta all'accumulo di ROS e al danno tissutale, attivano l'espressione di citochine pro-infiammatorie, come il fattore di crescita trasformante beta (TGF-β). Il TGF-β può, a sua volta, aumentare la produzione di ROS attraverso la soppressione degli enzimi antiossidanti, portando così a un feedback positivo che sostiene lo stress ossidativo, l'infiammazione e il danno tissutale. Il TGF-β, infine, favorisce il reclutamento dei fibroblasti e la deposizione locale dei componenti della matrice extracellulare. Nonostante diversi progressi siano stati fatti per comprendere al meglio questa patologia, ad oggi non sono disponibili approcci terapeutici di successo in ambito clinico.
È importante sottolineare che la terapia antiossidante post-radiazione ha dimostrato di ridurre significativamente la RIF nei modelli animali. Ciò suggerisce che è effettivamente possibile arrestare il feedback positivo tra accumulo di ROS e infiammazione alla base della malattia.

L'astaxantina (3,3′-diidrossi-β-β′-carotene-4,4′-dione; ASX) è un chetocarotenoide della xantofilla presente in diversi organismi marini e d'acqua dolce, inclusi microrganismi, crostacei e pesci. L'ASX è un potente antiossidante, 10 volte più potente di altri carotenoidi, come la luteina e il β-carotene, e fino a 100 volte più dell'α-tocoferolo. L'ASX potrebbe, quindi, essere utilizzata per ridurre o prevenire la fibrosi indotta da radioterapia. L'ASX, tuttavia, non è solubile nei fluidi biologici a base acquosa ed è sensibile alla temperatura, alla luce e all'ossigeno, tutti fattori che ne limitano la stabilità e la biodisponibilità e che possono essere controllati mediante incapsulamento dell'ASX in opportune matrici chimiche. L'incapsulamento di ASX in particelle di dimensioni micrometriche potrebbe

anche rappresentare un'eccellente strategia per fornire ASX specificamente ai macrofagi e ad altre cellule immunitarie innate che sono caratterizzate dalla loro capacità unica di inghiottire, assorbire e degradare particelle di queste dimensioni attraverso la fagocitosi. Questa capacità non è condivisa dalle cellule tumorali e quindi in linea di principio le cellule tumorali non dovrebbero beneficiare di questo trattamento antiossidante.

Il progetto ha lo scopo di dimostrare la fattibilità di questo approccio terapeutico contro la RIF, anche se in un ambiente cellulare *in vitro*. I risultati indicano chiaramente che le microparticelle di ASX interferiscono con il feedback positivo tra ROS e TGF-β nelle cellule fagocitiche e che la pentossifillina, un farmaco attualmente utilizzato per il trattamento del dolore muscolare derivante da malattie delle arterie periferiche, amplifica gli effetti delle microparticelle dell'astaxantina sui macrofagi. Le strategie di trattamento che coinvolgono le microparticelle di ASX, eventualmente in combinazione con altri farmaci come la pentossifillina, dovrebbero essere ulteriormente studiate per esaminare il loro potenziale per ridurre l'infiammazione e inibire la fibrosi indotta dalle radiazioni.

Summary of the research project

Radiation-induced fibrosis (RIF) is one of the common adverse effects of radiotherapy (overall incidence between 10-20%) and it results in a multitude of symptoms that can significantly impact the quality of life of cancer patients. RIF is a complex multi-factorial process that ultimately results in an excess accumulation of collagen and other extracellular matrix components in many organs, especially in the lung, skin, small bowel, breast, liver, and kidney, that in turn impairs their own functions.

RIF is initiated by direct radiation-induced cell damage and by indirect mechanisms which, in turn, involve the generation of reactive oxygen and nitrogen species (ROS and RNS, respectively) through water radiolysis and activation of nitric oxide synthase. Central to RIF is the role of tissue-resident leukocytes, such as macrophages, which, in response to ROS accumulation and tissue damage, activate the expression of pro-inflammatory cytokines, such as transforming growth factor beta (TGF-β). TGF-β may, in turn, increase ROS production through suppression of antioxidant enzymes, thus leading to a positive feedback that sustains oxidative stress, inflammation and tissue damage. f-β, finally, promotes fibroblasts recruitment and local deposition of extracellular matrix components. Our understanding of the processes involved in the pathology of RIF have improved. However, to date no successful therapeutic approaches are available in the clinical setting. Importantly, it has been reported that post-radiation antioxidant therapy significantly reduces RIF in animal models. This shows that it is indeed possible to halt the positive feedback between ROS accumulation and inflammation at the basis of the disease.

Astaxanthin (3,3′-dihydroxy-*β*-*β*′-carotene-4,4′-dione; ASX) is a xantophyll ketocarotenoid present in several marine and freshwater organisms, including microorganisms, crustaceans and fishes. ASX is a potent antioxidant, with rate constants for radical scavenging approximately 10 times higher than other carotenoids, such as lutein and *β*-carotene, and 100 times more than that of *α*-tocopherol. ASX might, therefore, be used to reduce or prevent RIF. ASX, however, is not soluble in water-based biological fluids and is sensitive to temperature, light and oxygen, all factors that limit its stability and bioavailability and that can be controlled by ASX encapsulation into appropriate chemical matrices. Encapsulation of ASX into micrometer-sized particles might also represent an excellent strategy to deliver ASX specifically to macrophages and other innate immune cells that are characterized by their unique ability to engulf,

uptake and degrade particles of this size through phagocytosis. In contrast, tumor cells do not phagocytose and hence will not be provided direct protection against antioxidants conferred by ASX.

This project aims at demonstrating the feasibility of this possible therapeutic approach against RIF, albeit in a cell-based *in vitro* setting. The results clearly indicate that ASX microparticles interfere with the positive feedback between ROS and TGF-β in phagocytic cells, and that pentoxifylline, a drug currently investigated for its ability to reduce RIF, amplifies the effects of astaxanthin microparticles on macrophages. Treatment strategies involving ASX microparticles, eventually in combination with other drugs such as pentoxifylline, should be further studied to examine their potential to reduce inflammation and inhibit radiation-induced fibrosis.

INTRODUCTION

1. FIBROTIC DISEASES: A GENERAL OVERVIEW

Fibrosis is a common sequela of most chronic inflammatory pathologies and consists of excessive tissue scarring that can affect several organs. Fibrotic disease is a leading cause of morbidity and mortality, and imposes a major socio-economic burden on modern societies. In the United States, 45% of death can be attributed to this condition. Its worldwide incidence and the associated health-care burden are increasing and today fibrosis is one of major healthcare challenges facing modern medicine [1].

It is based on the dysregulated wound healing process after persistent inflammatory tissue injuries induced by different stimuli, including infections, autoimmune reactions, allergic responses, radiation, exposure to toxins, chemical mechanical insults and temperature extremes. Inflammatory reactions may persist for several weeks, months; the inflammation is often coincident with cell loss, and tissue remodeling [2]. Fibrosis leads to the replacement of normal tissue with connective tissue due to an excessive deposition of extracellular matrix components (ECM), including proteins (such as collagens and elastin), glycoproteins and proteoglycans (such as fibronectin, laminin and tenascin), glycosaminoglycans (such as heparin and chondroitin sulphates). When there is an imbalance between ECM synthesis and degradation, the formation of a permanent fibrotic scar can result. Fibrotic scars are a sign of late normal tissue injury and often impair normal organ function.

Most of the fibrotic diseases are characterized by a persistent inflammatory stimulus and a sustained production of growth factors, proteolytic enzymes and fibrogenic cytokines that collectively lead to remodeling and eventual impairment of normal tissues. Fibrotic changes occurs in various vascular diseases, such as cardiac disease, cerebral disease and peripheral vascular disease, as well as in virtually all of the main tissues and organ systems, including skin, lung, liver, bowel and kidney [3], resulting in individual organ manifestations or in systemic disorders. In *Table 1* [1], [4] the most consequential fibrotic disorders affecting human beings are listed.

Table 1. Common fibroproliferative diseases in humans

Major-organ fibrosis

- *Heart and vascular disease:* following a heart attack, scar tissue can impair the ability of heart to pump the blood.
- *Lung disease:* interstitial lung disease (ILD) includes different disorders with common manifestations, as pulmonary inflammation and fibrosis. Idiopathic lung fibrosis is the most common type of ILD.
- *Liver cirrhosis*: cirrhosis is the end-stage consequence of fibrosis and it is often irreversible and results in liver failure, or development of hepatocellular carcinoma and death. The major causes of cirrhosis are chronic hepatitis B and C infections, autoimmune and biliary diseases, alcoholic steatohepatitis and nonalcoholic steatohepatitis.
- *Kidney disease*: diabetes can cause damage and scarring of kidneys with eventual loss of function.
- *Disease of the eye:* an impaired vision can be caused by macular degeneration, diabetic retinopathy and proliferative vitreoretinopathy.
- *Pancreas disease:* it can be caused by autoimmune and hereditary pathologies; the etiology remains poorly understood.
- Bowel disease: Crohn's disease. The major cause are autoimmune disorders and pathogenic organisms.
- Brain: Alzheimer's disease and neurological complications due to AIDS are the contributing factors.
- Bone marrow: cancer and aging are the contributing causes.

Fibroproliferative disorders

- *Systemic and local scleroderma.*
- *Keloids and hypertrophic scars.*
- *Atherosclerosis and restenosis.*

Multi-organ scarring associated with trauma

- *Surgical complications:* the scarring process can cause pain, contracture and occasionally infertility.
- *Chemotherapy-induced fibrosis in cancer patients.*
- *Radiotherapy-induced fibrosis in cancer patients.*
- *Physical injury by blunt trauma.*
- *Burns.*

2. MECHANISMS OF WOUND HEALING AND FIBROSIS

Fibrosis scarring is characterized by pathological wound healing in which connective tissue replaces normal parenchymal tissue in an unregulated process that leads to tissue remodeling and the formation of a persistent scar. Under normal conditions, wound healing response is characterized by three distinct phases: injury, inflammation, and repair for a successful response. Under fibrotic conditions, wound healing response becomes pathogenic, unbalanced, and dysregulated; a persistent insult persists impairing normal tissue functions and ultimately leading to organ failure and, under extreme circumstances, death.

Fibrotic tissues and organs share the same macroscopic and microscopic features that characterize the pathogenesis of fibrosis. Specifically, macroscopically fibrotic organs usually display an uneven surface, are not elastic, but become hard, and pale [5] due to the accumulation of ECM components, contracted fibroblasts and reduced vasculature. Microscopically, features include lack of capillaries, infiltration of mononuclear cells, excessive presence of fibroblasts and ECM.

The pathophysiology of fibrosis has mostly been studied in the context of a specific organ or tissue damaged. Recent research into the underlying molecular mechanisms suggest that the loss of metabolic homeostasis and chronic low-grade inflammation appear to play a role in the pathogenesis of fibrosis. Moreover, recent evidences have indicated that the oxidative stress appears to link metabolic homeostasis and inflammation [5].

As reported in [6], at least five responses to injury-induced functional or physical disruption of epithelial cells can provoke tissue fibrosis. One is cell death, which can occur as a consequence of injury through either apoptosis or necrosis [6]. A second common response to damage is the dysregulation of metabolic pathways that lead to cell stress and activation. In chronic diseases, cellular stress is persistent and therefore such stressed cells are sources of pro-inflammatory cytokines, chemokines, growth factors that can promote fibroblasts activation and proliferation. A third injury-triggered epithelial alteration is the epithelial-to-mesenchymal transition (EMT) resulting in the decrease of the epithelial surface markers, e.g., E-cadherin, and an increase in mesenchymal markers, e.g., vimentin, N-cadherin, fibronectin, apha-smooth muscle actin (α-SMA). A fourth common response involves the interaction between integrins and TGF-β, a profibrotic cytokine, resulting in TGF-β activation. Finally, injured epithelial cells initiate both innate and adaptive immune responses with the involvement and

recruitment of immune cells, such as neutrophils, macrophages, and lymphocytes into the injured organs to drive tissue fibrosis [6].

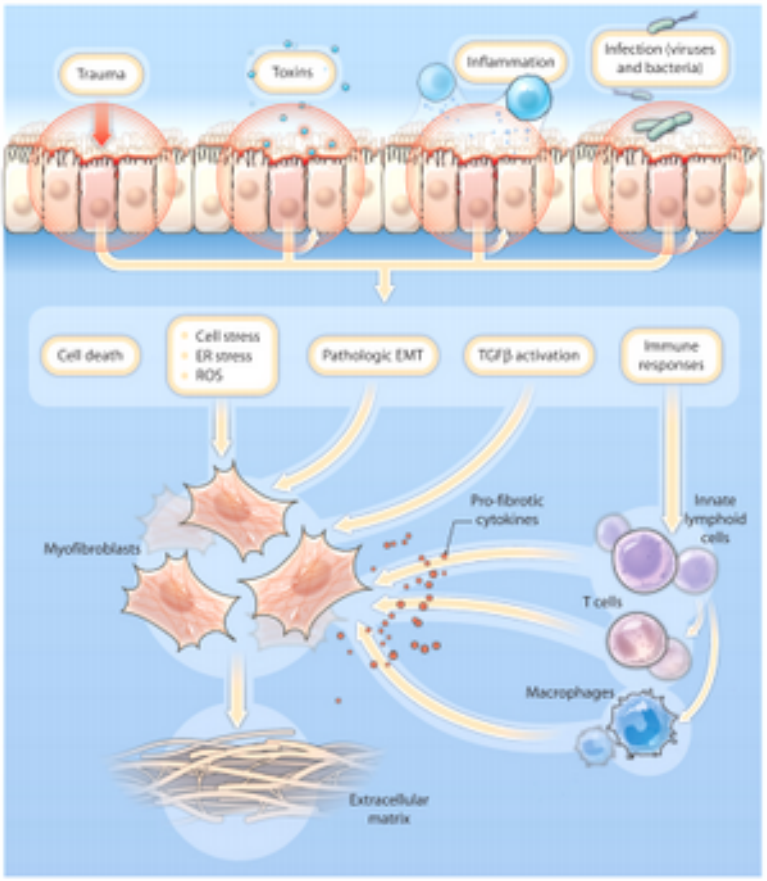

Figure 1. Mechanisms by which epithelial injury can lead to fibrosis [6]

Phase I: injury

The wound healing response is initiated by injuries to endothelial and epithelial cells, resulting in the disruption of normal tissue architecture. Damages to these cells result in cell stress and activation which lead to the release of inflammatory mediators that initiate the anti-fibrinolytic coagulation cascade. The anti-fibrinolytic cascade triggers blood-clot formation and formation of a provisional extracellular matrix.

Platelet recruitment, their degranulation and the clot formation increase vasodilatation and blood vessel permeability.
In addition epithelial and/or endothelial cells produce matrix metalloproteinases (MMPs) that cleave one or more ECM constituents and disrupt the basement membrane, allowing the inflammatory cells to be easily recruited to the site of injury.

Phase II: inflammation

In the injury phase epithelial and endothelial cells secrete growth factors, cytokines and chemokines that induce the recruitment and the proliferation of leukocytes, such as neutrophils, macrophages, eosinophils and lymphocytes across the provisional ECM.
Neutrophils are the most numerous inflammatory cells at the early stage of healing; after their degranulation and death, macrophages are called up. Activated macrophages and neutrophils eliminate dead cells, tissue debris and any invading organisms, and amplify the inflammation through the release of cytokines and chemokines. Stimulated by these factors, endothelial cells begin to surround the injured site and form new blood vessels as they migrate towards the center of the wound.
In the last stage of the inflammatory process, the inflamed micro-environment induces lymphocytes T to release pro-fibrotic cytokines and growth factors, in particular, TGF-β, IL-13 that in turn activate macrophages and fibroblasts. Specifically, fibroblasts are activated into α-SMA-expressing myofibroblasts and migrate to the lesion.

Phase III: fibroplasia

Myofibrobasts can originate from different cellular pools: 1) resident fibroblasts upon TGF-β activation; 2) bone marrow cells; 3) epithelial cells that undergo the mesenchymal transition. After activation, myofibroblasts promote the wound contraction, a process characterized by the migration of the edges of the wound to the center [2].
In a normal healing process, at the end, the collagen fibers become more organized, blood vessels are restored to their normal structure and epithelial and

endothelial cells divide and migrate over the basal layers to restore the injured tissue to its normal appearance (repair process).
However, in the case of chronic inflammatory damages, the normal healing process is disrupted, as myofibroblasts are continuously activated and persistently generate ECM components. In fibrosis, the synthesis of ECM components, in particular collagen, exceeds the rate at which they are degraded. This leads to the formation of a permanent scar (fibrosis).

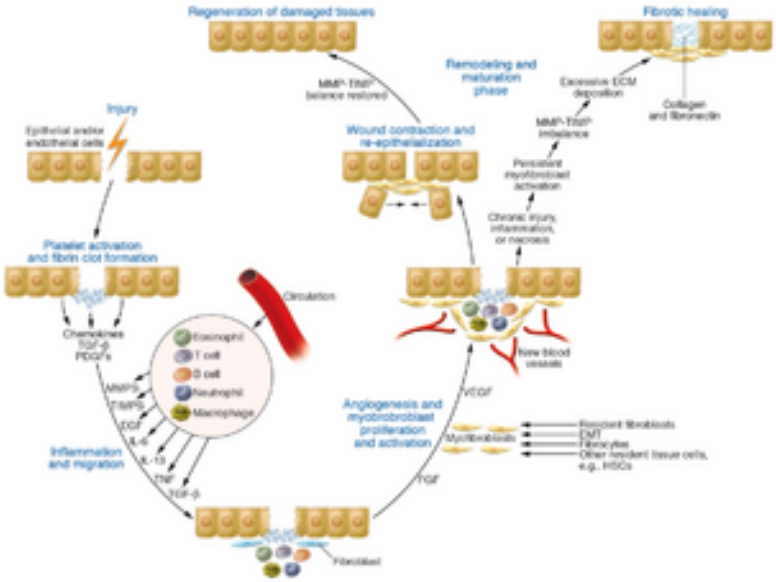

Figure 2. Outcomes of wound healing: tissue regeneration or fibrosis [2]

2.1 Immune response and development of fibrosis

Chronic inflammation is characterized by considerable infiltration of mononuclear cells, including macrophages, lymphocytes, eosinophils and plasma cells. Specifically lymphocytes move to the injured area and, following contact with various antigens, become activated and in turn produce lymphokines that switch on macrophages and other local inflammatory cells. Thus, activation of adaptive immune system is fundamental and crucial in many chronic inflammatory pathologies, as reported in many experimental models of fibrosis, $CD4^+$ T cells, also called T helper cells, play a prominent role in the progression of the disease [4]. Th1 cells stimulate a cellular immune response, participate in the inhibition of

macrophage activation and stimulate B cells to produce immunoglobulins (IgM, IgG1) that bind to particular antigens eliciting an immune response. Th2 stimulates the humoral response, promotes B cell proliferation and induces antibody production (e.g., IL-4). Studies conducted with multiple cytokine-deficient mice have demonstrated that liver fibrosis is strongly linked with the development of a $CD4^+$ Th2 cell response, involving IL-4, IL-5, IL-13, IL-21 [4]. Among the factors leading to fibrosis, Th2 cytokines were firstly recognized to show strong pro-fibrotic properties. Conversely, anti-fibrotic activity has been reported for Th-1 associated cytokines (e.g., IFN-γ, IL-12).

3. ROLE OF MACROPHAGES IN FIBROSIS

Cells of the monocyte/macrophage lineage are central actors of the immune response following tissue injuries, and macrophages orchestrate all stages of tissue damage, repair and fibrosis. Consequently, it is important to fully understand the mechanisms that contribute to the development of fibrosis disease, and to deeply analyze these cells and their function in both physiological and pathological conditions.

3.1 Macrophages: origin, phagocytosis, and polarization

Macrophages are white blood cells situated in all tissues whose main functions are phagocytosis of pathogens, cellular debris, dead cells, tumor cells and activation of lymphocytes and other immune cells. Thus, macrophage cells play a central role in the immune system.

Macrophages were first discovered in the late 19th century by Ilya Metchnikoff (1845-1916), honored as the "father of innate immunity" for the discovery of the phagocytosis process and the phagocytic cells, and in particular macrophage cells, responsible of it.

Macrophages are evolutionarily conserved phagocytes that evolved more than 500 million years ago. In the 1960s, van Furth proposed that macrophages mainly originated from circulating adult blood monocytes that differentiate from their precursor in the bone marrow. This has been the prevailing view for the following 40 years [7]. However, in the last few years, researchers have found that many tissue resident macrophages have an embryonic origin and persist into adulthood as resident and self-maintaining populations.

In the early stage of the embryonic process, macrophages are first detected in the extraembryonic yolk sac ("primitive hematopoiesis"). During this stage, macrophages are the only white blood cells produced. Then, definitive hematopoietic stem cells (HSCs) come up from the aorta-gonad-mesonephros and originate all immune lineages. HSCs migrate to the fetal liver which serves as the major hematopoietic organ during the remainder of embryonic development. Only in the perinatal period do traditional bone marrow HSCs become the primary site of hematopoiesis [7].

Yolk-sac-derived macrophages and definitive-HSC-derived macrophages differ in their transcription factor usage and in their expression of surface markers.
After birth, macrophages persist into the adulthood as resident and self-maintaining populations and monocytes derived from bone marrow can replenish tissue resident macrophages following injuries, infections, inflammations [8].

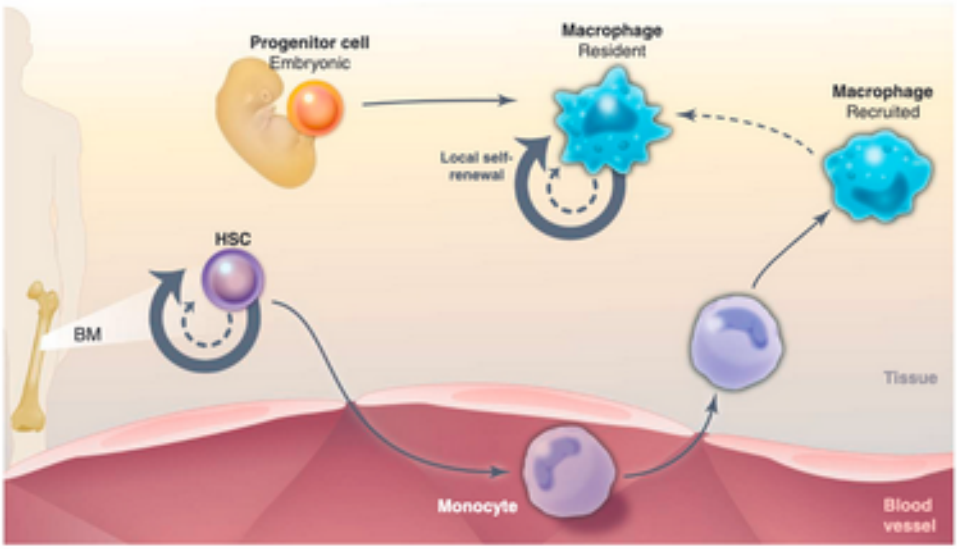

Figure 3. Origin of macrophages [9]

Macrophages are widely distributed, either as resident cells or monocyte-derived cells that infiltrate into tissues [7], in virtually all tissues and organs of adult mammals, where they can represent up to 10-15% of the total cell number in quiescent conditions [10], performing specialized functions. Macrophages take different names depending on their localization, for example alveolar macrophages in the lungs, Kupffer cells in the liver, osteoclasts in the bone marrow, microglia in the nervous system, Langerhans cells in the skin, peritoneal macrophages in the intestine and histiocytes in the connective tissue, as shown in *Figure 4*.

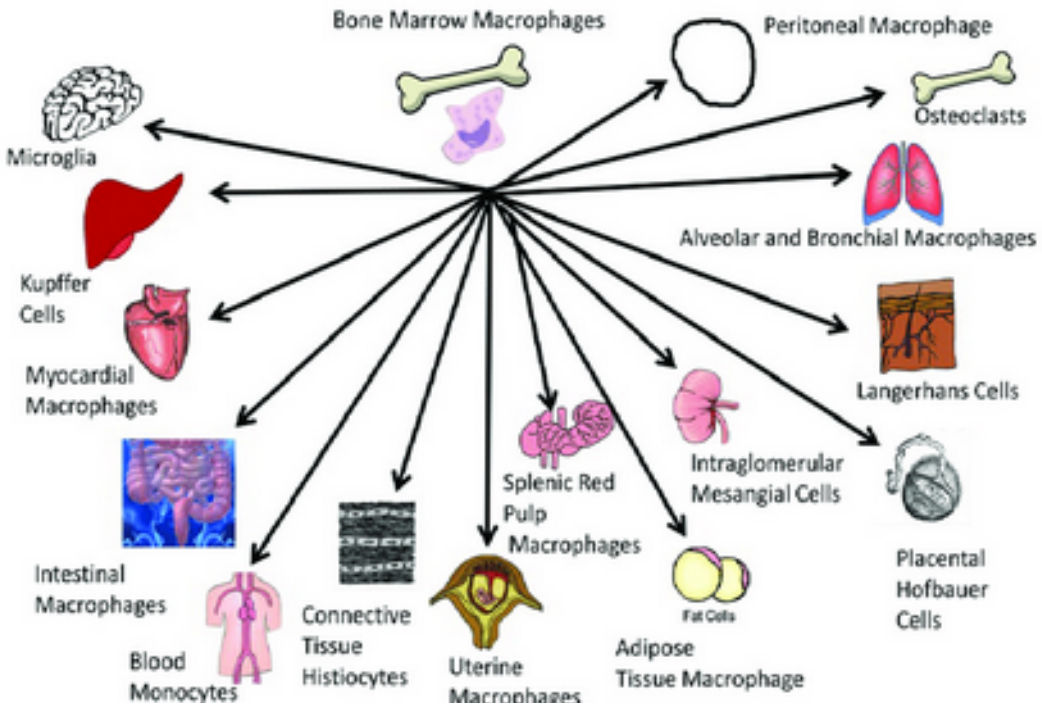

Figure 4. Example of different macrophage populations associated with different tissues are illustrated [11]

These populations of macrophages possess distinctive transcriptional profiles that allow them to be considered as many different and unique classes of macrophages. However, the functions of macrophages are basically the same in all tissues: they are central players in tissue development, in immune surveillance, they fight against and eliminate pathogens and they contribute to the maintenance of tissue homeostasis.

Table 2 summarizes the functions of resident macrophages in the human body. Different macrophages functionalities and activities, needed to keep homeostasis, reflect the differences in their origin, distribution and changes in tissue micro-environments. The maintenance of homeostasis can be perturbed by chronic insults which cause an anomalous amplification of macrophages activities and consequently leads to a causal association between macrophages and diseases.

Table 2. Macrophages functions and the pathological consequence of their anomalous activation in the main tissues [10]

Macrophages (MΦ)	*Tissue*	*Functions*	*Pathologies*
Microglia	Brain	Brain development, immune surveillance, synaptic remodeling	Neurodegeneration
Osteoclasts	Bone	Bone modeling and remodeling, bone resorption, support to hematopoiesis	Osteoporosis, osteopetrosis, arthritis
Heart MΦ	Heart and vasculature	Surveillance	Atherosclerosis
Kupffer cells	Liver	Toxin removal, lipid metabolism, iron recycling, erythrocyte clearance, clearance of microbes and cell debris from blood	Fibrosis, impaired erythrocyte clearance
Alveolar MΦ	Lung	Surfactant clearance, surveillance for inhaled pathogens	Alveolar proteinosis
Adipose tissue-associated MΦ	Adipose tissue	Metabolism, adipogenesis, adaptive thermogenesis	Obesity, diabetes, insulin resistance, loss of adaptive thermogenesis
Bone marrow MΦ	Bone marrow	Reservoir of monocytes, waste disposal	Disruption of hematopoiesis
Intestinal MΦ	Gut	Tolerance to microbiota, defense against pathogens, intestinal homeostasis	Inflammatory bowel disease
Langerhans cells	Skin	Immune surveillance	Insufficient healing, fibrosis
Marginal zone MΦ, red pulp MΦ	Spleen	Erythrocyte clearance, iron processing, capture of microbes from blood	Impaired iron recycling anerythrocyte clearance

Inflammatory MΦ	All tissues	Defense against pathogens, protection against dangerous stimuli	Chronic inflammation, tissue damage, autoimmunity
Healing MΦ	All tissues	Branched morphology, angiogenesis	Cancer, fibrosis, epithelial hyperplasia

3.2 Heterogeneity and polarization of macrophages

Macrophage cells display a huge heterogeneity and flexibility in their biological activities that depend on the differences in their origins, distribution and changes in the microenvironment. Indeed, macrophages possess a considerable plasticity that allow them to efficiently respond to environmental signals and change their phenotype. Early signals are typically generated by innate immune cells and can exert effects on the physiology of macrophages. Depending on their physiology resulting from their varied activations, macrophages are categorized in phenotypically distinct subpopulations.

A dichotomy has been proposed for macrophages activation: classic *vs* alternative, also M1 and M2, respectively [12].

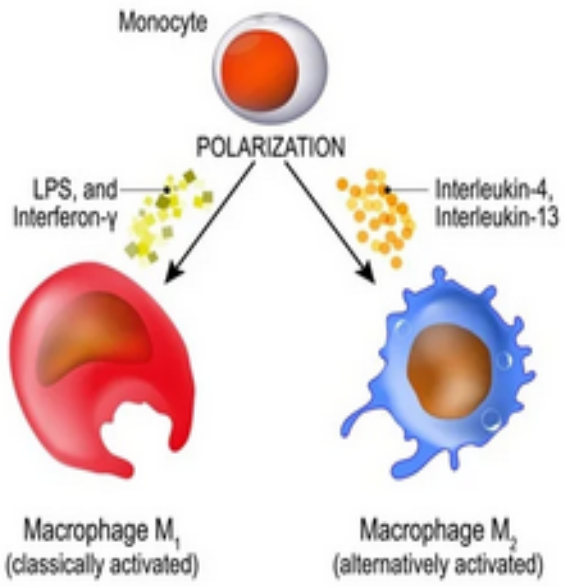

Figure 5. Macrophage activation (https://www.azolifesciences.com/article/What-is-Inflammatory-Macrophage-Polarisation.aspx).

3.2.1 Classically activated macrophages (M1)

In the 1960s, George B. Mackaness introduced the term “macrophages activation” to describe the microbicidal activity of macrophages against a secondary exposure to the bacillus Calmette-Guerin (BCG) and Listeria [12]. The observation became known as the “classical macrophage activation”. Then, Mills and colleagues found that classically activated macrophages (M1) respond to interferon-gamma (IFNγ), lipopolysaccharide (LPS), granulocyte-macrophage colony stimulating factor (GM-CSF), and tumor necrosis factor (TNF) stimuli [12]. IFNγ is the main cytokine linked with M1 activation and the main product of Th1 cells. Natural killer (NK) cells are the principal source of IFNγ.
Following an infection or stress, NK cells produce IFNγ that in turn primes macrophages to release pro-inflammatory cytokines (e.g IL-1-beta, IL-12, IL-18, IL-23) and to produce high amount of reactive oxygen and nitrogen species (ROS and RNS, respectively), for example through the up-regulation of the NADPH oxidase and the inducible nitric oxide synthase (iNOS), respectively. This leads to drive antigenic specific Th1 and Th17 cell inflammatory responses. Generally, NK cells only transiently produce IFNγ. In order to sustain a population of M1 macrophages, the adaptive immune response, provided by T helper 1, is tipically necessary. Classically activated macrophages phenotypically express high levels of major histocompatibility complex class II (MHC II), CD68, CD80 and C86. They exhibit inflammatory functions and are implicated in initiating and sustaining inflammation in the context of the host defense, and if this process is not finely controlled, it is detrimental to the health of the host.

3.2.2 Alternatively activated macrophages (M2)

In the 1990s, it was discovered that interleukin-4 (IL-4) induced different effects on macrophage gene expression compared to that of IFNγ and LPS. In contrast to the classical activation of macrophages by IFNγ, this activation induced by IL-4 was described as “alternative activation” (https://www.bio-rad-antibodies.com/static/2015/innate/macrophage-polarization-mini-review.pdf). In particular, basophils and mast cells are important early producers of IL-4, but other granulocytes can also contribute.
Alternative activation can be induced also by fungal cells, immune complexes, helminth infections, apoptotic cells, IL-13, IL-10, TGF-β, and M-CSF. The early production of IL-4 converts resident macrophages into a population programmed

to activate the inflammatory responses and expression of markers. In particular IL-4 stimulates macrophage to switch on the arginase enzyme and to release high amount of IL-10 and low levels of IL-12. Arginase enzyme converts arginine into ornithine, a precursor of polyamines and collagen, thereby contributing to the production of extracellular matrix. The development and maintenance of wound-healing macrophages is carried out by adaptive immune responses. Alternative activated macrophages can be detrimental to the host, since a dysregulated wound-healing process can lead to tissue fibrosis. Indeed, it was demonstrated that macrophages that lacked expression of IL-4 receptor failed to induce uncontrolled fibrosis, and treatment with antibodies specific for IL-4 caused a reduction in fibrosis and a decrease in the accumulation of wound-healing macrophages [13].

It has recently been demonstrated that *in vitro* macrophages are capable of complete repolarization from M2 to M1, and can reverse rapidly their polarization depending on the chemokine environment (https://www.bio-rad-antibodies.com/static/2015/innate/macrophage-polarization-mini-review.pdf).

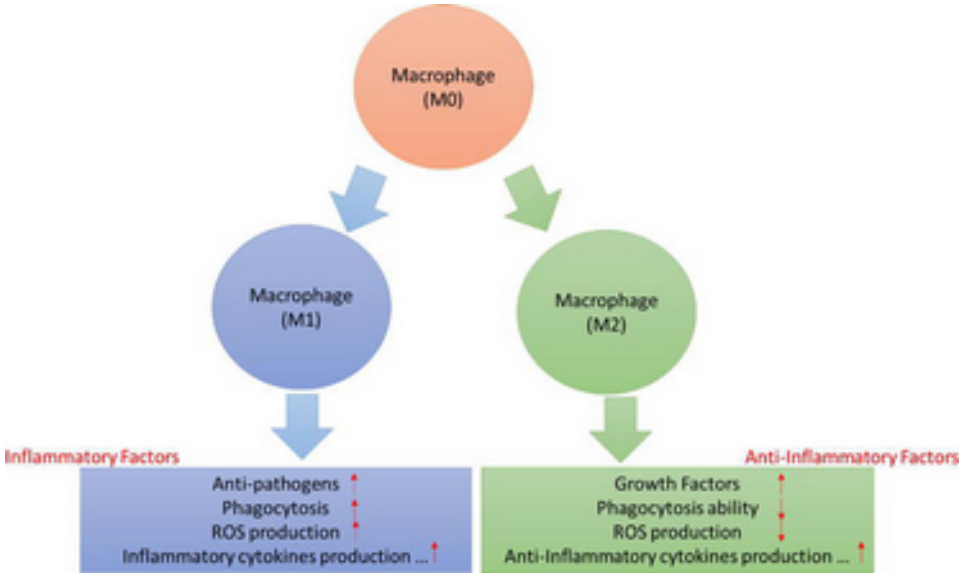

Figure 6. M1 and M2 macrophages activities [14]

The classification of macrophages in M1 and M2 populations is now considered an oversimplification that does not describe accurately the whole spectrum of macrophages. Other populations of macrophages have been discovered such as the population of tumor associated macrophages (TAM), and the population of macrophages expressing T cell receptors and CD169, which do not fit the criteria used to distinguish between M1 and M2. TAMs were first identified as having M2-like phenotype, but subsequent studies [15] have shown that they express both M1 and M2 phenotypes. These macrophages induce tumor progression and a poor prognosis by promoting angiogenesis, immune suppression, lymphogenesis, stroma remodeling, tumor invasion and metastasis. They can be recruited to the tumor sites either from the surrounding tissues by the tumor itself, through the release of chemotactic molecules, or from circulating monocytes that infiltrate in the tumor and mature into TAMs. The current classification of macrophages is complex and further research is needed to fully understand the role of the different macrophage populations in both physiology and pathology (*Figure 7*).

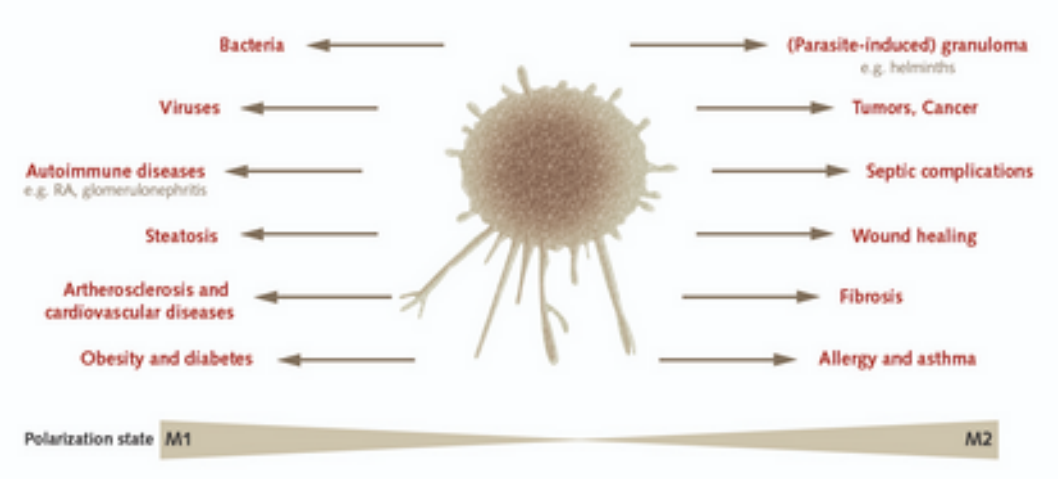

Figure 7. Macrophage plasticity and polarization in different types of pathologies (https://promocell.com/cells-in-action/macrophage-plasticity-black-white/).

3.3 Phagocytosis: a peculiar ability of macrophage cells

Cells have evolved several strategies to internalize particles, nutrients, solutes, including pinocytosis, receptor-mediated endocytosis, and phagocytosis.
Pinocytosis consists of the uptake of fluids and solutes. Receptor-mediated endocytosis refers to the process that allows macromolecules, viruses and small particles to enter cells. Pinocytosis and endocytosis share a clathrin-based mechanisms and occur independently of actin polarization.
By contrast, phagocytosis is defined as the receptor-mediated engulfment of large particles (> 0.5 μm) into plasma membrane-derived vacuoles called phagosomes [16]. Phagocytosis is mediated by an actin-dependent mechanism which is also independent on clathrin.
Only specialized cells, termed "professional phagocytes", are capable of performing this process with high efficiency, and further coordinate the adaptive immune response by presenting antigens to lymphoid cells. Neutrophils, dendritic cells, osteoclasts, eosinophils, monocytes, and macrophages are some of these cells [16], [17]. Rabinovitch *et al.* [18], however, have shown that other cells may have an intermediate phagocytic ability under certain circumstances, and proposed the term "paraprofessional phagocytes".
Phagocytes recognize a large number of different particles that can be ingested, including all sorts of microbial pathogens, apoptotic cells, and foreign substances.
The recognition of specific particles is achieved thanks to different receptors that can distinguish ligands on the target particles. The receptors expressed on the plasma membrane of phagocytes are classified into non-opsonic or opsonic receptors. Non opsonic receptors can identify directly determinants inherent to the particle. Examples include mannose receptors, CD14, detectin-1, and scavenger receptor A (SR-A) which bind to damage- or pathogen-associated molecular patterns (DAMPs and PAMPs, respectively). In particular mannose receptors bind to mannan, CD14 to lypopolysaccharide-binding protein, and detectin-1 to polysaccharides of some yeast cells, and SR-A to lipopolysaccharide (LPS) on Gram negative bacteria and on *Neisseria meningitidis*.
Opsonic receptors recognize, interact and digest host serum factors (opsonins) bound to foreign particles. Opsonins operate as a bridge between the phagocyte and the particle to be ingested. Opsonins include antibodies, fibronectin, complement, and milk fat globulin. The best characterized opsonic phagocyte receptors are the Fc receptors (FcR) and the complement receptors (CR, e.g CR3) that binds respectively to the constant portion of immunoglobulin (Ig) G or IgA antibodies and iCR3 deposited on the particle after complement activation [16].

After recognition of targeted particles, the receptors trigger a series of signaling cascades that lead to changes in membrane remodeling and in the actin cytoskeleton in order to extend the membrane around the particle. This process is called "formation of pseudopods". At the point of contact, a depression of membrane (the phagocytic cup) is formed. Then, the membrane surrounds the target particle and within a few minutes it closes at the distal end, leaving a new phagosome [16]. During this part of the process, the receptors grab and collaborate to complete the formation of the phagosome.

The maturation process leads to the transformation of the phagosome into a microbicidal vacuole called a "phagolysosome". The maturation process is subdivided into four stages: early, intermediate, late and phagolysosome. During this process the composition of the membrane is modified to include molecules that control the membrane fusion. It is regulated by GTPase Rab5 and Rab7.

GTPase Rab5 determines the fusion of new phagosome with early endosomes. GTPase Rab7 is required for the fusion of the phagosome with late endosomes. At the same time new intraluminal vesicles are formed and contain molecules planned to degrade and move the late phagosome and the lysosome. The process ends with their fusion into phagolysosomes.

Moreover, during this process, the phagosome get increasingly acidic by the action of a proton-pumping V-ATPase and abundance of degradative enzymes. At the beginning the early phagosome is mildly acidic (pH 6.1-6.5), whereas the phagolysosome is highly acidic (pH as low as 4.5). The phagolysosome further contains hydrolytic enzymes, (e.g., cathepsins, proteases, lipases, and lysozymes) and NADPH oxidase that increases the production of reactive oxygen species. All these features of phagolysosome are fundamental to killing microorganisms, digesting them, releasing digested products and finally contributing to the host defense. Indeed, phagocytosis efficiency is increased during inflammation, oxidative stress and xenobiotic agents.

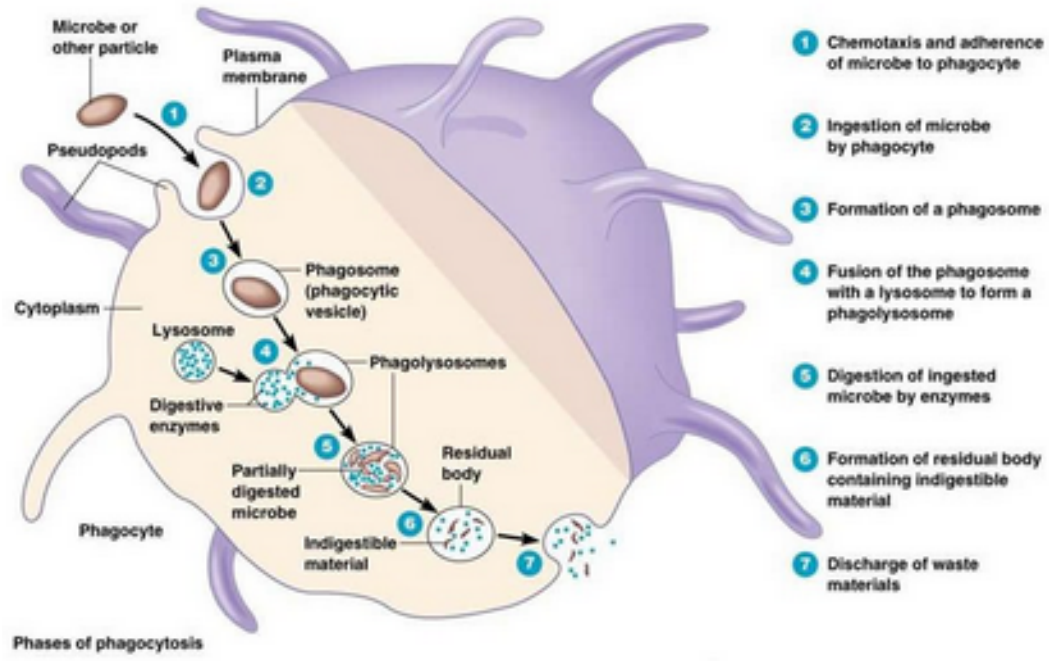

Figure 8. Phagocytosis steps (https://microbenotes.com/phagocytosis-introduction-mechanism-steps-and-example/).

Considering that macrophages and other mononuclear phagocytes are central regulators of a broad spectrum of inflammatory diseases by their accumulation and immunological effector functions, phagocytosis has been evaluated as a target for therapeutic treatment. Macrophages can ingest large particles, whereas all other non-phagocytic cells are not able to take up > 0.5 μm particles. Exploiting the ability of macrophages to ingest a wide range of exogenous and host-derived particulates presents the opportunity to utilize cytotoxic particles greater than > 0.5 μm to selectively kill/switch off macrophages. This offers a therapeutic option to inflammatory and tissue injury diseases in which macrophages activity has been implicated. It has been demonstrated that pathogen-derived delivery systems could reduce phagocyte mediated inflammation and diseases 1) by the reduction of inflammatory cytokines directly in mononuclear phagocytes and 2) inflammatory cell infiltration inhibition [19].

3.4 Macrophages: central regulators of inflammation and fibrosis

- Macrophages in tissue injury and inflammation

Macrophages responding to infections and sterile tissue injuries are activated by inflammatory signals (e.g PAMPs and DAMPs) in their microenvironment and develop into classical activated M1 macrophages. M1 macrophages synthesize and release a myriad of pro-inflammatory and cytotoxic molecules, including cytokines (e.g., IL-1, IL-12, IL-23, TNFα), chemokines, and reactive oxygen and nitrogen species, that are responsible for amplifying the inflammation and attracting other immune cells, such as neutrophils and natural kill cells. Further, M1 macrophages have enhanced phagocytic abilities and increased expression of co-receptors required for antigen presentation [21].
In particular:
- TNFα and IL-1 upregulate adhesion molecules and stimulate the endothelium to produce chemokines. TNFα also sensitizes neutrophils and macrophages to produce ROS and RNS, and, along with IL-1, it induces the release of proinflammatory mediators including IL-6, platelet activating factor (PAF), prostaglandins, matrix metalloproteinases, and various chemokines from macrophages and other cell types [22].
- chemokines have been characterized as being in one of two major structurally distinct groups: C-C chemokines, which induce migration and activation of macrophages/monocytes and lymphocytes, and C-X-C chemokines, which are primarily neutrophil chemoattractants and activators. Continuous local release of chemokines at sites of injury is thought to mediate the ongoing migration of effector cells into inflammatory lesions [22].
- ROS and RNS (e.g., superoxide anion, hydrogen peroxide, hydroxyl radical, nitric oxide, and peroxynitrite) are produced in high amounts by macrophages via enzyme-catalyzed reactions. These reactive species are needed to destroy invading pathogens and foreign materials. Specifically, ROS are generated via membrane-associated NADPH oxidases. This enzyme produces superoxide anion that rapidly dismutates to hydrogen peroxide anion and then in the presence of transition metals forms hydroxyl radicals. RNS are generated by the NOS-2 enzyme that catalyzes the oxidation of L-arginine to nitric oxide and citrulline. Nitric oxide reacts rapidly with superoxide anion to form peroxynitrite, a relatively long-lived cytotoxic oxidant.
A persistent pro-inflammatory phenotype of macrophages is responsible for turning acute inflammation into a chronic process that leads to loss of tissue and a variety of chronic inflammatory and autoimmune pathologies.

- Macrophages in the resolution of inflammation

For the resolution of inflammation, the "waste elimination process" is fundamental. It consists of the removal of dead cells, in particular neutrophils that undergo apoptosis and are taken up by macrophages. The limitation or cessation of monocytes infiltration to the injured sites avoids the persistent exposure of all immunostimulatory elements to immune cells. During this phase, macrophages switch their phenotypes from classical activated M1 macrophages (inflammatory) to alternatively-activated M2 macrophages (anti-inflammatory). M2 macrophages secrete several anti-inflammatory mediators, such as IL-4, IL-13, IL-10, and TGF-β. A key regulator of these process might be the circulating serum amyloid P that is responsible for opsonizing dead cells in damaged tissue, and the IL-10 seems to be the predominant cytokine that strongly activate M2 macrophages and orchestrate the resolution of inflammation. It was demonstrated that injection of M2 macrophages into mice was protective in terms of the inflammatory cytokine expression and accumulation of pro-inflammatory macrophages [21]. Further, depletion of M2 macrophages from sterile wounds not only delays wound healing but also leads to apoptosis of endothelial cells [21]. Therefore, the anti-inflammatory phenotype of macrophages is mandatory for an efficient resolution of inflammation.

- Macrophages in tissue repair and fibrosis

The process for the resolution of damaged tissues is in general subdivided into regeneration and repair (*Figure 9*). Regeneration consists of the proliferation of cells to replace the injured tissues and lost structures and leads to a complete reconstitution of the lost or damaged tissue. In contrast, in the repair process, the replacement of damaged tissues is incomplete, and can result in structural derangement, characterized by formation of a scar. The contribution of regeneration and scarring depends on the regenerative capacity of the tissue and the severity and nature of the injury. For example, liver and skeletal muscle have high regenerative ability, whereas brain and heart healing proceeds rapidly through processes of wound closure and fibrotic scarring at the expense of tissue structure and function [23].

When the injury is severe and persistent, regeneration is not possible, and an insufficient resolution results in fibrosis and dysfunction of the tissue.

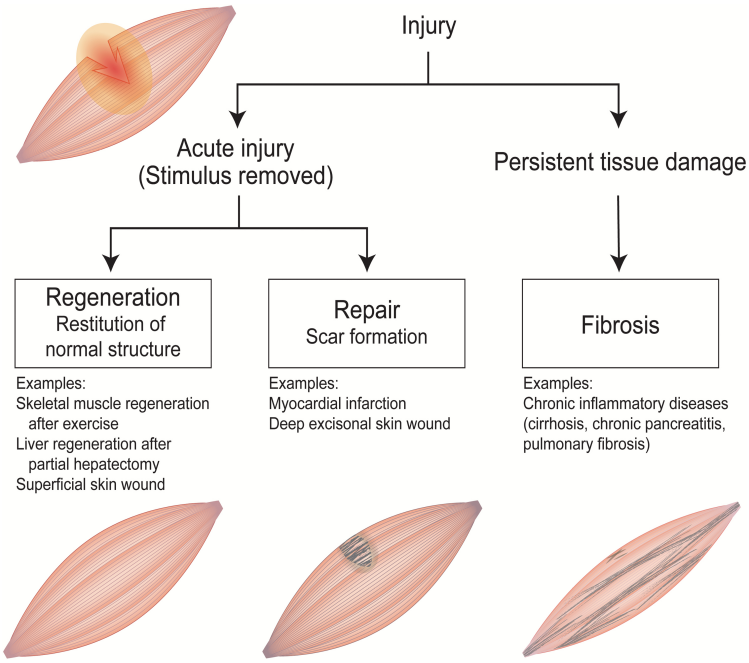

Figure 9. Regeneration and repair after injury [23]

Inadequate repair is associated with the presence of alternatively-activated M2 macrophages that contribute to tissue fibrosis, through the production of several growth mediators, supporting mesenchymal healing response, fibroblasts activation, and ECM secretion. M2 macrophages express arginase that synthesizes glutamate and proline necessary for the collagen synthesis, therefore promoting fibrogenesis. Furthermore, M2 macrophages release TGF-β, and other profibrotic factors, such as CTGF, CCL17, CCL22, and IGF1. TGF-β induces the activation of fibroblasts into myofibroblasts that drive the fibrotic process. Utilizing the varied roles of macrophages in its phases of tissue repair in health and disease might be an attractive therapeutic target to limit both scarring and fibrosis.

4. RADIATION-INDUCED FIBROSIS: A LATE SIDE EFFECT OF RADIOTHERAPY

4.1 Radiation therapy for the treatment of cancer

Cancer is a complex pathology with a multifactorial etiology and characterized by cells with uncontrolled proliferative potential, evasion of apoptosis and ability to metastasize to different organs in the body [24]. Cancer is a leading cause of death worldwide, accounting for over 10 million deaths in 2020. The most common cancers in 2020 (in terms of new cases) were: breast (2.26 million cases), lung (2.21 million cases), colon and rectum (1.93 million cases), prostate (1.41 million cases), skin (non-melanoma) (1.20 million cases) and stomach (1.09 million cases) cancers (https://www.who.int/news-room/fact-sheets/detail/cancer). It is estimated that cancer affects 1 in 3 people in the United States and the International Agency for Research on Cancer (IARC) has predicted that by 2030 approximately 26 million new cancer cases and 17 million cancer death will occur each year worldwide [25].

Nowadays, many treatment and management options for cancer are used to cure, to shrink or to stop the progression of a cancer, including surgery, chemotherapy, radiation therapy. Radiation therapy or radiotherapy is a cost-effective single modality to treat many types of cancer and it accounts for approximately 5% of the total cost of cancer care [26].

Approximately 50% of all cancer patients receive radiotherapy during their course of illness, with an estimation that radiotherapy contributes to around 40% toward curative treatment [26]. Under some situations of inoperable disease, radiotherapy is the only option available. Some indications require the combination of radiotherapy with other treatment modalities, such as surgery and chemotherapy or immunotherapy. Radiation can be used before surgery, with the goal to shrink tumor, and after to destroy microscopic tumors that are not removed by surgery [26]. There are two approaches to administer radiation: external beam radiation and brachytherapy. External beam radiation is delivered from outside to the cancer site by photons (i.e., x-rays and γ-rays), electrons (i.e., β-particles), protons or particle radiation (e.g., α-particles, carbon ions, etc.); these are called ionizing radiations because their energy absorption is sufficient to break chemical bonds and produce ionizations. This is the most common modality in the clinical practice. Brachytherapy or internal radiation consists of the administration of radioactive

sources that act from inside the body. It is used especially for gynecological and prostate cancers.

Table 3. Examples of cancers treated with radiation therapy [26]

Early cancers curable with radiotherapy	*Cancers curable with radiotherapy in combination with other modalities*
Skin cancers (Squamous and Basal cell)	Breast carcinomas
Prostate carcinomas	Rectal and anal carcinomas
Lung carcinomas (non-small cell)	Locally advanced cervix carcinomas
Cervix carcinomas	Locally advanced head and neck
Lymphomas (Hodgkin' s and low grade	carcinomas
Non-Hodgkin's)	Locally advanced lung carcinomas
Head and neck carcinomas	Advanced lymphomas
	Bladder carcinomas
	Endometrial carcinomas
	CNS tumors
	Soft tissue sarcomas
	Pediatric tumors

4.2 Principles of radiotherapy

The overall goal of radiotherapy is to damage and eventually to kill cancer cells by interfering with their reproductive potential. Ionizing radiation deposition is through different chemical mechanisms. Photons produced by modern radiotherapy machines are of sufficient energy (~ 6 MV) to damage DNA molecule both directly, and mostly indirectly through the production of reactive chemical species from water radiolysis. Ionizing radiations induce double strand breaks and single strand breaks in DNA molecules, as shown in *Figure 10*. Typically, most single strand DNA breaks are repairable because the cell has the complementary, undisturbed DNA strand to use as a template. However, if the

DNA break cuts across both DNA strands, the genomic integrity is compromised. The damage is manifest when the cell attempts cell division and the result is usually cell death [26].

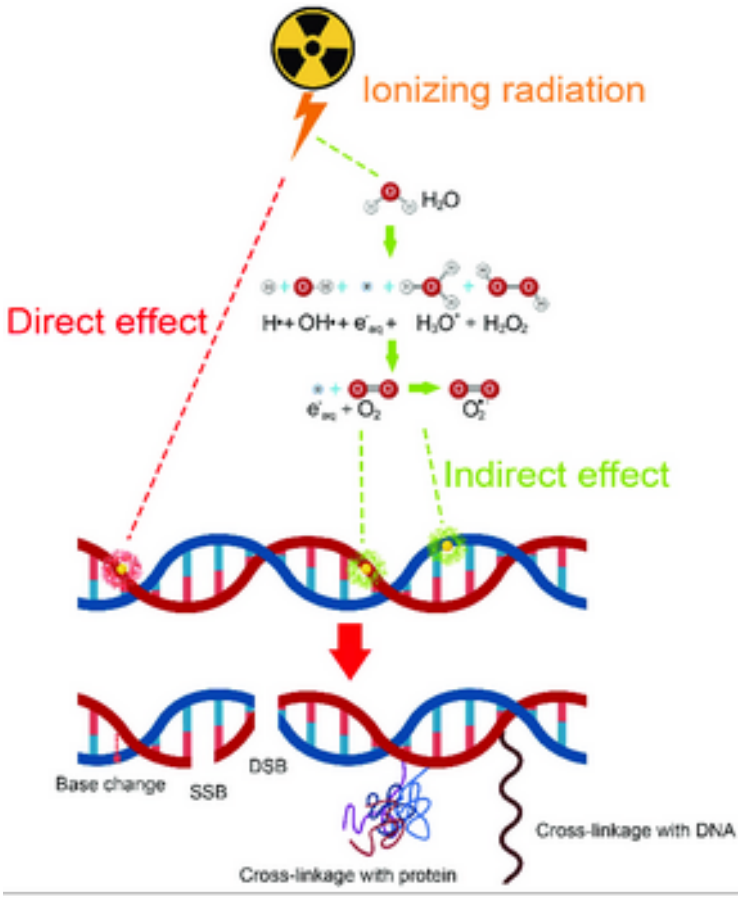

Figure 10. Schematic of ionizing radiation actions [27]

4.2.1 Primary effects of ionizing radiations

4.2.1.a Water radiolysis and reactive oxygen species

Ionizing radiation is non-specific in its deposition of energy. Most radiation absorption is with water, since water makes up the majority of our bodies; thus,

radiation absorption leads primarily to water radiolysis. Radiation can also directly interact with lipids, carbohydrates, and proteins; the consequence of these interactions is minor due to biological redundancy. In contrast, there is only one double stranded copy of DNA and absorption of radiation energy either directly or indirectly through hydrolysis (i.e., free radicals formed through the interaction of radiation with water), can produce lethal consequences. Eighty percent of a cell is composed of water, and therefore understanding the process of the radiolysis of water yield insight into an understanding of the interaction of radiation with living tissue. Water radiolysis consist of the decomposition of water due to ionizing radiation and results in both excitations and ionizations leading to the production of free radicals that consequently combine with and damage biological molecules [28]. In fact, most of the free radicals form recombined to re-form water; others combine with biological molecules that damage the cell.
In an aerobic cellular environment at physiological pH, the majority of species formed during the radiolysis process are $O^{2-\bullet}$, $^{\bullet}OH$- and H_2O_2 [28]. Consequently, in biological systems water radiolysis determines the formation of organic radicals causing protein inactivation and lipid peroxidation.

4.2.1.b Production of reactive nitrogen species

Ionizing radiation can induce the cellular activity of nitric oxide enzyme that leads to the production of large amounts of reactive nitrogen species, in particular nitric oxide ($^{\bullet}NO$). Nitric oxide is an inactive molecule but, if it reacts with $O^{2-\bullet}$, generates the peroxynitrite anion ($ONOO^-$). This radical reacts, strongly and with low selectivity, with several cellular molecules, such as lipids, proteins, thiols, and DNA bases. Whereas reactive oxygen species (H_2O_2 and $O^{2-\bullet}$), that are less reactive, diffuse a longer distance away from the originating site; peroxynitrite anion reacts only with nearby molecules and it is not able to react as a second messenger [28]. Moreover, these RNS enhance cellular damage in the presence of catalytic redox metal ions, e.g copper and iron ions.

Therefore, in irradiated cells under ambient oxygen, water radiolysis species and activation of nitric oxide synthase are the most important sources of ROS/RNS, and sustain damages to DNA, including DNA breaks, base damage, DNA-protein cross links, destruction of sugar, telomere dysfunction and finally cell death.

4.3 Types of radiotherapy-induced cell death

Radiotherapy does not kill cancer cells instantly, as shown in *Table 4,* but cancer cells begin to die hours, days or weeks after the treatment.

Table 4. Time scale of radiation interaction [29]

Time (s)	*Event*
Physical stage	Energy transfer
10^{-18}	Ionizing particle traverses a molecule:
10^{-15}	Ionization
10^{-14}	Excitation: molecular vibration, molecular dissociation, electron thermalization
Chemical stage	Formation of radical species and molecular products
10^{-12}	Diffusion of free radicals
10^{-10}	Free radical reactions with the solute
10^{-8}	Formation of molecular products
10^{-5}	Completion of chemical reactions
Biochemical stage	
1s-1h	Enzymatic reactions, repair process
Biological stage	
1h-100yrs	Genomic instability, aberration, mutation, cell killing, fibrosis, carcinogenesis

Remarkably, ionizing radiation induces DNA damage not only in cells exposed to ionizing radiation but also in their neighboring non-exposed cells and cells far from the irradiated area through intercellular communication mechanisms, the movement of toxic cytokines through gap-junction. This effect is termed

radiation-induced bystander-effect (RIBE). Furthermore, the progeny of non-irradiated cells show the same symptoms of the parent cells and exhibit perturbation of oxidative homeostasis and a wide range of damages to lipid, protein, and DNA.

Radiation induces different types of cell death: apoptosis, mitotic catastrophe, necrosis, senescence and autophagy. Apoptosis, a programmed cell death, has been implicated in the mechanisms involved in cancer and radiation therapy. Most solid tumor cell death occurs primarily as mitotic catastrophe that can result in the formation of giant cells with multiple nuclei after aberrant mitosis. Necrosis, a process characterized by cell swelling and breakdown of cellular membranes, is seen less frequently after large radiation exposures. Senescence, that is the loss of cell proliferative ability, is observed in cells subjected to an intensive oxidative stress following DNA injury. Autophagy is a more recently observed phenomenon and consists of the digestion of cell itself involving authophagic, lysosomal compartment. Nowadays knowledge of the mechanisms responsible for the death of irradiated cell is increasing, even if much remains to be understood and fully elucidated in the cell death pathways after radiation exposure.

4.4 Radiation-induced fibrosis: a complication of radiation treatment

4.4.1 Clinical presentation and etiology

Radiation-induced fibrosis (RIF) is a severe, yet incurable, irreversible long-term complication of normal tissues after external beam radiation treatment in cancer patients. Approximately 60% of cancer patients receive radiotherapy as part of their therapeutic regimens and 16-28% of them develop this adverse effect. The onset of RIF occurs between months and years after radiotherapy, and it progresses in severity with time [30]. RIF occurs in many organs, including mostly breast, skin, lung, bowel, liver, and kidney. It results in a multitude of symptoms that impact strongly the patients' quality of life. In general, it may manifest as skin induration and thickening, muscle shortening and atrophy, limited joint mobility, lymphedema, mucosal fibrosis, ulceration, fistula, hollow organ stenosis, and pain [31].

Clinical severity of RIF is influenced by several factors, including the treatment-related factors (total dose of radiotherapy and dose per fraction, the volume of tissue treated, other previous or current treatments, such as chemotherapy and

surgery, and the duration of therapy); patient-related factors (genetic susceptibility, age, physiological status); comorbidity factors (preexisting connective tissue disease, cardiovascular disease, diabetes mellitus, and hypersensitivity). Despite technology-driven improvements in the delivery of radiation to better target the tumor area, normal tissue toxicity continues to occur, and it is a key consideration for the treatment of any condition with radiotherapy [32]. The doses opted for use in therapy are generally a compromise between the dose that successfully destroy cancer in the majority of patients and the dose that induces adverse effects in the smallest subset.

4.4.2 Pathogenic mechanisms of RIF

Mechanisms of RIF are similar to that of any chronic wound healing process [31]. Following the initial injury of radiation exposure, an acute response leads to inflammation and then to fibroblasts recruitment and activation with the deposition of ECM components, as shown in *Figure 11*.
Essentially, the multi-step process of RIF includes the oxidative stress generation, microvascular injury, recruitment and migration of inflammatory cells to the inflammatory sites and finally the activation of fibroblasts into myofibroblasts.

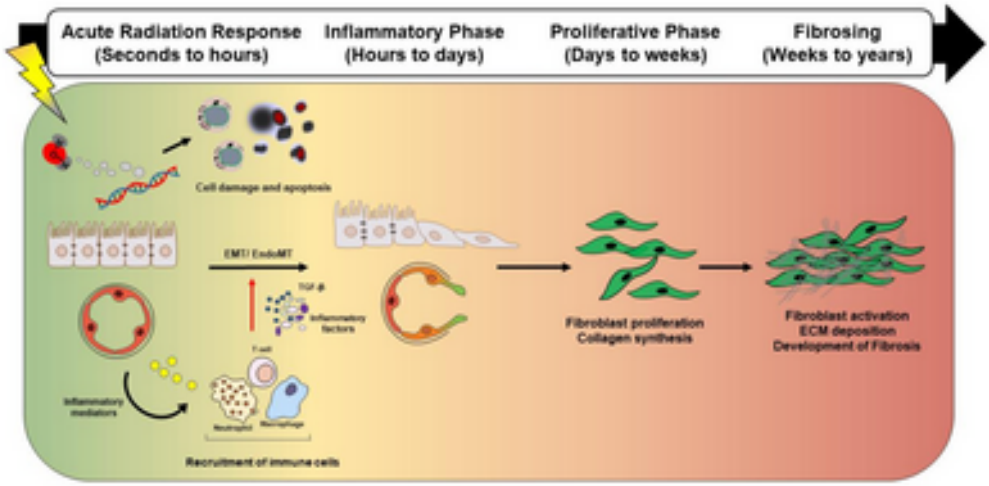

Figure 11. Schematic representation showing distinct and overlapping stages of RIF [33]

5.4.2.a Oxidative stress

It is firmly established that oxidative stress, in particular an imbalance in ROS production, is implicated as an important molecular mechanism underlying fibrosis in a variety of organs [34].
The term “oxidative stress” encompasses all the molecular, cellular, and tissue abnormalities resulting from excess ROS production and/or depleted antioxidant defenses [34]. Ionizing radiation favors electron leakage from the electron transport chain and disrupts enzymatic scavengers of ROS, including the superoxide dismutases (SODs), catalase (CTL), and glutathione peroxide. This results is an increase in reactive species.
Excess of ROS or deficiency of SODs and CTL are responsible to:
- damage lipids, proteins, and DNA of living cells in aerobic conditions (oxidative stress);
- production and release of the TGF-β. Excessive amount of ROS, after radiation exposure, determine the maturation and the activation of this pro-fibrotic cytokine. Specifically, ROS oxidizes cysteine residues and change the conformation of the latency-associated peptide (LAP), destroying the covalent bond between TGF-β and LAP. This allows TGF-β to bind its receptors and initiate an intracellular signaling cascade. Additionally, it was demonstrated that there is a vicious cycle between TGF-β and ROS, as they are interlinked to each other via feedback and feed-forward control mechanisms [36].
- differentiation of fibroblast into myofibroblasts by mediating epigenetic regulation in fibroblasts, such as DNA methylation, hystone methylation, and acetylation [36].

4.4.2.b Microvascular injury and hypoxia

Microvascular arterioles, capillaries and venules allow the delivery of oxygen, nutrients to, and the elimination of metabolic wastes from tissue parenchymal cells. Vascular injury is prominent in the microvascular layer, as endothelial cells are highly sensitive to the damaging effects of radiation. After radiation exposure, the sub-endothelial ECM components are exposed to platelets that promote excessive secretion of von Willebrand factor, tissue factor, and platelet-activating factor, while reducing NO, prostacyclin, and transmembrane glycoprotein thrombomodulin (TM) production, as well as its fibrinolytic activity [36]. This leads to an antifibrinolytic-coagulation cascade responsible for vascular occlusion.

The reduction of TM levels causes an insufficient local scavenging of thrombin that results in procoagulant and pro-inflammatory effects regulated by the activated endothelial protease-activated receptor-1 (PAR-1). Clinical and preclinical studies have demonstrated that the up-regulation of PAR-1, after ionizing radiation, is due to the direct oxidative damage and downregulation of TM at the gene expression level with upregulation of radiation-induced inflammatory cytokines [36], e.g., TNFα, TGF-β, IL-1, and IL-6.
The damages to vascular endothelial barrier promote the release of different factors, such as vascular endothelial growth factor (VEGF), platelet-derived growth factor (PDGF), that determine the permeabilization of the vessels and consequently the recruitment and proliferation of inflammatory cells.
The major effects of microvascular injury are tissue ischemia and hypoxia. Hypoxia promotes the production of radical species from NADPH oxidase enzyme, mitochondria, and Ca^{2+} flux. Hypoxia is a major sign of fibrosis as it causes the loss of endothelial cells, rarefication of capillaries and subsequent malperfusion [37].

4.4.2.c Continuous inflammatory response

Damage to DNA molecules and other macromolecules and cell death, in general, in response to radiation exposure result in the release of DAMPs recognized by pattern recognition receptors (PRRs) that activate a pro-inflammatory response. Neutrophils are the first cells that migrate to the site of injury and are responsible for removing cellular debris. Then, they extravasate and transmigrate into tissues and release high amount of pro-inflammatory cytokines which amplify the production of ROS and aggravate the local inflammation. Subsequently, macrophages are considered the key players not only in initiating, but also in sustaining and amplifying the inflammation. They originate from the differentiation of monocytes into M1 and then M2 macrophages. Ionizing radiation activates macrophages. Activated M1 macrophages release inflammatory factors, e.g., TNFa, IL-1β, IL-6, IL-12, and IL-23, and produce and secrete ROS in large quantitatives. Activated M2 macrophages release TGF-β and increase fibroblast proliferation and their activation into myofibroblasts, largely involved in fibrosis. Specific to lung fibrosis, radiation injuries have 2 phases: an acute phase, called radiation pneumonitis, and a late phase, termed as radiation-induced lung fibrosis. Prevailing studies suggest that the presence of chronic inflammation eventually causes lung fibrosis [36].

4.4.2.d Promotion of fibrosis by activated fibroblasts

After radiation exposure, fibroblasts are the major source of ECM and facilitate the development of fibrosis. In fibrotic diseases, fibroblasts are defined as "activated fibroblasts" or "myofibroblasts" as they are more metabolically active in ECM production and have a higher ability to migrate in the damaged tissues (refer to *Figure 12*). Fibroblasts are hugely heterogeneous within a single organ and also between organs. This heterogeneity may result from different origins and modes of activation.

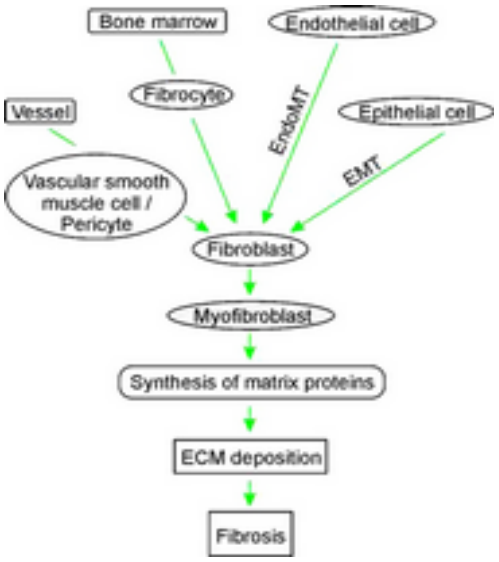

Figure 12. Fibroblasts as major ECM producers [37]

A major source of activated fibroblasts identified in scarred tissue is the resident fibroblast population that proliferates and migrates to the injured site, partially stimulated by TGF-β [38]. In addition to resident fibroblasts, activated cells may also derive from bone-marrow fibrocytes, and from endothelial and epithelial cells that undergo the transition to a mesenchymal phenotype. Active fibroblasts may also derive from vascular smooth muscle cells and pericytes. Activation of fibroblasts into myofibroblasts is promoted by TGF-β, a cytokine produced mainly by infiltrating inflammatory cells (in particular macrophages). TGF-β is considered the most potent and ubiquitous profibrogenic cytokine and plays a central role in the development of fibrosis involved in nearly all organ systems [36]. Its mRNA and/or protein expression is enhanced in fibrogenic conditions, both in organ systems and in experimental fibrosis models. Indeed, administration of anti-TGF-β antibody or inhibitor to TGF-β receptors ameliorates the fibrosis [40], [41]. In mammals, it exists in three isoforms, TGF-β1, TGF-β2, and TGF-β3, all present in fibrotic tissues.

The synthesis and maturation of TGF-β are convoluted and involve several steps. TGF-β is initially translated in a 390- to 412-amino acid pre-pro-protein. After the elimination of the signal peptide, maturation of the pro-TGF-β is completed in the trans-Golgi network (TGN) by endopeptidases such as furin [39] (refer to *Figure 13*). Then, the propeptide is cleaved and the latency associated peptide (LAP) and the TGF-β monomer are released. Two TGF-β monomers generate a dimer and two free LAPs bind non-covalently to the dimer. Subsequently, the inactive protein complex, named "the large latent TGF-β complex" is secreted in the extracellular space. Overall the large extracellular complex is formed by TGF-β-LAP and the latent TGF-β binding protein (LTBP) [36].

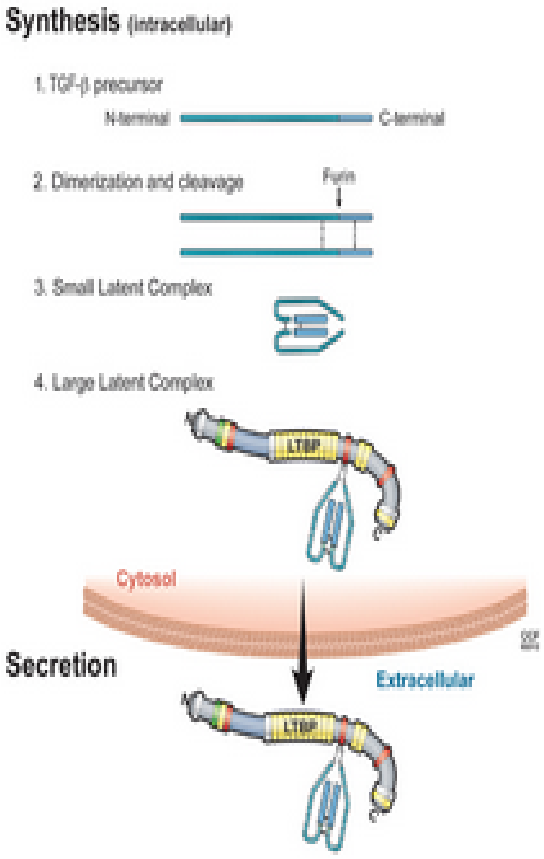

Figure 13. TGF-β processing [40]

To become mature and bind receptors, TGF-β must be released by the complex. Different molecules induce the maturation of this cytokine, and consequently the removal of the LAP and LTBP, such as thrombospondin-1, integrins, pH, and ROS. Notably, high levels of ROS are not only associated with fibrosis, but also with diseases that share high TGF-β1 levels, like diabetes and cancer. Mature TGF-β binds to serine and threonine kinase receptors, the type II (TβRII) and type I (TβRI) receptors on the cell membrane. This leads to the formation of an heterocomplex, in which TβRII activates TβRI by phosphorylation of threonine and serine residues. Then, activated TβRI recruits and phosphorylates Smad2 and Smad3 that form a complex with Smad4 that translocates into the nucleus to regulate gene transcription by binding to the Smad binding elements localized in the promoter region of the target genes. Further, several studies demonstrated that TGF-β explicates its profibrogenic activity through other non-canonical pathways,

specifically the mitogen activated protein kinase (MAPK) pathways, Rho-like GTPase pathways, and phosphatidylinositol-3-kinase (PI3K) pathways [36].

TGF-β is a multifunctional protein as illustrated in *Figure 14*. One of its major biological effects is to promote the epithelial- and endothelial- mesenchymal transformation, the proliferation and recruitment of fibroblasts to the wound site, and synthesis of structural matrix proteins. TGF-β is responsible for inducing phenotypic changes of fibroblasts to highly efficient matrix-producing myofibroblasts. Further, to avoid degradation of newly synthesized ECM components, TGF-β blocks the expression of matrix degradation enzymes, e.g., matrix metalloproteinase, and stimulates the expression of matrix metalloproteinase inhibitors.

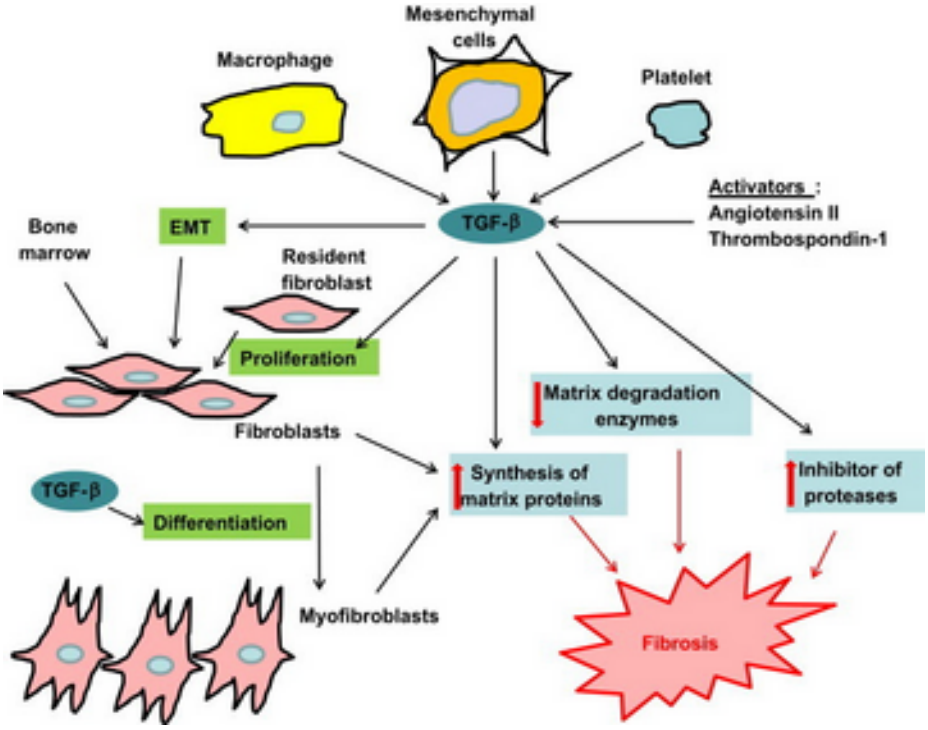

Figure 14. Biological effects of TGF-β [38]

Evidence indicates that there is a reciprocal regulation of TGF-β and ROS that supports the fibrosis [36].

TGF-β causes redox imbalance. It promotes, both mitochondrial and via induction of NADPH oxidase, ROS production in different types of cells. Ishikawa *et al.* demonstrated that in mouse mammary epithelial cells, TGF-β enhanced the cytoplasmic and mitochondrial ROS levels [42]. Jain *et al*. showed that TGF-β increased mitochondrial ROS production by blocking complex III activity [43]. They also reported that antioxidants which target mitochondria or genetically interfering with Complex III activity reduced TGF-β-induced expression of profibrotic genes.

TGF-β stimulates the expression and hence the activity of Nox enzymes (termed also NADPH oxidases), including Nox1, Nox2, Nox3, and Nox4, all important ROS producers. In particular, Nox4 stimulation mediates differentiation of fibroblast into myofibroblasts, apoptosis of epithelial and endothelial cells, and epithelial-, endothelial-mesenchymal transition. Boudreau *et al.* described that TGF-β enhanced ROS production by inducing Nox4 in human breast epithelial cells (e.g., MCF10A), and the knockdown of Nox4 expression significantly decreased ROS levels and fibronectin mRNA expression [44]. Jarman *et al.* reported that administration of a low-molecular-weight Nox4 antagonist reduced the progression of fibrosis in mice with bleomycin-induced lung fibrosis [45].

In addition, several studies suggested that there is a crosstalk between mitochondria and NADPH oxidases: mitochondria-derived ROS contributed to the increase in Nox expression in response to TGF-β, whereas Nox-generated ROS caused mitochondria dysfunction and increased ROS production [36]. Jain *et al.* revealed that, through the increase in mitochondria ROS levels, TGF-β stimulated the expression of α-SMA and CTGF, profibrotic proteins [43].

Furthermore, TGF-β suppresses the antioxidant defense system that include several molecules and enzymes, such as glutathione (GSH), superoxide dismutases (SODs), catalase (CTL), and glutathione peroxidases (GPXs). In human lung alveolar epithelial cells [46] and in fibrotic areas of usual interstitial pneumonia [47], TGF-β1 reduced the expression of gamma-glutamylcysteine synthetase (γ-GCS), the limiting enzyme of GSH synthesis. Also, the reduction of γ-GCS and consequently GSH, due to TGF-β1, enhanced the lipid and protein peroxidation in a mouse model of lung fibrosis [46]. Cui *et al.* demonstrated that, in *in vitro* fibroblasts and *in vivo* mouse lung tissue, TGF-β1 inhibited the extracellular SOD (EC-SOD) [48], a protective enzyme in several models of interstitial lung disease [36].

On the other hand, ROS intensifies TGF-β activity. Specifically, ROS activates TGF-β1, uncoupling it from LAP and LTBP, and upregulating TGF-β gene

expression [36]. Then, ROS are crucial in mediating many profibrotic effects of TGF-β, in particular the differentiation of fibrobrasts, the apoptosis of epithelial and endothelial cells, the endothelial- and epithelial- mesenchymal transition, and the ECM synthesis. Of note, epithelial apoptosis is juxtaposed with fibrosis, and it is believed to contribute importantly to fibrogenesis [36]. Lee *et al.* revealed that, in the lung of inducible TGF-β triple transgenic mice, the overexpression of TGF-β1 was followed by a transient epithelial apoptosis that moved on to inflammation and fibrosis [49].
Among all considerations, a further characterization of TGF-β pathways and its targeting should be carried out in order to provide new potential therapeutic options for fibrotic conditions.

4.5 Therapeutic strategies for RIF

Although progresses have been made in understanding the pathophysiology of radiation-induced fibrosis and novel treatment targets have been identified [50], no successful therapeutical treatments, to date, are available for this disease. However, results of clinical studies are difficult to compare because of variations in severity of RIF, method of RIF assessment, availability of efficient therapeutic drugs, treatment duration, and quality of trial design [51]. Treatment strategies can be summarized as: (1) anti-inflammatory treatment; (2) vascular therapy with pentoxifylline (PTX) and hyperbaric oxygen; and (3) antioxidant treatment [50].

- Anti-inflammatory therapies

Corticosteroids and non-steroidal anti-inflammatory drugs have been used to reduce late RIF since the 1950s. *In vitro* steroids inhibit the recruitment of macrophages, the synthesis of prostaglandins, leukotrienes and collagen. *In vivo* dexamethasone, a steroid drug, has been administered to treat liver injury, radiation-induced pneumonitis, and nephropathy in rats and it has been appeared to retard the onset of radiation-induced organ dysfunction [52], [53], [54].
Although steroids are used for their anti-inflammatory and immunosuppressive properties in clinical therapy for chronic RIF, no long-term effect on the underlying fibrosis has yet been shown [51].

Other immunosuppressive drugs, including D penicillamine and colchicine, may be acceptable for clinical use, but their marginal benefit must be weighed with their potential to cause serious adverse effects.

- Vascular-directed therapies

Pentoxifylline is a methylxanthine derivative that belongs to the class of drugs known as hemorrheologic agents, as it improves the flow properties of blood by decreasing its viscosity. In 1999, it was approved by the FDA for the treatment of vascular diseases, such as the intermittent claudication. Today, pentoxifylline is commercialized under several brand names (Trental, Pentoxil, Pentoxifylline) as an extended-release oral tablet.
It has three main properties [55]:
- improving the rheological properties of blood by suppressing both erythrocyte and platelet aggregation, reducing plasma fibrinogen, and increasing erythrocyte distensibility.
- anti-inflammatory, by lowering plasma levels of pro-inflammatory cytokines, such as TNFα, IL-1, IL-6, neutrophils activity and adhesion.
- antioxidative, may be due to its ability to decrease the production of superoxide via NADPH oxidase.
Further, in preclinical studies, pentoxifylline has been shown to inhibit serum- and IL-1β-driven fibroblast proliferation *in vitro*, as well as fibroblast collagen, glycosaminoglycans, and fibronectin production, while it enhanced collagenase activity [56].
For all these properties, pentoxifylline was considered in several fibrotic studies as a potential therapeutic solution to reverse radiation damages. Unfortunately, only high doses of PTX showed satisfactory results in terms of RIF resolution. High doses of PTX (600 mg orally four times a day) were not well tolerable by patients [56] (e.g., it caused more vomiting and central nervous system adverse effects than placebo). This suggests that PTX alone does not constitute a viable approach for the treatment of RIF [57].

Another vascular-directed treatment is hyperbaric oxygen therapy (HBO). In 1973, Mainous E. G. and Hart G. B [58] showed the efficacy of HBO against osteoradionecrosis, as it reduced tissue edema and increased angiogenesis, fibroblast proliferation and synthesis of collagen in irradiation-injured tissues. Evidence that HBO is beneficial to chronic fibrosis is not yet established [59], as

the literature is dominated by small trials with ill-defined recordings of complications [51].

Other treatments include drugs approved to manage high blood pressure, that have anti-inflammatory properties, including angiotensin-converting enzyme inhibitors (e.g., captopril, ramipril), and angiotensin II receptors antagonists (e.g., losartan). Animal studies have shown that these agents are effective in protecting the lung, kidney, skin, and heart from the effects of radiations [51], [60].
Recently statins have been enrolled in studies on healing, and pravastatin has been shown to have possible antifibrotic properties *in vitro* [61], but the administration of statins is correlated to the increase of complications, in particular post-operative bleeding adverse effect [62].

- Antioxidant therapies

In the 1980s, copper/zinc superoxide dismutase (Cu/Zn-SOD) was introduced for the treatment of severe inflammatory diseases. It was developed into a liposomal form (LipSOD) for the treatment of Crohn's disease, systemic sclerosis, Kawasaki's disease, and rheumatoid arthritis. Delanian and coworkers [51] showed for the first time in a phase II trial that LipSOD reversed established RIF, and demonstrated that in human-cultured pig myofibroblasts LipSOD decreased the expression of TGF-β, and the anticollagenase tissue inhibitor of metalloproteinase, with increased endogenous manganese (Mn)-SOD expression [51]. Brotons *et al.* showed that the treatment with Cu/Zn-SOD in cultured pig myofibroblasts downregulated the TGF-β gene expression and drove back the myofibroblast phenotype to a normal fibroblast phenotype. However, to date, SOD and its several formulations are not available for clinical use.
Vitamin E was taken in consideration for the treatment of RIF. Vitamin E (or α-tocopherol) is an antioxidant, it scavenges reactive oxygen species generated during oxidative stress. Fifty years ago it was observed that the deficiency of vitamin E was correlated with dysfunction of connective tissue repairs [57]. In studies of RIF lacking proper control arms, vitamin E has shown modest improvement [63] or no improvement in clinical symptoms and regression of fibrosis.
The combination treatments of vitamin E and pentoxifylline was investigated, as both alone were unable to manage RIF in patients, and with the idea that the combination of two compounds could be more successful thanks to different

mechanisms of radioprotection. Case reports of PTX plus vitamin E in patients with RIF have demonstrated clinical regression of fibrosis and improvement in clinical symptoms (e.g., skin tightness, dyspnea, pain) [63]. Further studies are necessary to clarify the biological properties and effects of this combined approach.

- Targeting Transforming growth factor-beta 1

TGF-β is the most extensively investigated cytokine involved in radiation fibrosis, as radiation increases its expression and induces its activation through proteolytic cleavage of the latent complex by ROS. Several animal studies of pulmonary radiation fibrosis have been undertaken to inhibit TGF-β, in particular TGF-β1, using both antibodies against TGF-β1 and inhibitors of TGF-β1 receptors. In a model of rat lung irradiation, the antibody 1D11 was given immediately after the last fraction of fractionated radiation. A reduction in alveolar septal wall thickness, macrophage activation and TGF-β1 and its downstream signal transduction protein was seen at 6 weeks and 6 months after radiation [50]. The administration of SM16, a small molecule inhibitor of TGF-β type 1 receptor kinase was effective in a similar animal model of radiation-induced lung fibrosis [64]. In other studies [50], the use of a human recombinant adenoviral vector carrying the gene for a TGF-β type II receptor has shown to elevate plasma levels of the receptor and to reduce levels of TGF-β in lung tissues, leading to ameliorate lung toxicity after radiation exposure. Unfortunately, to date, there have been no clinical trials of this therapeutic approach and the efficacy in humans has not yet been demonstrated.

AIMS OF THE PROJECT

Cancer patients previously treated with radiotherapy can develop long-term toxicities due to injuries in normal tissues that surround the tumor area. Radiation-induced fibrosis (RIF) is one of the common adverse effects of radiotherapy (overall incidence between 10-20%) and it results in a multitude of symptoms that significantly reduce the quality of life of the cancer patients. RIF is a complex multi-factorial process that ultimately results in an excess accumulation of collagen and other extracellular matrix components in many organs, especially in the lung, skin, small bowel, breast, liver, and kidney. Pathophysiological reactive oxygen species (ROS) and the response of normal cells to ROS stress are hypothesized to be central to the etiology of RIF. In addition, the transforming growth factor beta (TGF-β) plays a crucial role in the development of this condition.

It is well known that macrophages are central players of the immune response following normal tissue damages. Their persistent accumulation in irradiated sites prolong inflammation and consequently they can orchestrate all phases of the fibrotic process: they initiate, amplify and sustain the release of reactive oxygen and nitrogen species, pro-inflammatory and regulatory cytokines (e.g., TGF-β). Macrophages in turn promote fibroblast activation and leukocyte recruitment.

Progresses has been made to understand the pathology of RIF. However, to date no successful therapeutic approach is available in the clinical setting. Importantly, it has been reported that post-radiation antioxidant therapy significantly reduces RIF in animal models. This shows that it is indeed possible to halt the positive feedback between ROS accumulation and inflammation and reduce the severity of radiation injury.

Since macrophages are key regulatory actors in RIF, they may represent the natural target of anti-oxidant therapy. Eventually one might exploit the peculiar ability of macrophages to uptake μm-sized particulate material by phagocytosis and thus develop a macrophage-specific drug-targeting strategy.

The main aim of the project was indeed to explore this possibility, and to this purpose we sought to realize particles loaded with biologically active molecules. Particles have been obtained thanks to a collaboration with Sphera Encapsulation S.r.l. (Verona, Italy) and, as the drug, astaxanthin was selected for its biological activity.

Astaxanthin, *3,3'-dihydroxy-carotene-4,4'-dione*, is a naturally red-orange xanthophyll carotenoid pigment obtained from micro-algae *Haematococcus pluvialis* and marine organisms such as salmon, crustaceans and crab shells.

Astaxanthin (ASX) has proven anti-oxidative properties as it exhibits strong singlet oxygen/free radical scavenging activity, thereby protecting cell and biological membranes from oxidative damage. The pharmacologic potential of

ASX is now well recognized [65] and it could therefore play a key role in counteracting oxidative stress. Its biological activity is not limited to its antioxidant activity [65]. Indeed, ASX can protect animals, human beings included, against a wide range of diseases with excellent safety and tolerability [66]. A number of studies have shown that ASX treatments can modulate the functions of the immune system and control inflammation [66]. ASX could therefore play a key role in contrasting oxidative stress, a phenomenon caused by imbalance between production and accumulation of reactive oxygen species (ROS) in cells and tissues and detoxification of these reactive products through specific mechanisms. For all these considerations, ASX might therefore be used to reduce or prevent RIF.

ASX, however, is not soluble in water-based biological fluids and is sensitive to temperature, light and oxygen, all factors that limit its stability and bioavailability. These significant limitations may be addressed by ASX encapsulation into appropriate chemical matrices [66].

Encapsulation of ASX into micrometer-sized particles might represent, not only an excellent strategy to deliver ASX specifically to macrophages and other innate immune cells that are characterized by their unique ability to engulf, uptake and degrade particles of this size through phagocytosis, but also to protect and stabilize ASX.

Whey protein isolate isolate (WPI) was used as a shell material for the incorporation of the hydrophobic astaxanthin oleoresin. WPI is derived from milk, which has two important protein contents (β-lactoglobulins and α-lactalbumins), constituting 65% of the total weight of whey proteins [67], [68].

WPI-based drug delivery system have been investigated for delivering drugs and bioactive compounds [67], [68] as a promising carrier due to its excellent functional properties, such as emulsification, gelation and foaming, high drug binding capacity, biodegradability, and nontoxic properties. WPI has been used extensively to prepare nanosuspensions, nanoemulsions, hydrogels, nanoparticles, microparticles, and tablets [67]. The WPI-based microparticles have gained good reputation for being an innovative drug delivery system because WPI biopolymers can bind different hydrophobic and amphiphilic bioactive molecules and therefore can improve the solubility and bioavailability of the moiety [67].

To these purposes, we developed protein-based ASX-loaded microparticles, and we explored their biological activity *in vitro* with J774A.1 macrophage cells.

MATERIALS AND METHODS

Formulation of Astaxanthin-loaded WPI microparticles and empty WPI microparticles

Astaxanthin-containing oleoresin (ASTAPure® 10% oleoresin from *Haematococcus pluvialis*) was provided by Algatech (Ketura, Israel).
Astaxanthin-loaded microparticles were obtained by the technique described in the PCT/IB2019/059991 application. Five percent whey protein isolate (WPI, Carbery Food Ingredients, Ballineen, Ireland) resuspended in water and oleoresin (dissolved in ethyl acetate) were combined (ratio 9:1) and subjected to emulsification using Ultra-Turrax homogenizer (Ika, Staufen, Germany) at 13.500 rpm for 5 minutes. The emulsion was evaporated by rotary evaporator (Büchi Labortechnik AG, Flawil, Switzerland) and the particles were dried using a Mini-Spray dryer B-290 (Büchi Labortechnik).
Empty microparticles without oleoresin were obtained using the same procedure, adding ethyl acetate to the formulation.

Chemical and physical characterization of Astaxanthin-loaded microparticles

We quantified astaxanthin (ASX) in the microparticles in order to determine the loading capacity of WPI microparticles and the stability in time of astaxanthin, as light, UV, heat and oxygen can degrade this natural compound and lead to the loss of the antioxidant activity.
For these quantification purposes, the particles were digested enzymatically with porcine trypsin and amylase (Sigma-Aldrich, Merck KGaA, Darmstadt, Germany) at a final concentration of 2 mg/mL in phosphate buffer pH 7.0 for 4 h at 37 °C and ASX extracted with 2 volumes of ethyl acetate (Sigma-Aldrich) for 60 min, and then centrifuged at 21,000 x *g*.
ASX in the microparticles was quantified with an Evolution 201 spectrophotometer (Thermo Scientific, Waltham, MA, USA) at a wavelength of 480 nm as described in Reference [69].
The concentration of ASX was calculated following the equation:

$$[A]=\frac{10\times A_{480}\times DF}{E(1\%1cm)\times d} \qquad (1)$$

where [A] is the concentration of ASX expressed as mg/mL; A480 the sample absorbance at 480 nm; DF: dilution factor; E(1% 1 cm): ASX percent solution extinction coefficient ((g/100 mL)$^{-1}$ cm^{-1}) in ethyl acetate (2150); d: the optical path (cm).

As the dimension of particles is strongly important for our aims, the particle size was determined on dried samples upon dispersion in distilled water by laser diffractometry using a Malvern Master Sizer 3000 (Malvern Panalytical, Worcestershire, UK) with the following settings: particle refractive index, 1.9; particles absorption index, 0.01; water refractive index, 1.33; laser obscuration 12%.

Cells and cell cultures

J774A.1 (murine macrophage) and T47D (human breast carcinoma) cell lines were obtained from the European Collection of Authenticated Cell Cultures (ECACC, Salisbury, UK; ECACC numbers 91051511 and 85102201, respectively). Murine macrophages and human breast carcinoma cells were cultured in RPMI 1640 medium (Biochrom AG, Berlin, Germany) supplemented with 10% heat-inactivated foetal bovine serum (FBS), 2 mM glutamine (Sigma-Aldrich, St. Louis, MI, USA), and 10 mg/mL gentamicin (Biochrom) at 37 °C in a humidified 5% CO_2 atmosphere.
The mouse embryonic fibroblast MFB-F11 cell line [70] was kindly provided by Dr. Tony Wyss-Coray (Stanford University, Stanford CA, USA). These cells were cultured as described above, but, in culture media, we added 125 µg/mL hygromycin B Gold (InvivoGen, San Diego CA, USA), as indicated in [70].
Cells were routinely tested and shown to be negative for mycoplasma contamination using MycoAlert PLUS Mycoplasma Detection Kit (Lonza Walkersville Inc., Walkersville, MD, USA).

Microscopy

Cell morphology was routinely checked using an Evos (AMG, Life Technology) digital inverted microscope.
For confocal microscopy analyses, we cultivated J774A.1 and T47D cells in glass bottom µ-Slide IbiTreat chambers (Ibidi GmBH, Martinsried, Germany; 10,000 cells/well). 56 µg/ml ASX-loaded microparticles was added to cells. After 24 h at 37 °C, the cell samples were washed twice with cold sterile PBS 1x and cell membranes stained with an anti-CD11-FITC monoclonal antibody (clone M1/70, InvitroGen, Carlsbad, CA, USA) for 30 min at 4 °C. Cells were then washed with PBS 1x to remove excess antibody and fixed with 400 µL paraformaldehyde for 10 min at 37 °C. Cells were rinsed 3 times with PBS 1x and permeabilized with 0.1% Triton in 2% PBS-BSA. 1:4000 DAPI (4′,6-diamidino-2-phenylindole; Sigma-Aldrich, St. Louis, MI, USA) was used to stain nuclei, for 10 min at 37 °C and finally cells were washed again with PBS 1x. Images were taken with an SP5 confocal microscope from Leica Microsystems (Mannheim, Germany) equipped with a 63× objective (HCX PL APO λ blue 1.4NA OIL). We collected stacks of images at $\Delta z = 1$ µm. Image analyses were performed with ImageJ 1.47v software (https://imagej.nih.gov).

Cytotoxicity assays of microparticles

J774A.1 macrophage cells and T47D breast cancer cells were seeded at 5000 cells/well in flat-bottom 96-well plates in 180 µL RPMI medium containing serial dilutions of ASX-loaded particles or empty particles. Some cell samples were also left untreated for control purposes.
The incubation was prolonged for several days, and at each time point intracellular ATP was measured using the CellTiter-Glo® Luminescent Cell Viability Assay (Promega, Milan, Italy) following the manufacturer's instruction.
The CellTiter-Glo® Luminescent Cell Viability Assay is a method to determine the number of viable cells in culture based on the quantification of ATP content which reveals the presence of metabolically active cells. ATP content is directly proportional to the number of cells present in culture.
Luminescence was measured with a FLx800 Microplate reader (FLx800, Bio-Tek Instruments, Bad Friedrichshall, Germany). All measurements were carried out at least in triplicate.

Flow cytometry

A Guava easyCyte 5 flow cytometer (Merck Millipore, Billerica, MA, USA) was used. The instrument is equipped with a 488 nm, 20 mW, blue laser light. Light scattering is measured by means of a forward scatter (FSC) photodiode and a side scatter (SSC) photomultiplier. Three fluorescence channels, green, yellow and red, allowed for collection of cell-associated fluorescence at the same time, thanks to the following filters: green, 525/30 filter; yellow, 583/26; red, 680/30. Instrument calibration was routinely carried out using the Guava EasyCheck kit (Merck Millipore, Billerica, MA, USA) following the manufacturer's instructions. Raw listmode data were analyzed with the software Mathematica (Wolfram Research Inc., Champaign, IL, USA).
Flow cytometry analyses were carried out to determine the phagocytosis kinetics of astaxanthin-loaded microparticles and the intracellular ROS levels in J774A.1 cells.

- Phagocytosis kinetics

J774A.1 cells were seeded at 20,000 cells/well in flat-bottom 24-well plates in 2 mL RPMI medium containing 56 µg/mL ASX-loaded microparticles. Then, cells were treated with 100 ng/mL of IFNγ.
Some cell samples were also left untreated (without ASX microparticles and IFNγ) as control.
Flow cytometry analyses were carried out 1 hour after the treatments, and 1, 2, 3, and 4 days post treatments. The accumulation of ASX-loaded microparticles was detectable due to the property of oleoresin extract-containing ASX from *H. pluvialis* to emit yellow to red fluorescence when excited by light around 488 nm.

- ROS measurements

Cell-associated ROS levels were measured by flow cytometry using the cell permeable 2′,7′-Dichlorofluorescein diacetate (DCF-DA) fluorescent probe (Sigma-Aldrich, St. Louis, MO, USA). DCFA-DA allows one to quantitatively assess ROS in a live cell sample. This dye fluoresces green and measures hydroxyl, peroxyl, and other ROS activity within the cell. DCFA-DA passively diffuses into the cells, and the hydrolysis of the diacetate group by cellular esterase blocks the probe from leaving the cell, thus allowing for a measurement of intracellular ROS levels [71]. The deacetylated form of DCF is a highly fluorescent compound and so detectable by fluorescence.
Cells were seeded at 6×10^4 cells/well into the wells of 6-well culture plates in 3 mL growth medium and treated with 56 µg/mL ASX-loaded particles or empty particles for 5 h at 37 °C to allow phagocytosis. After washings with PBS 1x, cells were incubated with 500 µL of 50 µM DCF-DA for 30 min at 37 °C and further washed two times. Cells were then incubated with 3 ml of a solution containing 2.5mL complete medium and 0.5 mL of 0.1% (*w/w*) hydrogen peroxide in PBS 1x (final H_2O_2 concentration of ~ 0.017%) to increase intracellular ROS levels and mimic oxidative stress.

Irradiation

Irradiation of cell samples was performed with a Gammacell 40 irradiator (Atomic Energy of Canada Limited, Kanata, ON, Canada) equipped with a ^{137}Cs source. The dose rate was 0.6654 Gy/min and the measured uniformity was ±1.3% over the entire sample chamber. Both quality assurance and radiation safety are monitored by the Radiation Protection Service of the University of Verona.
Control non-irradiated ASX and cell samples were always kept in the irradiator room for the whole duration of the radiation treatments and processed in parallel with treated samples.

Analysis of Irradiated ASX-Loaded Microparticles by Thin Layer Chromatography and in J774A.1 cells

ASX-loaded microparticles were dissolved in RPMI medium and treated with a dose of 4 Gy γ-rays. The samples were then mixed with ethyl acetate (Sigma) at 1:2 volume ratio while stirring for 10 min at room temperature and finally sonicated for 1.5 h in an ultrasonic sonicator bath. The aqueous and the organic phases were then separated by centrifugation at 15,000 rpm for 5 min, the organic phase containing ASX oleoresin collected, and ethyl acetate removed by evaporation in an N2 saturated atmosphere.
Thin layer chromatography (TLC) was performed on silica gel F254 TLC aluminum sheets (Merck, Darmstadt, Germany) using as the elution solvent a mixture of hexane (60%) and acetone (40%).
In addition, irradiated ASX-loaded microparticles were administrated to J774A.1 cells to evaluate their viability for several days, and at each time point intracellular ATP was measured using the CellTiter-Glo® Luminescent Cell Viability Assay (Promega, Milan, Italy), (see cytotoxicity assays).

Effects of radiation on cells: ATP assay

J774A.1 cells were seeded at 5000 cells/well in flat-bottom 96-well plates in 200 µL RPMI medium containing either 56 µg/mL ASX-loaded particles or empty microparticles or left untreated as an additional control. Specifically, ASX-loaded and empty microparticles were administrated 2 and 1 days before radiotherapy or 1 and 2 days post radiotherapy. The cells were irradiated with a single dose of 4

Gy γ-rays and the ATP, as an indicator of cell viability, was measured 6, 8, and 12 days post exposure to radiation. All measurements were carried out at least in triplicate.

Effects of radiation on cells: statistical models and experiments

Quantification of radiation effects on J774A.1 cells was carried out as described earlier using an approach based on a novel probabilistic model [66], [72].
Briefly, the model computes the mean number of clonogens that survive irradiation as $S(D)\varepsilon\mu$, where $S(D)$ is the survival probability of clonogens (i.e., cells with self-renewing potential) irradiated with a dose D, and ε is the fraction of clonogens in a population of μ cells on average. If the cells are randomly and independently distributed, then the probability that they survive a given dose of radiation follows the Poisson distribution. Therefore, the probability that no clonogen survives is:

$$P_0 = e^{-S(D)\varepsilon\mu} \qquad (2)$$

and the probability that at least one clonogen survives is:

$$P = 1 - P_0 = 1 - \mathrm{e}^{-S(D)\varepsilon\mu}$$

Equation (2) can be straightforwardly translated into experiments by seeding the cells at different densities μ into a high number of independent wells. After ~ 20 days post-irradiation of 4 Gy, cell populations were scored as surviving or sterilized by careful microscopic analysis. These were carried out by two independent observers. The overall survival probability P was estimated as the ratio between the number of wells containing alive growing cells and the total number of seeded wells.

The survival probability of the clonogens $S(D)$ was then estimated by nonlinear fitting of Equation (2) to data. Precise estimation of this quantity, however, requires independent measurements of the multiplicative parameter ε, i.e., of the number of clonogens in the cell population. This was carried out by limiting dilution assays [66], [73]. The cells were seeded at different concentrations into the

wells of 96-well microplates. We prepared one plate for each tested cell density ranging from 1 to 20 cells/well. After 20-30 days, the wells showing absence of proliferating cell populations were counted. If the cells are randomly and independently distributed, then the fraction of negative wells (the ratio between the number of negative wells and the total number of seeded wells) obeys Poisson statistics [66], [73].

$$F_0 = e^{-\varepsilon\mu} \qquad (3)$$

where F_0 is the fraction of negative wells, μ the mean cell concentration expressed as the number of initially seeded cells per well, and ε is the fraction of clonogenic cells. The parameter ε was estimated by fitting Equation (3) to experimental data.

Measuring Bioactive TGF-β

Bioactive TGF-β was measured with a bioassay based on MFB-F11 cells [70]. These are fibroblasts cells isolated from *Tgfb1*−/− mouse embryos and stably transfected with a synthetic promoter element containing twelve CAGA boxes fused to a secreted alkaline phosphatase (SEAP) reporter gene. CAGA boxes are directly bound by activated Smad3, which, in turn, is activated through phosphorylation when TGF-β binds its receptor [70]. TGF-β is secreted by cells in association with a Latency Associated Peptide (LAP) [70] that has to be removed, e.g., by acid or heat denaturation to allow the binding of the cytokine to its receptor.
J774A.1 cells were seeded at 2000 cells/well in flat-bottom 96-well plates in 200 μL medium and treated with ASX-loaded microparticles at different days and with or without 100 ng/mL IFNγ, as described in the following *Schemes 1, 2* (P-ASX t-2, P-ASX t-1, P-ASX t0, P-ASXt+1 and P-ASXt+2 refer to treatments with ASX-loaded microparticles -2, -1, 0, +1 and +2 days with respect to IFNγ treatment. For the sake of comparison control treatments (i.e. absence of IFNγ) were named following the same code). One hundred μL of culture supernatants were carefully collected, centrifuged to remove cellular debris, and treated with 5 μL of 6M HCl solution at room temperature for 10 min to allow activation of TGF-β. The solutions were neutralized to pH 7.4 with the addition of 6M NaOH [70]. Fifty microliters of activated and neutralized supernatants were then given to MFB-F11

previously seeded at 10,000 cells/well in flat-bottom 96-well culture plates in 150 µL growth medium. After 48 h, the supernatants of MFB-F11 cultures were collected, centrifuged to remove any cellular debris, and SEAP activity measured using the chemiluminescent SEAP Reporter Gene Assay kit (Roche Diagnostic GmbH, Mannheim, Germany) following the manufacturer's instructions.
This is a chemiluminescent assay for the quantitative determination of the secreted alkaline phosphatase activity. The SEAP gene product is secreted from transfected cells (e.g., MFB-F11) and it is easily detected in a sample of culture medium, without destroying cells. It is based on the alkaline phosphate substrate (CSPD) that, after dephosphorylation by the alkaline phosphatase, results in an unstable anion that emits light at 477 nm. The light intensity is proportional to the concentration of the alkaline phosphatase. Luminescence was measured with a FLx800 Microplate reader (FLx800, Bio-Tek Instruments, Bad Friedrichshall, Germany). All measurements were carried out at least in triplicate.

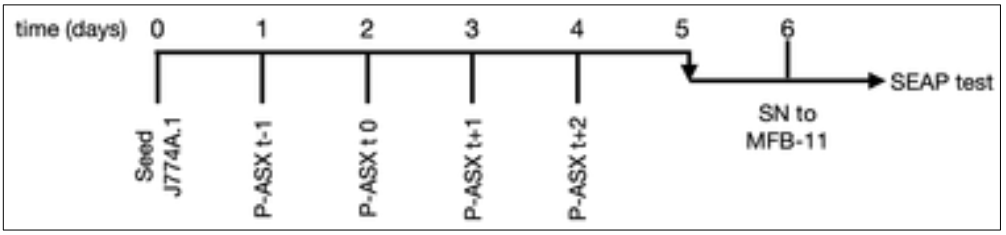

Scheme 1

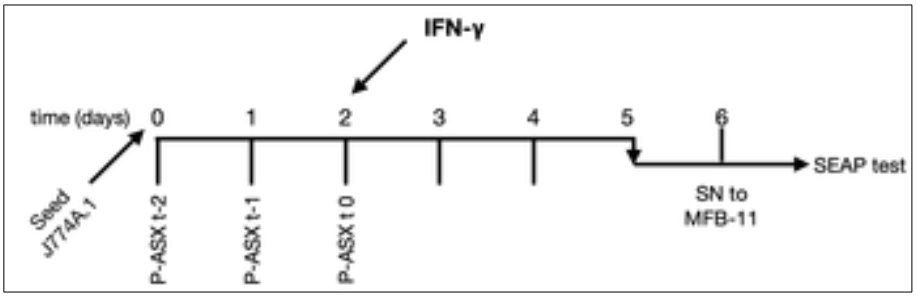

Scheme 2

Measuring TGF-β1 in J774A.1 cells supernatants by the Tgfb1 Chemi-Luminescenct ELISA assay

Aviva Systems Biology Tgfb1 Chemi-Luminescent ELISA Kit (Mouse) (OKCD03946, Avivasysbio, San Diego, CA, USA) is used for measuring the TGF-β1 in macrophage culture supernatants. This assay is based on standard sandwich enzyme-linked immuno-sorbent assay technology. An antibody specific for TGF-β1 has been pre-coated onto a 96-well plate. The supernatants were added to the wells, incubated and removed. A biotinylated detector antibody specific for TGF-β1 was added, incubated and followed by washing. Avidin-Peroxidase Conjugate was then added, incubated and unbound conjugate was washed away. Finally, a luminol substrate was added which was catalyzed by the HRP to produce light emission. The light emission was read by the luminometer (FLx800, Bio-Tek Instruments, Bad Friedrichshall, Germany). The light signal is proportional to the amount of sample TGF-β1 captured in well.
J774A.1 cells were seeded at 2000 cells/well in flat-bottom 96-well plates in 200 µL medium and treated two days after with ASX-loaded microparticles and with or without 100 ng/mL IFNγ, as described in the following *Scheme 3*. Samples were centrifuged for 20 minutes at 1,000 x g. and the particulates were removed. Samples were stored samples in aliquot at -20 °C for 24hours. One hundred µL of culture supernatants were treated with 1M HCl solution at room temperature for 10 min to allow activation of TGF-β.1and neutralized with 1.2M NaOH/0.5M HEPES, following manufacturer's instructions. 100 µL of activated samples were immediately assayed. All measurements were carried out at least in triplicate.

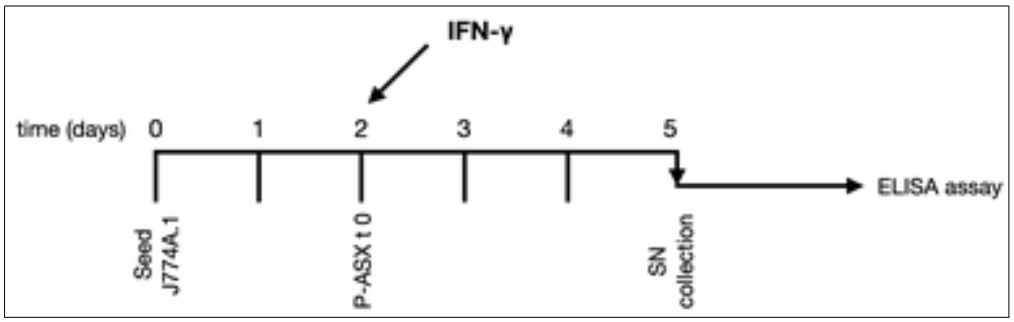

Scheme 3

Convertases activity assay

J774A.1 cells were seeded at 10,000 cells/well in a 96-well plate. Cells were cultured with and without 56 μg/ml of astaxanthin-loaded microparticles or empty microparticles. After 4 hours of incubation, cells were washed with PBS 1x and finally resuspended in the assay buffer (complete standard growth medium containing 0.25% Triton X-100, 1 mM $CaCl_2$). The convertases-specific fluorogenic substrate N-t-butoxycarbonyl-Arg-Val-Arg-Arg-7-amino-4-methylcoumarine (Boc-RVRR-AMC, Enzo Life Sciences, Farmingdale, NY, USA) was added at the final concentration of 100 μM. Fluorescence was recorded for 4 hours at 37 °C, using the FLx800 Microplate reader (excitation wavelength 360 nm; emission wavelength 460 nm). The background fluorescence of the substrate in the absence of cell extracts was measured in parallel and subtracted from the data.

Pentoxifylline powder

Pentoxifylline P1784-100G powder was provided by Sigma-Aldrich (St. Louis, MO, USA). When not specified, in all assays the final concentration of PTX was 8 μg/mL (28.7 mM), and ASX-loaded particles was 56 μg/mL.

Cytotoxicity assay of pentoxifylline in J774A.1 cells

J774A.1 cells were seeded at 5000 cells/well in 96-well culture plates in 200 μL RPMI medium containing different concentrations of PTX, from 1 μg/mL to 64 μg/mL. At each time point after treatments the intracellular ATP content was quantified using the Cell Titer Glo® Luminescent Cell Viability Assay (Promega, Milan, Italy) following the manufacturer's specification. Luminescence was measured with a FLx800 Microplate reader (FLx800, Bio-Tek Instruments, Bad Friedrichshall, Germany). All measurements were carried out at least in 4 replicates.

Phagocytosis kinetics

J774A.1 cells were seeded at 20,000 cells/well in six-well plates. Cells were incubated at 37 °C with 56 µg/mL of ASX microparticles for different days, and at each time point, phagocytosis of the microparticles was analyzed by flow cytometry. In fact, ASX oleoresin emits red fluorescence around 600 nm when excited by a blue laser light. In parallel assays, the cells were also treated with 8 µg/mL PTX.

Intracellular ROS detection

Macrophages were seeded in six-well plates at 60,000 cell/well in 3 mL of growth medium and treated with 56 mg/mL ASX particles, 8 µg/mL PTX or both for 5 h at 37 °C to allow phagocytosis. The cells were then washed twice with PBS 1×, and the medium was replaced with 500 µL of 50 µM DCF-DA. The experiment was performed as previously described in the subsection "ROS measurement", page 54.

Free radical scavenging: ABTS test

The free radical scavenging capacity of PTX was also studied using the ABTS radical cation decolorization assay which is based on the reduction of $ABTS^{+\bullet}$ radicals by antioxidants [74].
ABTS (Sigma-Aldrich, St. Louis, MO, USA) was dissolved in PBS to reach a final concentration of 7.4 mM. ABTS radical cation ($ABTS^{+\bullet}$) was produced by a chemical reaction of ABTS with 2.6 mM potassium persulfate (Sigma-Aldrich St. Louis, MO, USA). The reaction was carried out overnight, in the dark, and at room temperature. The $ABTS^{+\bullet}$ solution was then diluted in methanol to reach an absorbance of 0.75 at 734 nm. A BioTek PowerWave HT, microplate spectrophotometer (BioTek Instruments, Inc., Winooski, VT, USA) was used. Different concentrations of PTX dissolved in acetone (Sigma-Aldrich St. Louis, MO, USA) (20 µL) were allowed to react with 200 µL of $ABTS^{+\bullet}$ solution into the wells of a 96-well microplate kept in the dark. Absorbance kinetics were measured at room temperature starting at 5 min after initial mixing. All solutions were used

the same day of their preparation, and all determinations were carried out in triplicate.

Irradiation of cell samples

The cells were seeded at different densities into the wells of 96-well culture plates, 1 plate for each assayed cell density, and treated with 56 μg/mL of ASX microparticles and/or with 8 μg/mL PTX. After 24 h cells were irradiated with a dose of 4 Gy using a Gammacell40 irradiator (Atomic Energy of Canada Limited, Kanata, ON, Canada) equipped with a ^{137}Cs source. The experiment was conducted as previously described in the subsection "Effects of radiation on cells: statistical models and experiments", page 56.

Statistics

All assays were carried out in triplicate and repeated at least three times with different cell batches. Data were expressed as mean ± SE, where SE is the standard error of the mean. Statistical analyses have been performed with the open source software for statistical computing and graphics R (version 3.6.0) run under the free integrated development environment RStudio (version 1.0.153).
Nonlinear regression was carried out using the software Mathematica (v.12, Wolfram Research Inc., Champaign, IL, USA). The reduced χ^2, i.e., χ^2/df where df is the number of degrees of freedom, was used to determine the goodness of the nonlinear fits.

RESULTS

Astaxanthin and microparticles

1. Formulation of Astaxanthin-loaded WPI microparticles and empty WPI microparticles

Astaxanthin, *3,3'-dihydroxy-carotene-4,4'-dione* (refer to *Figure 15* **a)**), is a naturally red-orange xanthophyll ketocarotenoid pigment present in several marine and freshwater organisms, including micro-algae *Haematococcus fluvialis,* salmon, crustaceans, and shells of crabs. Astaxanthin exists in three different forms related to its two hydroxyl groups: 1) non-esterified form with both hydroxyl groups unmodified, 2) mono-esterified form with one hydroxyl group esterified with fatty acid, and 3) di-esterified form with both hydroxyl groups esterified with fatty acid [75]. These three forms exist in various ratios depending on the source of synthesis and it has been reported that astaxanthin extracted from *Haematococcus pluvialis* consists predominantly of the monoesterified form [75]. Astaxanthin is commercially available in oleoresin and in powder formulations (as shown in *Figure 15* **b)**, **c)**, respectively).

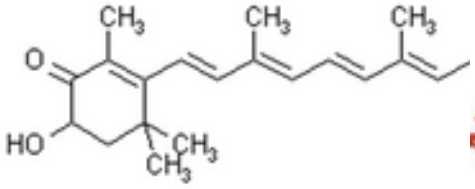

a)

b)

c)

Figure 15. ***a)*** *Chemical structure of non-esterified astaxanthin (https://it.wikipedia.org/wiki/Astaxantina).* ***b)*** *Astaxanthin-rich oleoresin (https://www.diytrade.com/china/pd/12760349/10).* ***c)*** *Astaxanthin powder (https://www.pngwing.com/en/free-png-khzet).*

We selected astaxanthin for this project because it has potent antioxidant and anti-inflammatory properties: it exhibits strong singlet oxygen/free radical scavenging activity, thereby protecting cell and biological membranes from oxidative damage. In 1991, for its biological activities it has been approved as a food supplement to promote human health [65].

We used WPIs because they are a class of natural molecules that have good functionalities and successful application in biomedical sciences and can be used to prepare microparticles loaded with bioactive compounds. Their amphiphilic properties allow them to interact with both hydrophobic and hydrophilic compounds and thus they can be used to attach drugs and ligands for targeting purposes.

The encapsulation of oleoresin rich in astaxanthin from *Haematococcus pluvialis* was carried out by an emulsification-solvent evaporation technique in which the lipophilic material is solubilized in ethyl acetate and emulsified with the water phase containing whey protein isolate (WPI), that acts as a stabilizer of oil-in-water interfaces. At the end the organic solvent is evaporated to form a core-shell particle (see scheme 4) and then, we obtained a red powder through the sprayer drying process. As control we prepared empty microparticles, that is microparticles made of whey proteins only, without loading astaxanthin oleoresin (see *Scheme 5*).

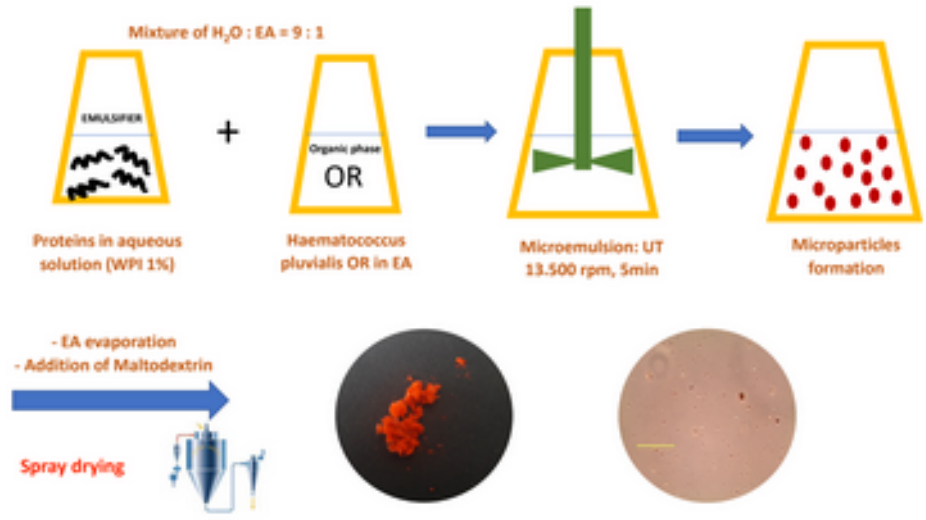

Scheme 4. Formulation of astaxanthin-loaded WPI microparticle

At the end of the process astaxanthin-loaded microparticles appear as a red powder, and they are visible at the microscope after dispersion in RPMI 1640 growth medium.

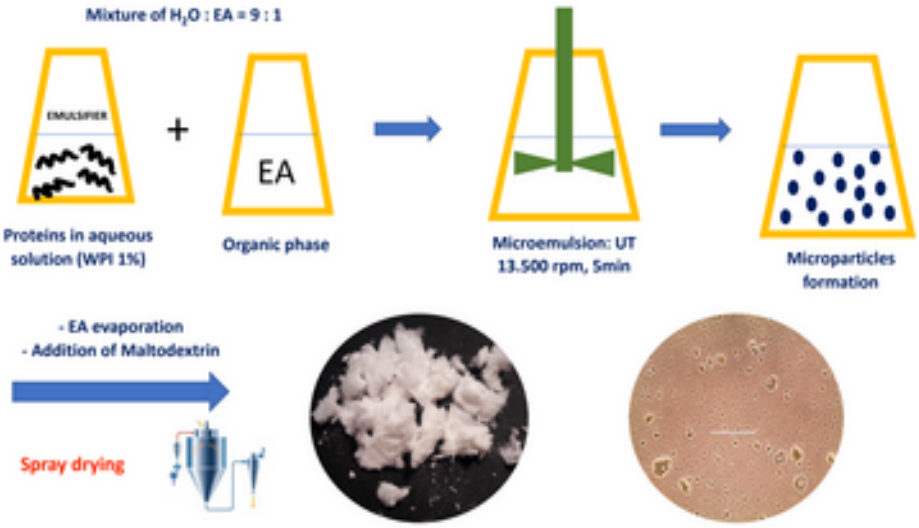

Scheme 5. Formulation of empty WPI microparticles

At the end of the process, empty microparticles appear as a white foamy powder, and they are visible after dispersion in RPMI 1640 growth medium.

2. Characterization of Astaxanthin-loaded WPI microparticles

2.1 Astaxanthin-loaded WPI particles dimension

Astaxanthin-loaded microparticles' dimension was measured by laser diffractometry, using a Malvern Mastersize 3000.
Laser diffraction spectrometry, is a widely used particle sizing technique for objects ranging from 0.02 μm to 2000 μm. This technique is applicable to powders and suspensions.
The suspension of microparticles is pumped through a measuring cell and is subsequently illuminated by a laser beam. The particles size distributions is measured from the angular variation in intensity of light scattered as the laser beam passes through the dispersed particulate sample. The angle of the laser beam and particle size have an inversely proportional relationship, where large particles scatter light at small angles relative to the laser beam and small particles scatter light at large angles. The angular scattering intensity data is then analyzed to calculate the size of the particles responsible for creating the scattering pattern, using the Mie scattering or Fraunhofer diffraction theory.
In *Figure 16*, astaxanthin-loaded particles size distribution is shown. The mean and the median particle sizes were 2.8 μm and 2.5 μm, respectively.
It is worth noting that specialized cells, such as macrophages, can internalize particles > 0.5 μm, with an optimal uptake of particles in the 1-10 μm range [76]. Thus, more than 50% of ASX particles can, in principle, be optimally phagocytised by macrophage cells.

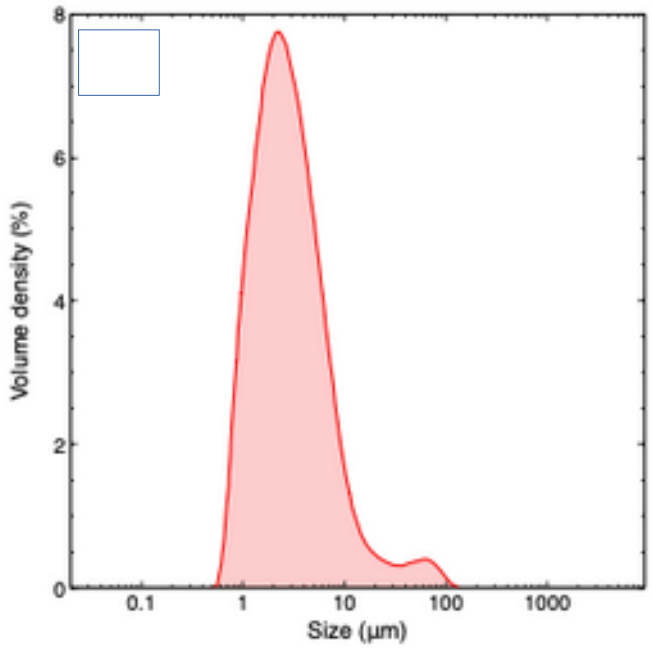

Figure 16. Distribution of particle size

2.2 Stability of astaxanthin-loaded microparticles

Astaxanthin is susceptible to oxidation, and therefore degradation, due to its highly unsaturated structure. Environmental factors such as oxygen concentration, heat, and light can influence its oxidation. The most noticeable change observed in astaxanthin degradation is the loss of its red color: its color turn from red to yellow/light brown during the degradation process.

To test the stability of astaxanthin microparticles we kept the preparation in the dark, under nitrogen atmosphere, and at -20 °C. Periodically, we measured the astaxanthin content of the particles.

Astaxanthin contributes to approximately 2.9% of the particles' mass (encapsulation efficiency) measured by spectrometry at 480 nm, after digestion of the protein particles with specific enzymes, porcine trypsin and porcine amylase to digest the protein envelope and maltodextrin respectively.

Figure 17 demonstrates that astaxanthin microparticles could be safely stored up to six months under the appropriate conditions, as the % of astaxanthin did not change in time. The ASX content was quantified through spectrophotometric analyses at 480 nm, after the enzymatic digestion of the microparticles.

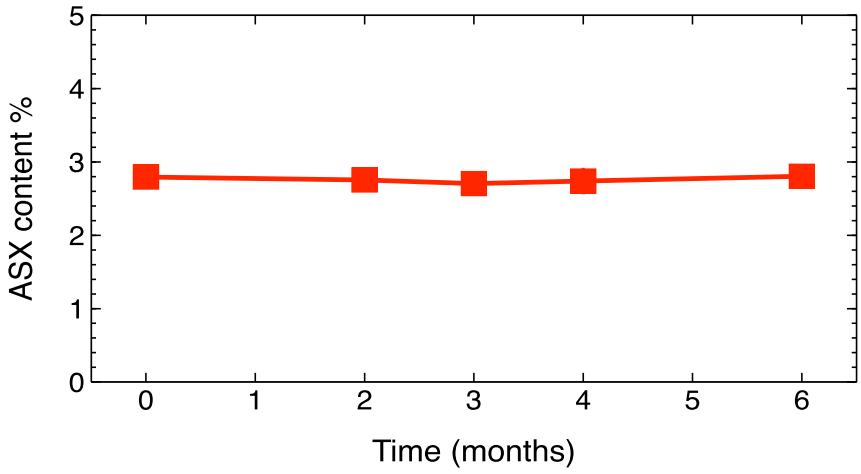

Figure 17. Storage stability of particles

2.3 Stability of irradiated astaxanthin-loaded WPI microparticles

In anticipation of future studies, we examined the chemical stability of astaxanthin encapsulated into WPI microparticles after radiation exposure, since radiolytic products might contribute to astaxanthin degradation.
It is known that irradiation can affect the composition of fat materials in saturated and unsaturated fatty acids, as well as the chemistry of fats with a high antioxidant content [77]. Since we planned to use astaxanthin-loaded microparticles with cells subjected to radiation it was important to assay whether ASX itself could resist radiation-induced degradation.
Figure 18, shows thin layer chromatography analyses of astaxanthin extracted from non-irradiated and from microparticles irradiated with a dose of 4 Gy.
We examined differences in absorption spectra of astaxanthin extracted from irradiated and non-irradiated WPI microparticles (*Figure 19*).
In both experiments, the data show that astaxanthin molecules were not degraded by radiation exposure at a single dose of 4 Gy radiations.

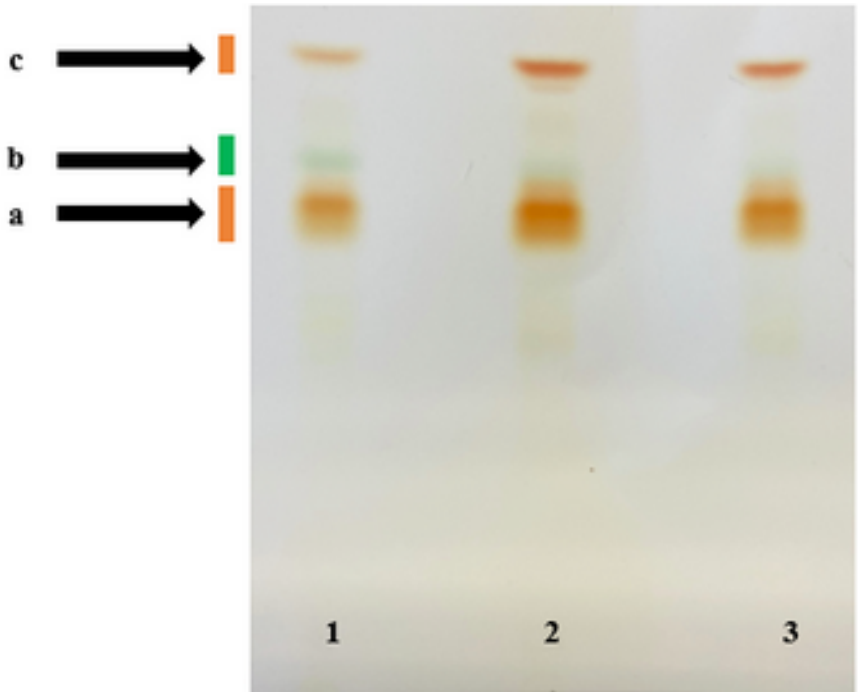

Figure 18. Thin layer chromatography of astaxanthin

*Lane 1: astaxanthin oleoresin from Haematococcus pluvialis; lane 2: astaxanthin oleoresin extracted from non-irradiated particles or from irradiated particles with a dose of 4 Gy (lane 3). Arrows show the bands corresponding to mono-esterified astaxanthin (**a**), chlorophylls (**b**), and di-esterified astaxanthin (**c**). Differences are not appreciable.*

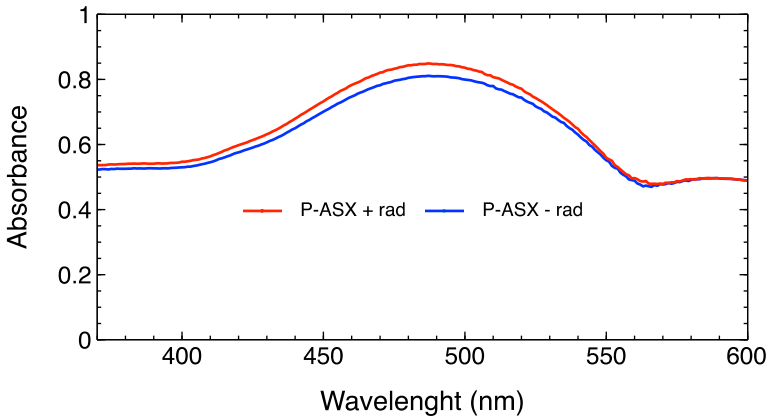

Figure 19. Absorption spectra of astaxanthin

Astaxanthin extracted from irradiated particles is shown as red line, and from non-irradiated particles in blue line. No differences between the two lines were detectable.

In vitro biological activities of
Astaxanthin-loaded microparticles

1. Phagocytosis of Astaxanthin-loaded microparticles in J774A.1 macrophages

The main goal of this project is to target specifically macrophage cells exploiting their peculiar ability to internalize micro-sized particles. All other cells, tumor cells included, are not able to uptake and digest particles of this size. In particular, in all non-phagocytic cells the optimal particle size for internalization is around 100-300 nm.

We investigated microparticles uptake by both J774A.1 macrophages and T47D tumor cells using both confocal microscopy and flow cytometry. In these assays we exploited the intrinsic fluorescence of astaxanthin oleoresin [78].

Data in *Figure 20* show that ASX-loaded microparticles accumulate in J774A.1 cells (panel **a, c**), but not in T47D cancer cells (panel **b**).

We used IFNγ, a key activator of macrophages and well known to stimulate phagocytosis in myeloid cells [79]. Treatment with IFNγ indeed increases cell associated fluorescence (flow cytometry assay) and, thus, causes higher accumulation of ASX-loaded microparticles in J774A.1 cells (panel **d**).

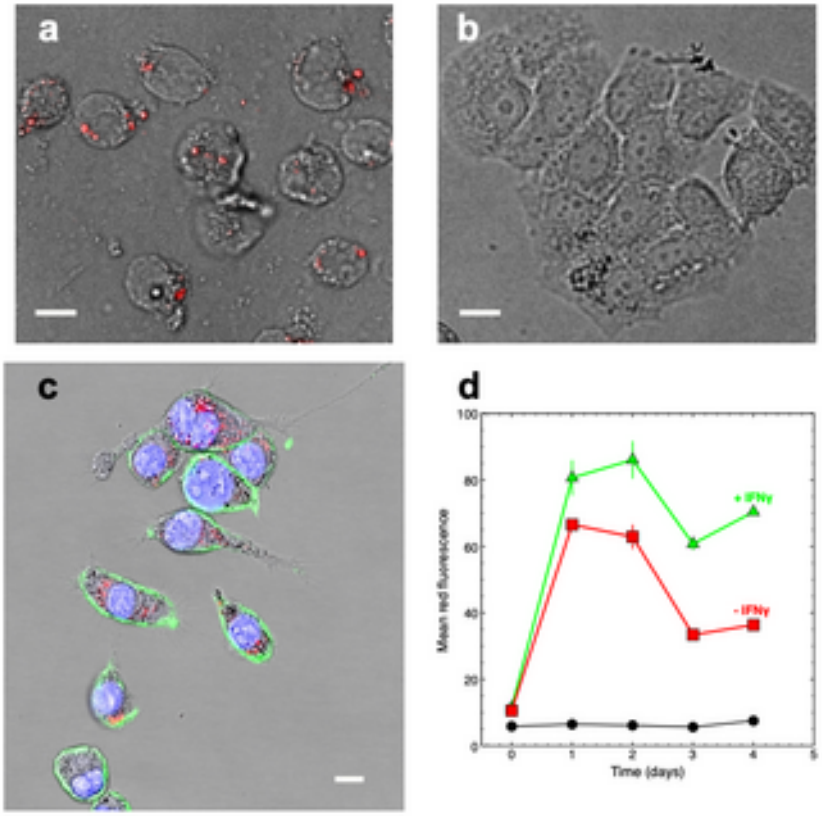

Figure 20. Phagocytosis of ASX-loaded microparticles in J774A.1 macrophages

*Raw fluorescence microscopy images obtained with J774A.1 macrophages (**a**) and T47D tumor cells (**b**). Particles loaded with ASX oleoresin are fluorescent and are found associated with macrophage cells only. (**c**) Mid optical section of J774A.1 cells obtained by confocal microscopy shows intracellular localization of ASX particles. Green fluorescence: cell membranes labelled with anti-CD11-FITC antibodies; blue fluorescence: cell nuclei; red fluorescence: ASX particles. Fluorescence signals are superimposed to the bright-field optical channel to show cell structures. In (**a**)-(**c**), a white bar 15-µm long has been added to set the microscopic length scale. Phagocytosis kinetics as measured by flow cytometry with J774A.1 cells (**d**). The data shows that ASX particle fluorescence rapidly accumulates in the cells and that treatment of the cells with INFγ further increases cell associated fluorescence. Black circles: cell autofluorescence; red squares: cells treated with 56 µg/mL ASX particles at 37 °C; green triangles: cells treated with 56 µg/mL ASX particles and 100 ng/mL INFγ at 37 °C.*

2. Cytotoxicity of Astaxanthin-loaded microparticles on J774A.1 cells

We tested if microparticles and the corresponding empty particles had unwanted effects on reducing J774A.1 cells proliferation or exhibited direct cytotoxic effects.
At the same time, we tested these microparticles in T47D cells in order to exclude any potential beneficial effects in cell proliferation.
Empty and astaxanthin-loaded microparticles were added in various doses to cell culture media containing J774A.1 macrophages. The cells were allowed to grow under the continuous presence of the various treatments and intracellular ATP levels were determined as the function of time.
Data in *Figure 21* show that both empty and ASX-loaded microparticles were not cytotoxic, but rather conferred to cells a slight growth advantage at later times of the J774A.1 cell growth kinetics.
This effect was probably due to the whey proteins used to make the particles' shell that, after phagocytosis and intracellular proteolysis, fed the cells with an extra-source of nutrients.
Indeed, this effect was not observed with non-phagocytic T47D cells that do not internalize ASX-loaded microparticles (see, e.g., *Figure 22*).

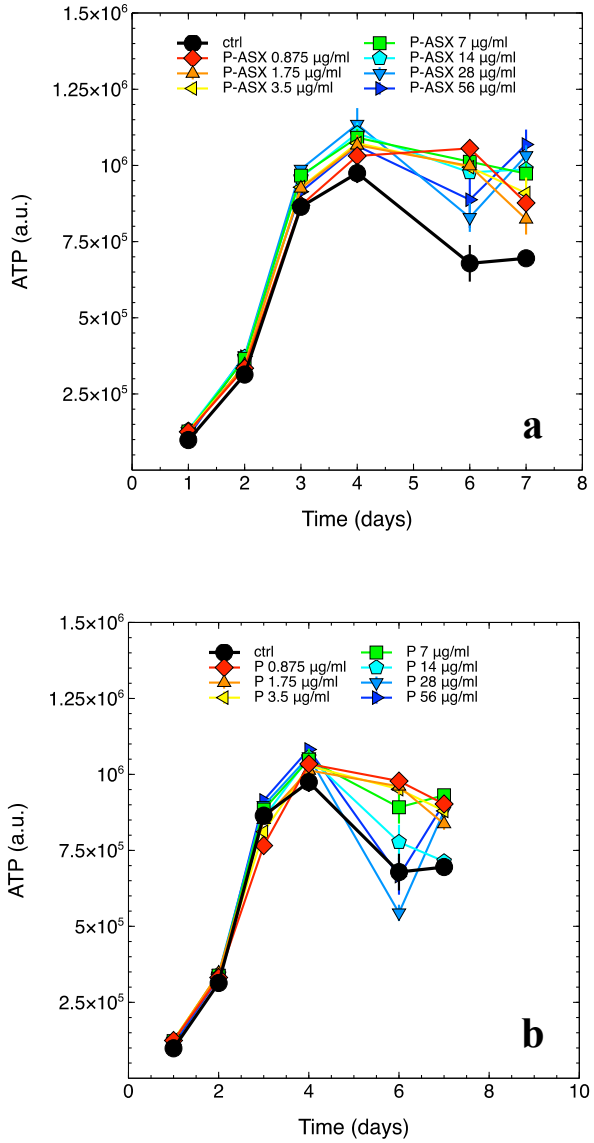

*Figure 21. Cytotoxicity of ASX-loaded (**a**) and empty microparticles (**b**)*

*ATP levels in J774A.1 cells as the function of treatment time with the indicated doses of empty (P, (**a**)) or ASX-loaded (P-ASX, (**b**)) microparticles. In both panels, the growth of untreated control cells is shown for comparison (black line and circles).*

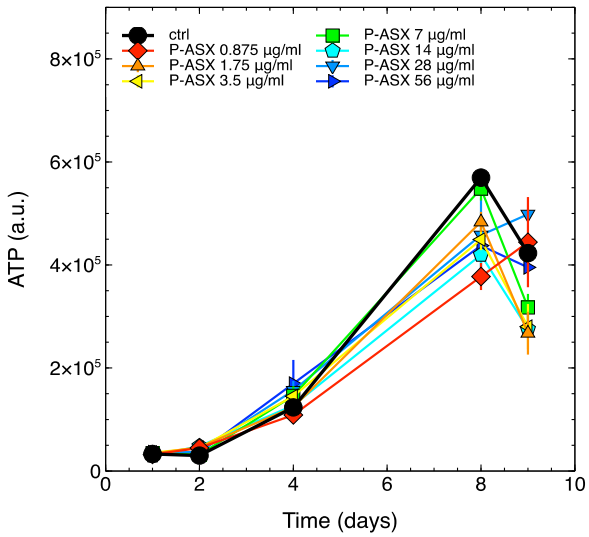

Figure 22. Cytotoxicity of ASX-loaded microparticles in T47D cells

ATP levels in J774A.1 cells as the function of treatment time with the indicated doses of ASX-loaded (P-ASX) microparticles. The growth of untreated control cells is shown for comparison (black line and circles).

In anticipation of future studies involving ASX particles exposed to radiation, the cytotoxicity of irradiated particles was measured. Previously irradiated ASX-loaded particles (with 4 Gy γ-radiations) were added into the culture medium of macrophage cells. As shown in *Figure 23*, the ATP levels in J774A.1 cells exposed to previously irradiated ASX particles were unchanged compared to untreated cells (control, black line). This demonstrates that irradiated ASX particles are non-toxic to the cells.

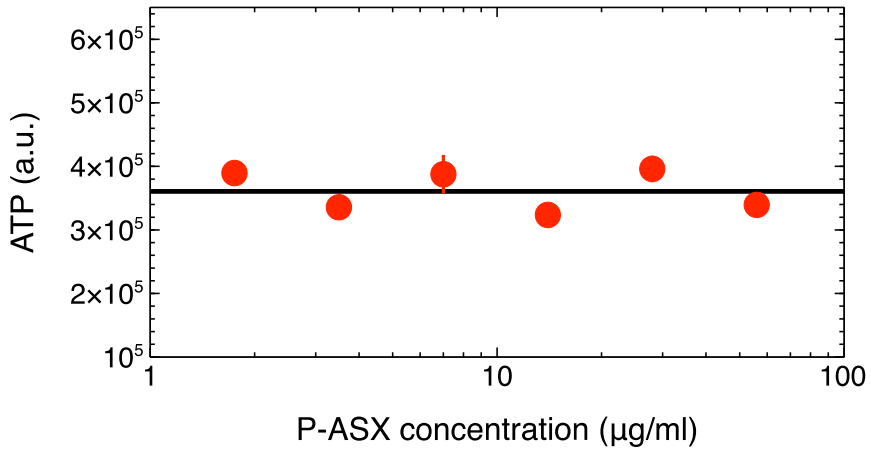

Figure 23. ATP levels for J774A.1 exposed to previously irradiated astaxanthin-loaded microparticles

Since ASX-loaded microparticles were not cytotoxic, the particles at the highest assayed dose of 56 µg/mL were used for the following experiments.

3. Effects of Astaxanthin-loaded microparticles on intracellular ROS levels

We developed a flow cytometry assay to measure at the single cell level the activity of ASX entrapped in WPI particles on intracellular ROS.
Macrophages, including J774A.1 cells, produce normally intracellular ROS and to increase/modulate the accumulation of ROS, we treated J774A.1 cells with hydrogen peroxide (H_2O_2).
Exposure to hydrogen peroxide is a widely used procedure to cause oxidative damage/stress in cellular models, as exogenous hydrogen peroxide can penetrate into biological membranes and enhance the formation of other reactive oxygen species. The Fenton's reaction between H_2O_2 and Fe^{2+} ions generates the highly reactive OH radical and is thought to be the main mechanism for oxidative damage [80].
Intracellular ROS in J774A.1 were detected using the fluorescent DCF-DA probe as described in the *Materials and Methods* section.
Treatments with a single administration of 56 μg/mL astaxanthin-loaded microparticles reduced intracellular ROS accumulation due to H_2O_2 by ~ 75% of control untreated cells (see *Figure 24*).
Thus, phagocytosis of ASX particles protects macrophage cells from oxidative stress.

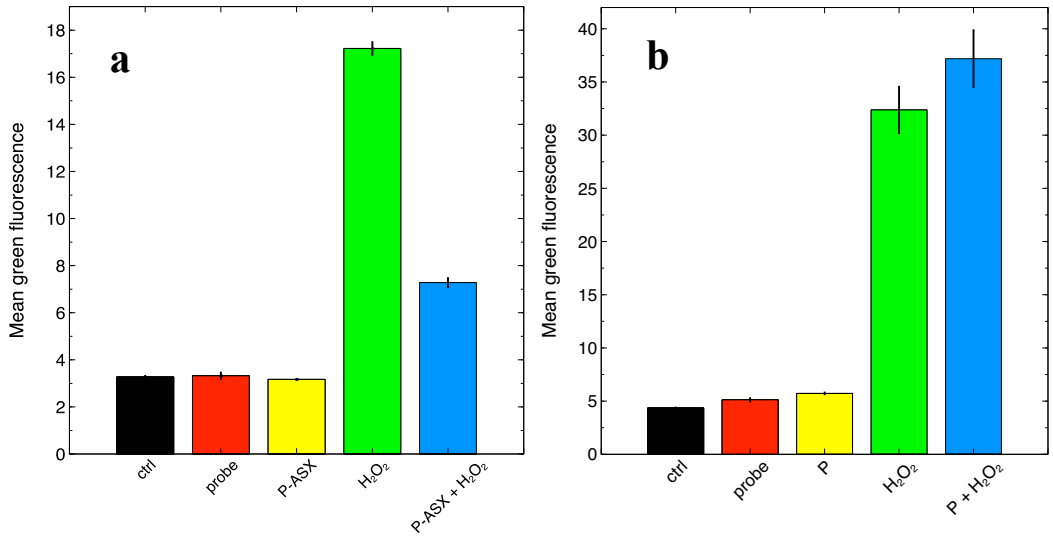

Figure 24. Determination ROS levels at the single cell level by flow cytometry using the fluorescent probe DCF-DA

***(a)** Experiments carried out with ASX-loaded microparticles (P-ASX). The reported differences are statistically significant ($F_{4,20} = 5828$, $p < 2 \times 10^{-16}$, ANOVA test). ASX-loaded microparticles can significantly reduce intracellular H_2O_2-induced ROS accumulation ($p < 10^{-8}$, Tukey-HSD post-hoc test). In both panels, the labels refer to: ctrl, cell autofluorescence; probe, fluorescence measured with cells loaded with the DCF-DA probe; P or P-ASX, fluorescence measured from cells loaded with DCF-DA and treated with empty (P) or ASX-loaded (P-ASX) microparticles; H_2O_2, fluorescence measured from cells loaded with DCF-DA and treated with H_2O_2; P or P-ASX + H_2O_2, fluorescence measured from cells loaded with DCF-DA, treated with H_2O_2 and with empty (P) or ASX-loaded (P-ASX) microparticles. (**b**) Experiments carried out with cells treated with empty microparticles (P). Overall, the reported differences are statistically significant ($F_{4,20} = 284.5$, $p < 2 \times 10^{-16}$, ANOVA test). H_2O_2 significantly increases intracellular ROS with respect to controls, but ROS levels in cells treated with H_2O_2 and empty particles were not statistically different from cells treated with H_2O_2 alone, suggesting that, within the power of the measurement, empty particles cannot reverse intracellular H_2O_2-induced ROS accumulation ($p = 0.85$, Tukey-HSD post-hoc test).*

4. Effect of radiation and of Astaxanthin-loaded microparticles treatment on J774A.1 cells

As shown above, ASX microparticles can protect J774A.1 macrophages from oxidative stress. Intracellular ROS levels also increase as a consequence of water radiolysis in irradiated cells. We, therefore, assayed whether ASX particles could protect J774A.1 from radiation damage. The clonogenic assay is the standard quantitative test in experimental radiation biology [81], but, for their biological characteristics, we were unable to perform this assay with J774A.1 macrophages despite several attempts (*Figure 25*).

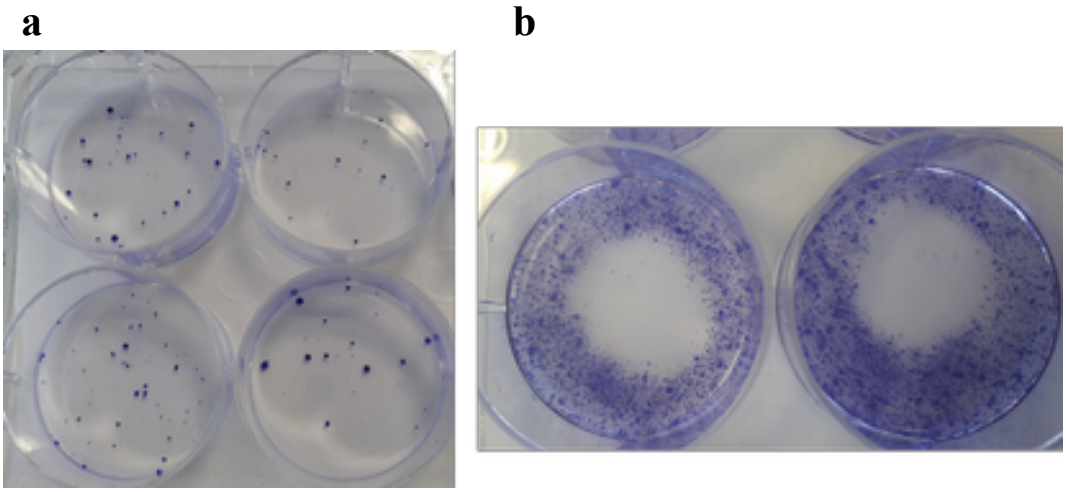

*Figure 25. Clonogenic assay performed with T47D cells (**a**) and J774A.1 cells (**b**)*

J774A.1 cells do not form measurable colonies and therefore the clonogenic assay could not be performed with these cells.

It was first investigated if ASX microparticles could confer to irradiated J774A.1 a selective advantage in long-term growth assays. As shown in *Figure 26*, treatment with ASX—but not empty microparticles—provides a growth advantage to irradiated macrophages as evaluated by ATP content of the cell populations. The maximum effect is observed for cells treated with ASX microparticles 1 day before radiation treatment (*Figure 26*).The effect appears to be transient because

in these assays cells are cultured in a closed environment, and, at later times, the toxic effects caused by nutrient deprivation and accumulation of waste molecules in growth media dominate cell growth kinetics.

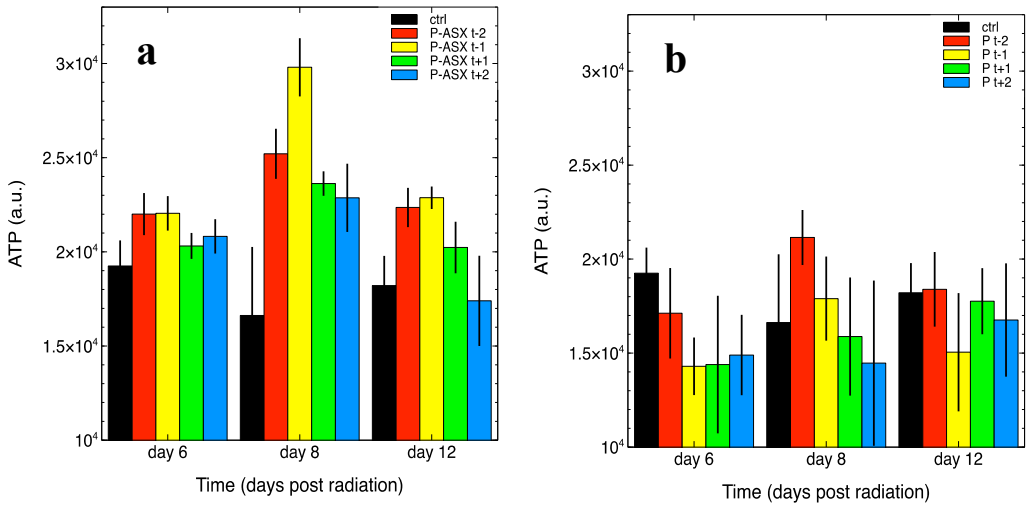

Figure 26. Effects of 56 μg/mL of ASX-loaded microparticles and empty microparticles on irradiated J774A.1 cells through the quantification of the metabolically active cells (ATP assay).

*Cells were either left untreated (ctrl) or treated with ASX-loaded microparticles (P-ASX, (**a**) or with empty particles (P, (**b**))) 2 and 1 days before radiotherapy (−2 and −1, respectively, in both panels) or 1 and 2 days after radiotherapy (+1 and +2, respectively, in both panels) with a dose of 4 Gy γ-rays. ATP was then measured at the indicated time points.*

The radio-protective effects of ASX particles was also quantified using a recently-developed experimental approach to measure the survival probability of irradiated cells [72]. The method is based on a probabilistic model of the cell survival after radiotherapy (see the *Materials and Methods* section) and, importantly, it takes into account the self-renewing (i.e., clonogenic) potential of non-irradiated cell clones which must be determined in independent limiting dilution assays. This is an important point in the present case because, as shown in *Figure 21 (**a**)*, ASX microparticles can positively influence cell survival of non-irradiated cells. This is also confirmed in *Figure 27* that shows a slightly higher, albeit not significant,

clonogenic potential of cells treated with ASX microparticles (37.7 ± 3.3%) as compared to control untreated cells (33.5 ± 2.9%).
Nonlinear fit of the data with Equation (2) indicates that the surviving fraction $S(D)$ of cells exposed to 4 Gy γ-rays and treated with ASX microparticles is ~ 1.53 times higher with respect to that of control cells. Thus, ASX microparticles confer a slight but significant survival advantage to cells irradiated with a dose of 4 Gy γ-rays.
Experiments shown in *Figure 27* require a careful measurement of the number of cells seeded in each well of multiwell culture plates that are subjected to radiation. Since ASX microparticles affect cell growth (also see *Figure 21* (***a***)), particles were added to cells just before radiation treatments. As shown in *Figure 26 (**a**)*, this might not be the best choice as ASX microparticles appear more efficient in protecting cells if given one day before radiation.

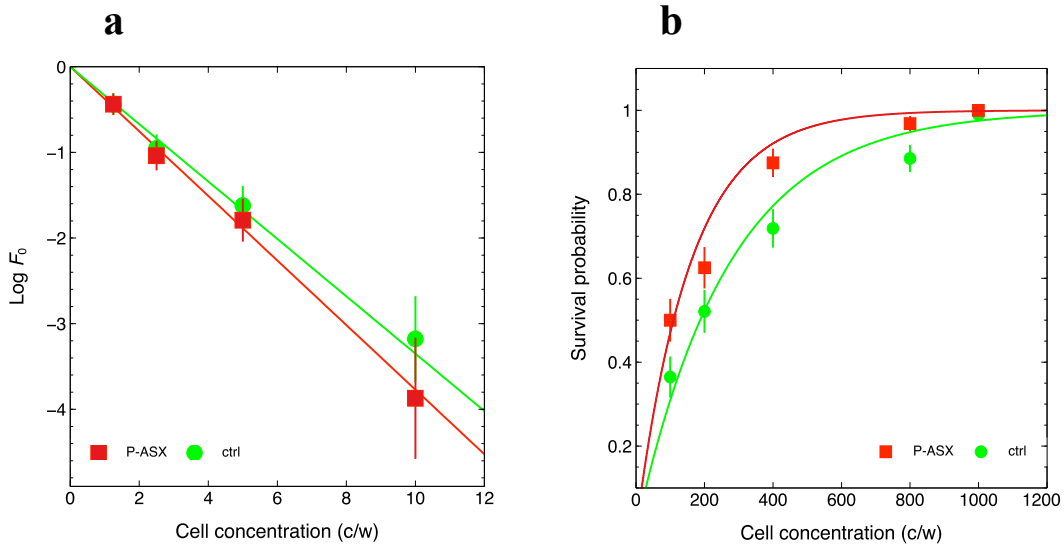

Figure 27. Effects of 56 µg/mL of ASX-loaded microparticles on irradiated J774A.1 cells

*(**a**) Limiting dilution assays with untreated cells (ctrl) or with cells treated with ASX microparticles (P-ASX). Linear regression weighted on experimental error of log-transformed data with the linearised model described by Equation (3) allows to estimate the clonogenic potential of the cells (i.e., parameter ε in Equation (3)) under both treatment conditions. The results are: ctrl, εctrl = 0.335 ± 0.029, r2 = 0.99; P-ASX, εP-ASX = 0.377 ± 0.033, r2 = 0.99. Linear regression of all data factorised per treatment with an extended linear model let us to conclude that the difference between εctrl and εP-ASX is not statistically significant (p = 0.148). (**b**) Survival probability of independent populations of untreated (ctrl) or ASX microparticles (P-ASX) treated cells using the method described in the Materials and Methods section and developed in Reference [72].*

Nonlinear fits of experimental data with Equation (2) allows to estimate the fraction of the cells surviving radiation treatments (here a 4 Gy dose of γ-rays). The results are: ctrl, S(D)ctrl = 0.0110 ± 0.0007, goodness-of-fit statistics $\chi^2/d\,f = 2.05$; P-ASX, S(D)P-ASX = 0.0168 ± 0.001, goodness-of-fit statistics $\chi^2/d\,f = 2.9$. The difference between S(D)ctrl and S(D)P-ASX was statistically significant ($Z = 4.49$, $p = 3.5 \times 10^{-6}$).

5. Secretion of bioactive TGF-β by macrophages treated with ASX-loaded microparticles

Secretion of active TGF-β in culture supernatants of J774A.1 cells was first evaluated using a bioassay based on MFB-F11 cells [70]. These cells were kindly provided by the laboratory of Tony Wyss-Coray at Stanford University (CA, USA) that developed a new cell-based reporter assay for measuring the bioactive TGF-β.

MFB-F11 cells have been engineered to activate secreted alkaline phosphatase (SEAP) transcription and secretion in response to TGF-β binding to its receptor [70], specifically mouse embryonic fibroblasts from *TGFb1*$^{-/-}$ mice were stably transfected with a synthetic promoter containing twelve CAGA boxes fused to the SEAP reporter gene.

Living cells release a protein complex formed by TGF-β and LAP, and this complex must dissociate to allow TGF-β to bind its receptor and start the intracellular signaling cascade in target cells. Dissociation of the protein complex is usually obtained by acid denaturation of the LAP peptide [70]. Thus, SEAP quantification in the culture supernatants of MFB-F11 cells is proportional to the amount of active TGF-β secreted by J774A.1 cells.

J774A.1 macrophages constitutively secrete TGF-β [82]. Indeed the supernatants of J774A.1 cells, only when subjected to acid denaturation, induces SEAP release by MFB-F11 cells, thus revealing TGF-β-LAP complex secretion by J774A.1 cells (*Figure 28*).

Treatment of J774A.1 macrophages with ASX-loaded microparticles significantly reduces the accumulation of bioactive TGF-β in culture supernatants. IFNγ (interferon gamma) does not improve the release of TGF-β-LAP complexes from J774A.1 cells (*Figure 29*). However, as also shown in *Figure 20*, IFNγ can increase cellular uptake of ASX-loaded microparticles and, as a consequence, their effect on TGF-β secretion. Indeed, a significantly greater reduction of bioavailable TGF-β is observed when J774A.1 cells are treated with both IFNγ

and ASX microparticles (*Figure 28*). In addition, a higher concentration of IFNγ anticipates the inhibitory effect of ASX microparticles on bioactive TGF-β secretion. Of note, empty particles do not significantly affect TGF-β secretion either in untreated J774A.1 cells ($p = 0.29$, one-way ANOVA followed by Tukey-HSD post-hoc test) and in cells treated with 50 ng/mL IFNγ ($p = 0.12$, one-way ANOVA followed by Tukey-HSD post-hoc test).

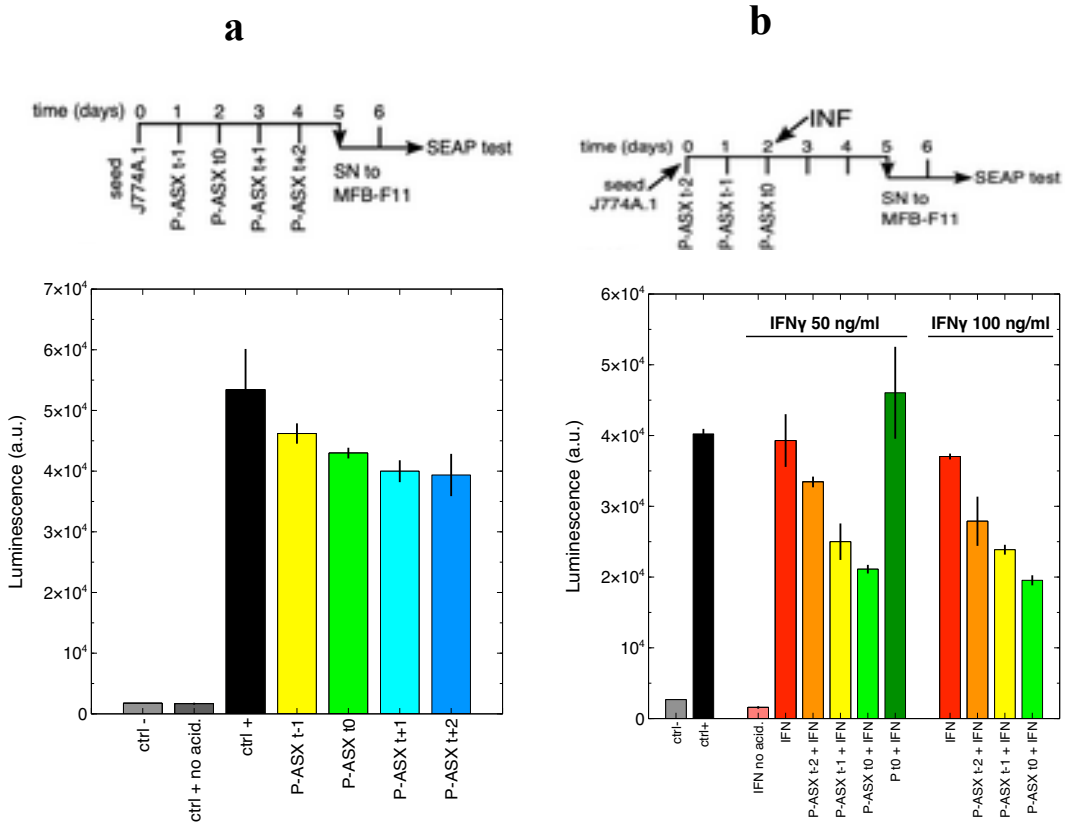

Figure 28. Treatment of J774A.1 macrophages with ASX-loaded microparticles

***(a)** The cells were treated with ASX microparticles following the scheme sketched on top of the panel. At day 5 the supernatants from J774A.1 cells were administered to MBF-F11 cells and after 2 more days secreted alkaline phosphatase (SEAP) activity in the culture supernatants (SN) of these cells was measured. Bar labels refer to: ctrl -, untreated MBF-F11 cells; ctrl +, MBF-F11 cells treated with J774A.1 cells supernatants subjected to acid denaturation (to dissociate the TGF-β-LAP complex and activate the cytokine); ctrl + no acid, in this case J774A.1 cells supernatants are not subjected to acid denaturation; P-ASX (t−1, t0, t+1, t+2), treatment of J774A.1 cells with ASX microparticles at the time*

*points indicated on top of the panel. The differences in the data shown in this panel are statistically significant ($F_{5,11}$ = 41.8, p = 8.6 × 10^{-7}, ANOVA test). Only ASX particles given at day 3 and 4 after J774A.1 cell seeding significantly inhibit TGF-β secretion (p = 0.027 and p = 0.02, respectively, Tukey-HSD post-hoc test). (**b**) The cells were treated with ASX microparticles following a slightly modified scheme with respect to that described above. As shown in the diagram on top of the panel, at day 2 the cells were also treated with two different concentrations of IFNγ (interferon gamma). Inhibition of TGF-β secretion by ASX microparticles is greater than that observed in panel (**a**), an effect that is probably correlated to the higher uptake of the particles in IFNγ-treated macrophages (see, e.g., Figure 20). Bar labels are as in panel (**a**) with the following additions: IFN no acid, MBF-F11 cells treated with supernatants, not subjected to acid denaturation, from IFNγ-stimulated J774A.1 cells; IFN, MBF-F11 cells treated with acid-denatured supernatants from IFNγ-stimulated J774A.1; Pt0 + IFN, MBF-F11 cells treated with acid-denatured supernatants from J774A.1 cells treated with IFNγ and empty microparticles. Treatment with IFNγ at 50 ng/mL does not significantly increase bioactive TGF-β secretion by J774A.1 cells but significantly increases the inhibitory effect of ASX microparticles administered at day 1 and 2 after J774A.1 cell seeding (p = 0.006 and p = 0.001, respectively, Tukey-HSD post-hoc test). Treatment with IFNγ at 100 ng/mL do not significantly increase bioactive TGF-β secretion by J774A.1 cells but significantly increases the inhibitory effect of ASX microparticles administered at day 0, 1, and 2 after J774A.1 cell seeding (p = 0.04, p = 0.003 and p = 0.0006, respectively, Tukey-HSD post-hoc test).*

TGF-β1 secretion was also evaluated in J774A.1 cells by a chemiluminescent ELISA assay to further confirm the previous results obtained with the biological assay.

Treatment of J774A.1 macrophages with ASX-loaded microparticles does not significantly reduce the accumulation of bioactive TGF-β1 in culture supernatants. Moreover, the administration of both IFNγ and ASX-loaded microparticles does not decrease the release of the cytokine (p = 0.97, one-way ANOVA followed by Tukey-HSD post-hoc test).

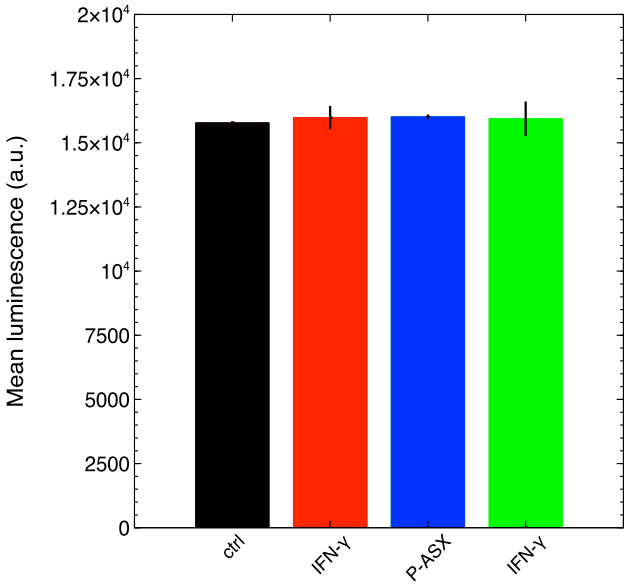

Figure 29. Quantification of TGF-β1 by the chemiluminescent ELISA assay

The cells were treated with either IFNγ, or ASX microparticles, or both following the scheme sketched on top of the panel. At day 5 the supernatants (SN) from J774A.1 cells were collected and the quantification of TGF-β was performed. Bar labels refer to: ctrl, untreated cells; IFNγ, cell treated with 100ng of IFNγ; P-ASX, cells treated with 56 μg/mL of astaxanthin-loaded microparticles; P-ASX + IFNγ, cell treated with both IFNγ and ASX-loaded microparticles. Treatment with IFNγ at 100 ng/mL does not significantly increase bioactive TGF-β1 secretion and moreover the treatments with ASX microparticles and the combination of ASX microparticles and IFNγ does not alter significantly TGF-β secretion. (p_{IFN} = 0.975, p_{ASX} = 0.964, $p_{ASX+IFN}$ = 0.987, Tukey-HSD post-hoc test).

To better analyze these controversial results, the intracellular processing of TGF-β was investigated.

TGF-β is synthesized as a single pro-peptide molecule that is then processed along the intracellular secretory pathways by furin convertase, a proteolytic enzyme that cuts the pro-peptide to form a complex made of mature TGF-β and the LAP peptide [83]. The unprocessed peptide can be recognized by monoclonal antibodies but it is not bioactive on target cells.

Several plant diterpene molecules inhibit furin [84], and it is tempting to speculate that ASX might inhibit it, as well being a tetraterpene molecule.
To test whether astaxanthin could inhibit convertase, we used the convertase-specific fluorogenic substrate Boc-RVRR-AMC (refer to *Figure 30*).
J774A.1 macrophages treated with ASX-loaded microparticles show significant inhibition of protein convertase activity (*Figure 31*). The results indicate that the reduction of active TGF-β secretion might indeed be explained by ASX inhibition of intracellular convertases. It is worth noting that the experiments shown in *Figure 31* might underestimate the inhibitory activity of ASX (see the *Discussion* section for further comments on this point).

a

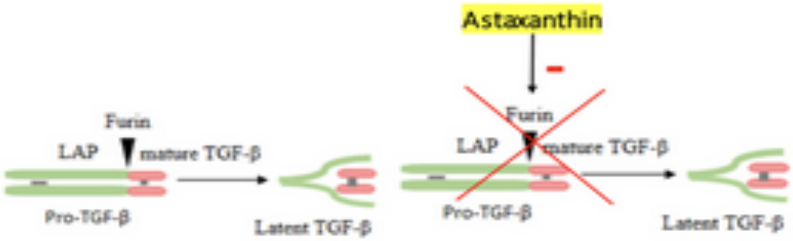

b

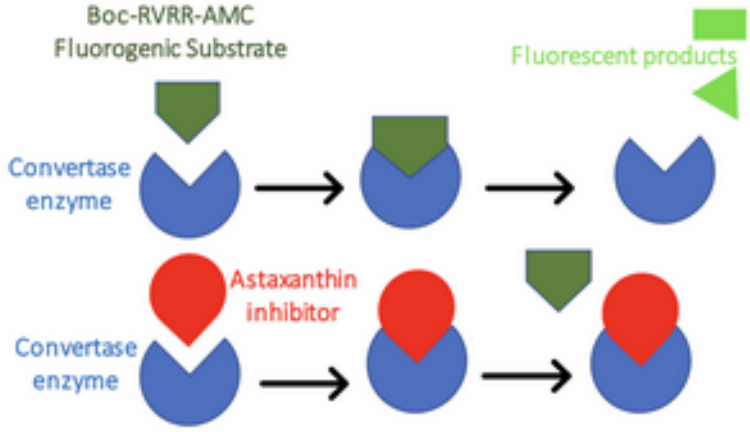

*Figure 30. Schematic representation of hypothetical inhibition of furin by astaxanthin (**a**), and inhibition of protein convertase activity by time-dependent cleavage of the convertases-specific fluorogenic substrate Boc-RVRR-AMC (**b**).*

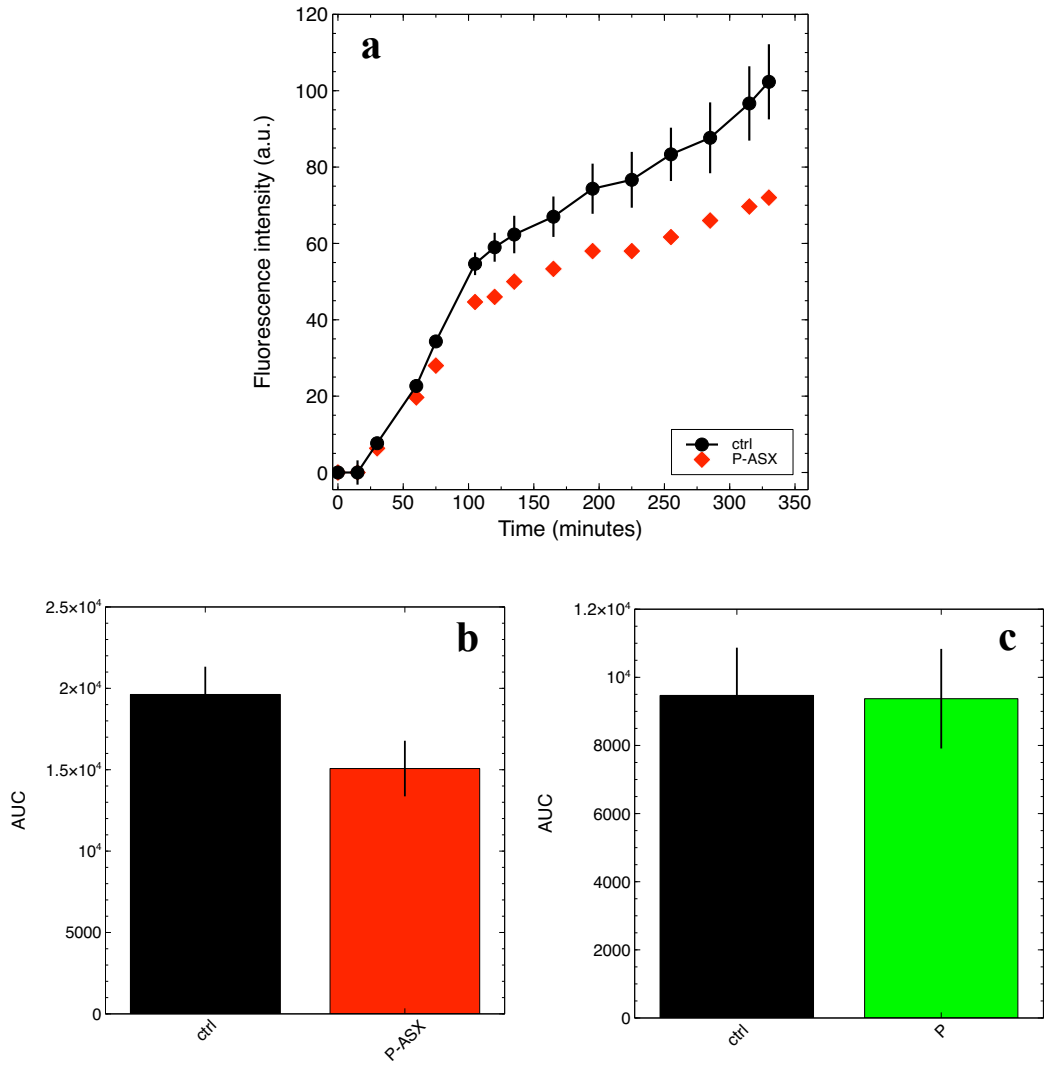

Figure 31. ASX-loaded microparticles inhibit the activity of intracellular convertases in J774A.1 cells

*The activity of intracellular convertases was measured in cell extracts using the convertases-specific fluorogenic substrate Boc-RVRR-AMC. (**a**) Fluorescence kinetics measured for cells treated with ASX-loaded microparticles (P-ASX) or left untreated (ctrl). (**b**),(**c**) The overall amount of substrate conversion by convertases was quantified as the area beneath the fluorescence kinetics curves (AUC) as those shown in (**a**) and obtained in independent assays with cells treated with ASX-loaded particles (P-ASX, (**b**)) or empty particles (P, (**c**)). ASX treatments significantly inhibit convertases activity ((**b**), p = 0.028 Student-t test), an effect that is not observed for empty particles ((**c**), p = 0.94 Student-t test).*

Combination treatments of
Astaxanthin-loaded microparticles and Pentoxifylline

1. Cytotoxicity of Pentoxifylline on J774A.1 macrophages

To the best of our knowledge no information is available on the safety of pentoxifylline (PTX) in J774A.1 macrophages. It was therefore assayed whether PTX could alter the growth kinetics of these cells. Intracellular ATP content was measured at different time points of the growth curve obtained with independent cell populations continuously exposed to different PTX concentrations, and the results are shown in *Figure 32*.
PTX, at all assayed concentrations, did not alter the proliferation of J774A.1 cells.

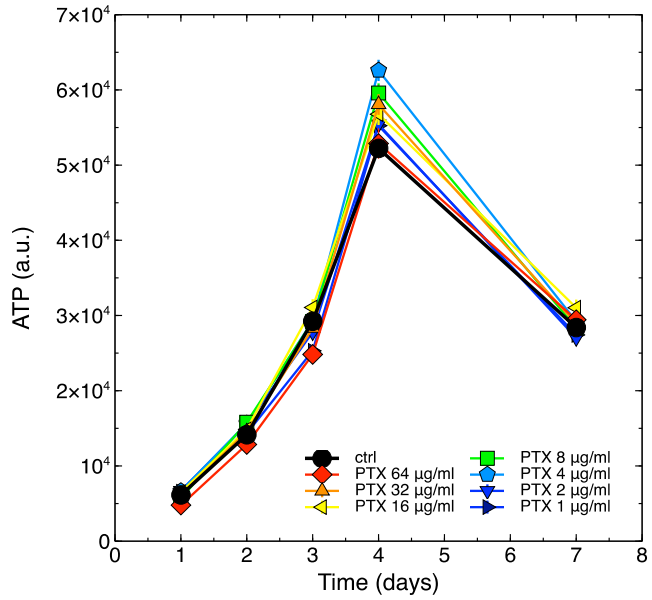

Figure 32. Growth kinetics of J774A.1 cells exposed to different concentrations of PTX

Pentoxifylline was administered to the cells at the indicated final concentrations at the beginning of the growth assays, and ATP was then measured. Cell populations were also left untreated as controls (black circles marked as ctrl). The error bars correspond to calculated standard errors and are not clearly visible in this figure because they are masked by the symbols (min. and max. coefficient of variation, CV = 100∗SE/mean, 0.75% and 6.0%, respectively).

2. Pentoxifylline does not alter phagocytosis of Astaxanthin-loaded microparticles in J774A.1 cells

Central to our treatment strategy is the idea that antioxidant molecules can be delivered specifically to macrophages (and other phagocytes) if loaded into particles of appropriate size that can be taken up by these cells through phagocytosis.
Bessler *et al.* [85] reported that PTX inhibit the phagocytosis induced by latex particles (~ 0.8 µm diameter) in monocytes and polymorphonuclear leukocytes in a dose-dependent manner. The critical PTX concentration at which the inhibitory activity became significant was 10 µg/mL [85].
We therefore assayed whether a slightly lower PTX concentration, namely 8 µg/mL, could inhibit phagocytosis of ASX microparticles in J774A.1 cells.
Figure 33 shows that 8 µg/mL PTX did not inhibit phagocytosis of ASX microparticles in J774A.1 macrophages.

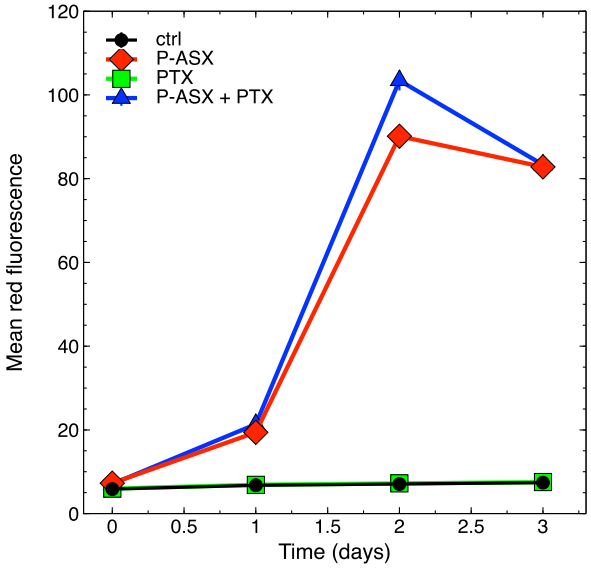

Figure 33. Phagocytosis kinetics of ASX microparticles

The cells were exposed to ASX microparticles (P-ASX) and were either treated or left untreated with PTX at a final concentration of 8 µg/mL. Phagocytosis was measured by flow cytometry thanks to the fluorescence emission of the ASX-containing oleoresin encapsulated into the protein particles. In this figure cell autofluorescence of control untreated cells (ctrl) or of cells treated with PTX only is also shown. Values are given as

mean ± SE. The error bars correspond to calculated standard errors and are not clearly visible in this figure because they are masked by the symbols (min. and max. coefficient of variation, CV=100∗SE/mean, 0.45% and 5.1%, respectively).

3. Effects of PTX and ASX microparticles on intracellular ROS levels

PTX has been reported to have antioxidant activity [55], and more importantly to have a synergic effect with other antioxidants, such as vitamin E, in combined treatments [86]. We previously showed that ASX microparticles could significantly reduce intracellular ROS levels in J774A.1 cells treated with H_2O_2 to induce oxidative stress [66], and we therefore wondered whether PTX could also improve the effects of ASX particles. *Figure 34* shows that the intracellular ROS levels in J774A.1 macrophages decreased when PTX and ASX microparticles were given alone or in combination.

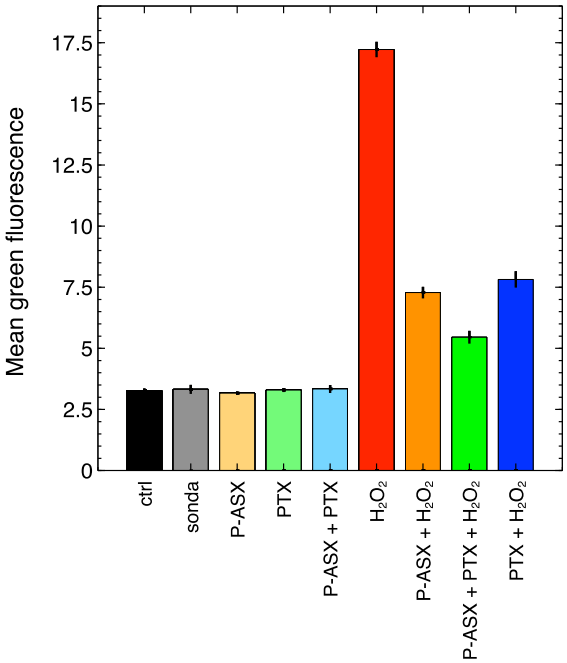

Figure 34. Effects of PTX and ASX-loaded microparticles on intracellular ROS as evaluated by flow cytometry with the DCF-DA probe

Cell fluorescence was almost equal for untreated cells (cell autofluorescence, ctrl) or cells treated with DCF-DA (probe), ASX microparticles (P-ASX), PTX or with P-ASX and PTX. Cell fluorescence significantly increased in cells loaded with DFC-DA and treated with H_2O_2, but treatments with PTX and ASX microparticles given alone or in combination significantly suppressed the effects of H_2O_2 (see Figure 35 and Table 5 for statistical details). Data are the mean ± SE of 4 independent samples.
Two-way ANOVA analyses indicated that PTX and ASX microparticles significantly interacted to reduce the intracellular ROS levels induced by hydrogen peroxide treatment in J774A.1 cells (Figure 35 and Table 5).

Two-way ANOVA analyses indicated that PTX and ASX microparticles significantly interacted to reduce the intracellular ROS levels induced by hydrogen peroxide treatment in J774A.1 cells (*Figure 35 and Table 5*).

Table 5. Two-ways ANOVA analysis of the antioxidant effects of PTX and ASX microparticles given alone or in combination to J774A.1 cells

Treatment	**df** [1]	**SS**	**MS**	***F***	***p***
P-ASX	1	97.4	97.4	381.9	1.8×10^{-10}
PTX	1	122.1	122.1	478.9	4.9×10^{-11}
PTX and P-ASX	1	41.2	41.2	161.4	2.6×10^{-8}
Error	12	3.1	0.255		
Total	15	263.8			

1 df, degrees of freedom; SS, sum of squares; MS, mean squares.

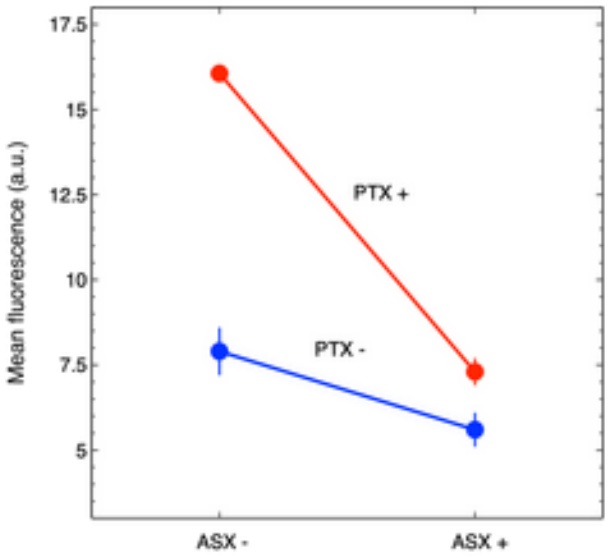

Figure 35. Graphical representation of the synergic effect of PTX and ASX microparticles on intracellular ROS reduction in J774A.1 cells

The two lines would be expected to be parallel if there were no synergic effects [84]. Formally, synergism is demonstrated by two-ways ANOVA statistical analysis (see Table 5).

4. Radical-scavenging activity of PTX and ASX-containing extract in a cell-free assay

Data in *Figures 34, 35* and *Table 5* indicate that PTX is an intracellular ROS scavenger. We further investigated its activity in a well-controlled cell-free assay, i.e., ABTS assay, in the attempt to explore whether the drug could react with free radicals on its own. As the control we used ASX-containing extracts that have an acknowledged antioxidant activity [88]. This result is somewhat expected since in a previous study PTX showed poor scavenging activity using DPPH assay [74]. This behavior is probably due to the lack of hydroxyl groups on PTX structure that underpin the scavenging activity of other potent antioxidants, such as vitamin E and phenolic compounds [89].

Figure 36 shows that PTX had no radical-scavenging activity at the assayed concentrations. We therefore concluded that the effects observed for PTX on

intracellular ROS levels likely depend on the ability of the drug to activate cellular detoxifying pathways (see also the *Discussion* section for a further examination of this point).

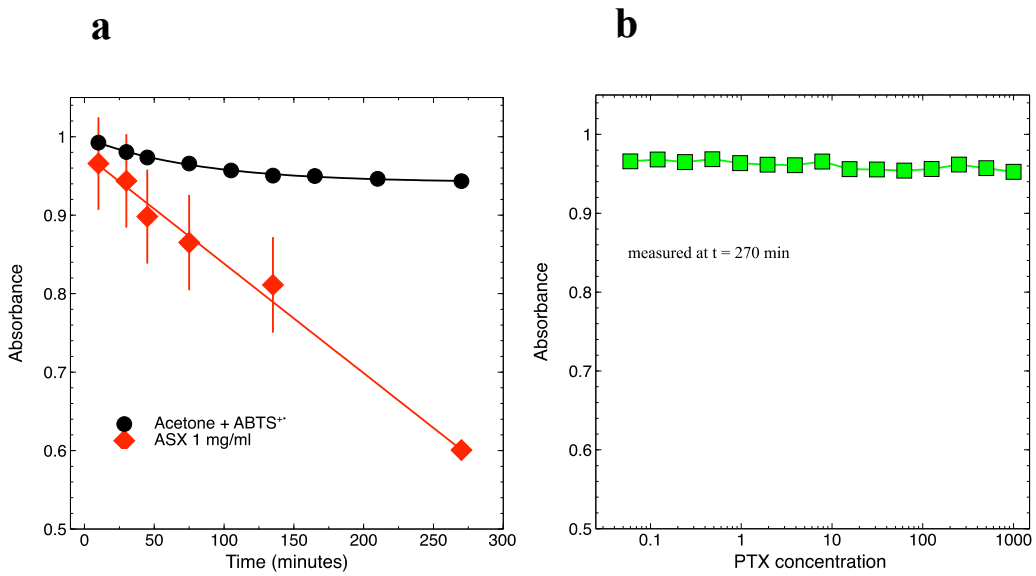

Figure 36. Antioxidant activity of PTX and ASX extracts in a cell free assay

*(**a**) Antioxidant kinetics of ASX extracts compared to the spontaneous decay of ABTS cation radicals ($ABTS^{+\bullet}$) in acetone solvent. (**b**) Antioxidant kinetics of PTX overlapped those of $ABTS^{+\bullet}$ in acetone at all assayed concentrations. For the sake of clarity, in this panel only the final time-point is showed, i.e., the measurements carried out after 270 min for all PTX concentrations.*

5. Effects of PTX and ASX microparticles on irradiated cells

Ionizing radiation initiate oxidative stress in biological samples through water radiolysis that ultimately leads to cell death [28]. Since PTX and ASX microparticles cooperated to significantly reduce intracellular ROS (*Figures 35* and *34* and *Table 5*), we investigated whether they could also increase the survival of irradiated cell samples when given alone or in combination to cells before radiation treatments.

Figure 37 shows the results of experiments with J774A.1 macrophages. ASX microparticles and PTX, given alone or in combination, did not alter significantly the clonogenic potential of the J774A.1 cells (parameter ε) if compared to that of control untreated cells, but significantly increased the survival of irradiated cells (parameter $S(D)$). The survival of irradiated cells increased progressively when the cells were treated with ASX microparticles, PTX or ASX particles in combination with PTX.

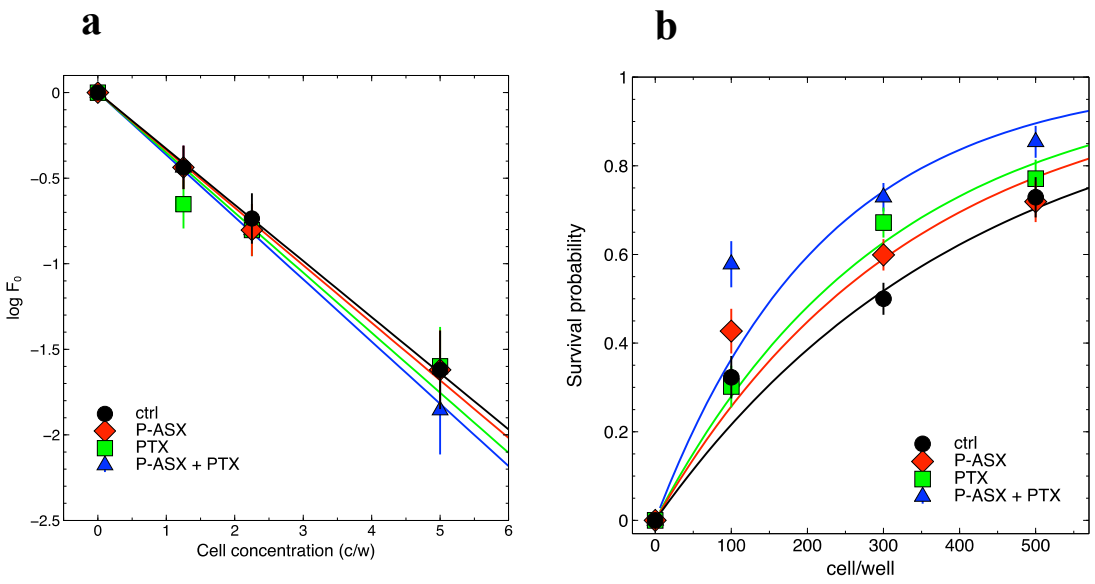

Figure 37 Effects of PTX and ASX microparticles on irradiated J774A.1 macrophages

***(a)** Limiting dilution assays were performed with non-irradiated cells to estimate ε in Equation (2). Cells were seeded at each indicated density into the wells of 96-well culture plates and treated with ASX microparticles (P-ASX) and PTX, either alone or in combination (ASX + PTX), or left untreated (ctrl), F_0 is the fraction of cells where no*

proliferation was observed at the end of the observation period (~ 30 days). When the cells are randomly and independently distributed, F_0 is expected to obey Poisson statistics with parameter ε. Linear fitting of log-transformed data provided the following estimates: $\varepsilon_{ctrl} = 0.328 \pm 0.0325$, $\varepsilon_{P\text{-}ASX} = 0.336 \pm 0.036$, $\varepsilon_{PTX} = 0.351 \pm 0.036$, $\varepsilon_{P\text{-}ASX+PTX} = 0.364 \pm 0.038$. The differences in the parameter ε were not statistically significant (ANOVA test, p = 0.9).

***(b)** Survival probability of independent cell populations treated with ASX microparticles (P-ASX), PTX, P-ASX in combination (ASX + PTX) or left untreated (ctrl), and then irradiated with a single dose of 4 Gy γ-rays. Non linear fits with Equation (2) allowed to estimate the fraction of the cells surviving radiation treatments. The results are: $S(D)_{ctrl} = 0.0071 \pm 0.0005$ ($\chi^2/df = 1.5$), $S(D)_{P\text{-}ASX} = 0.0086 \pm 0.0006$ ($\chi^2/df = -12.2$), $S(D)_{PTX} = 0.0095 \pm 0.0007$ ($\chi^2/df = 1.7$), $S(D)_{P\text{-}ASX+PTX} = 0.0131 \pm 0.001$ ($\chi^2/df = 2.1$). All observed differences in estimated parameter values were statistically significant (ANOVA test, $p = 1.5 \times 10^{-12}$) followed by Tukey post-hoc test.*

DISCUSSION

Radiation-induced fibrosis is a long-term, yet incurable, progressive side effect of radiotherapy in cancer patients. It may manifest as a systemic disorder that affects almost every part of the body exposed to radiation, as skin, lungs, gastrointestinal, urinary, lymphatic systems, joints, and mucosae. Furthermore, it remains a major obstacle for thoracic irradiation of lung, esophageal and breast tumors, where it causes severe lung injuries in up to 37% of treated patients [90]. Specifically, radiation induced pulmonary fibrosis is a common complication in 5-50% of patients [91], which significantly limits their quality of life even after successful eradication of the tumor itself. In breast cancer patients, the commonly reported incidence of radiation-induced fibrosis (RIF) is 10-15%, although 23% has been reported [92].

It is considered a multifactorial disorder that is initiated by an altered accumulation of reactive oxygen species (ROS) and consequently imbalance between their production and elimination through the activation of specific detoxifying mechanisms (e.g., antioxidant enzymes SOD, catalase), as the consequence of water radiolysis. This prominent mechanism of pathogenesis, accounts for 60-70% of the total tissue damage, in both intracellular and extracellular compartments, and not only to cancerous cells but also to irradiated and non-irradiated normal cells. This latter effect in non-irradiated normal cells is due to the so-called off-target effects caused by the propagation of radiation-related dangerous signals, such as ROS, other reactive molecular species, cytokine, ATP, and extracellular DNA, from irradiated to non-irradiated normal cells.

In turn, these signals activate immune cells, in particular macrophages, that can further contribute to ROS production and consequently to initiate, sustain and amplify the inflammatory cascade. Unresolved inflammation leads to the dysfunction of tissues (fibrosis), characterized by an increase in collagen deposition, poor vascularity, and scarring. In this last phase, TGF-β cytokine, mainly produced and released by macrophage cells, is a key molecular actor in RIF, as responsible for the recruitment and activation of fibroblasts and consequently deposition of collagen and other extracellular matrix components.

For all consideration, radiation-induced fibrosis is considered a multifactorial disorder and consequently a single therapeutic strategy is unlikely to be sufficient for its resolution, but it requires a distinct global approach, possibly by inhibiting different critical pathways involved in this condition. Up to now, the therapeutic options used in the clinic include only supportive management strategies (e.g., steroids and other anti-inflammatory drugs), and their efficacy, however, is far from being satisfactory [91].

Therefore, the lack of available efficacious treatments and the severity of the symptoms associated with RIF call for efforts to develop novel therapeutic strategies that could help to limit the side effects of radiotherapy.

The present study may contribute to this purpose. We exploited the ability of macrophage cells to uptake particulate. In this way, we could specifically deliver usefulness compounds formulated into micro-size particles to phagocytic cells, the only cells that can uptake material within this size, and modulate this process by adding specific cytokines, specifically IFNγ, a well know stimulant of the cellular uptake.

Microparticles loaded at least with 2% of astaxanthin were realized. Astaxanthin is a well known hydrophobic antioxidant and, thanks to its chemical properties, it inhibited the H_2O_2-induced intracellular ROS production in J774A.1 cells.

In all biological experiments, ASX oleoresin was not tested as an additional control for several reasons. ASX oleoresin is insoluble in the cell culture medium. It can be dissolved in dymethyl sulfoxide (DMSO). DMSO, even at low concentrations, is toxic for the cells and could alter the beneficial effects of astaxanthin. Astaxanthin oleoresin and astaxanthin itself have a poor bioavailability that limits their direct use as drugs. The encapsulation of astaxanthin in an envelope made of whey protein isolate represents a strategy to improve astaxanthin stability and bioavailability.

While ROS scavenging by astaxanthin is well documented in the scientific literature, we reported a preliminary innovative activity of this molecule, its ability to inhibit the production/release of bioavailable TGF-β that remains to be fully explained at the molecular level.

It was demonstrated that astaxanthin inhibits the activity of intracellular convertases, a class of enzymes responsible for the post-translational processing and maturation of several cytokines. TGF-β is activated by furin convertase along the secretory pathway, and the observed enzyme inhibition by astaxanthin might explain the reduction in the release of bioactive TGFβ by the cells, not revealed by the chemiluminescent ELISA assay, as the latter test can not distinguish between processed, active TGF-β form from unprocessed one.

However, to the best of our knowledge, no probes are commercially available to specifically quantify furin activity, and the Boc-RVRR-AMC substrate used here is not an exception. Thus, the present results do not formally provide a demonstration of the molecular events behind the observed ASX effects on TGF-β. ASX inhibition of intracellular convertases might, nonetheless, have been underestimated in this assay. It was noted that only tiny amounts of the widely exploited convertases-specific substrate Boc-RVRR-AMC are internalized in J774A.1 cells, and this did not allow us to monitor convertases activity in living

cells. The activity of these enzymes could only be measured on cell extracts, and cell lysis might have altered the chemical equilibrium between ASX and convertases, thus masking at least part of the ASX inhibitory activity on these enzymes.

We also attempted to purify TGFβ from culture supernatants by immunoprecipitation with the goal to analyze its biochemical structure, but the experiments failed because of the relatively low concentration of the cytokine.

ASX microparticles reduced not only the intracellular ROS levels in macrophages exposed to oxidative stress, but also inhibited their secretion of bioactive TGF-β, indicating, although within the limitations of a pre-clinical *in vitro* study, that the treatment strategy developed to target specifically phagocytic cells could indeed be effective.

The effects of ASX microparticles can be further potentiated by combination treatment with pentoxifylline. Pentoxifylline was not toxic for macrophage cells, did not interfere with phagocytosis of ASX microparticles, but at the same time could significantly reduce the oxidative stress in J774A.1 macrophages under oxidative stress conditions. Cell-free assays, however, clearly showed that pentoxifylline had no direct antioxidant activity on its own. It has been reported that this drug may have indirect antioxidant effects in neutrophils where it may reduce the superoxide production via NADPH oxidase [55]. It has also been shown to contribute to the maintenance of GSH levels, mitochondrial viability and in general to have protective effects against malathion-induced oxidative damage to rat brain mitochondria *in vivo* [93]. The antioxidant activity of the dimetylxanthine derivative, therefore, appears to depend on its ability to modulate intracellular detoxifying pathways. The results are in line with this interpretation of the molecular mechanisms of action of PTX. Importantly, the drug showed synergistic antioxidant effects with ASX-loaded microparticles in J774A.1 cells and significantly contributed to increasing the survival of irradiated macrophages.

These findings collectively show that both direct and indirect mechanisms can be activated to restore intracellular ROS levels and protect cells from oxidative injury. PTX has also a well-acknowledged anti-inflammatory activity, since it can inhibit TNFα production and signaling [56]. Given in combination with ASX microparticles, that on their own inhibit active TGF-β release by targeted macrophages, might result in more effective treatments against inflammation and fibrosis.

As final considerations, I would like to discuss about two potential routes of administration to deliver astaxanthin-loaded microparticles.

- Drug delivery for lung fibrosis

A possible way to administer ASX microparticles for the treatment of radiation-induced lung fibrosis might be by inhalation of aerosols. Current therapeutic options for lung fibrosis following radiotherapy include only supportive management strategies, such as anti-inflammatory treatment using steroids; their efficacy, however, is far from being satisfactory [94]. More recently, it was shown that nintedanib, a multiple tyrosine kinase inhibitor, and pirfenidone, a TGF-β inhibitor, exhibit anti-inflammatory and antifibrotic effects in experimental murine irradiation mice and these drugs are now in clinical use for the treatment of pulmonary fibrosis [94]. However, clinical trials have also shown that adverse reactions often occur during treatment. The systemic and chronic daily doses can lead to off-target toxicities and significant patient discomfort [95]. Therefore, there is a need to increase the effectiveness and reduce the overall toxicities of the active compounds that can be achieved by their encapsulation within nanoparticle or microparticle [95] and by their delivery directly to the lungs.
Pulmonary delivery is a developing technology in which medication is inhaled through lungs and enters the bloodstream through the alveolar epithelium [96].
The size of particles is fundamental to determine their deposition site. The size of particulate matter in an aerosol can range from 0.001 to more than 100 μm [97]. The aerosol particles can be divided into coarse particle (bigger that 2 μm), fine particles (0.1-2 μm), ultrafine particles (smaller than 0.1 μm).
Astaxanthin loaded microparticles have a mean diameter of 2 μm and therefore particles with an aerodynamic size between 1-5 μm are delivered to the smaller airways of bronchioles and alveoli by sedimentation, a deposition process governed by gravitational forces, particle velocity and aerodynamic size. It is possible to speculate that astaxanthin-loaded microparticles can reach the deep spaces of the lungs.
Pulmonary drug delivery possesses favorable properties: it is a non-invasive route of administration, and it avoids first bypass metabolism [97].
As lungs are one of the major ports of entry of foreign substances into the body, in the body, they have multiple physiological clearance mechanisms aimed at degrading and eliminating exogenous materials. In the deep lungs, resident alveolar macrophages, thanks to their phagocytic functions, are responsible for the

clearance of exogenous elements, as alveolar macrophages are recognized as a first line of cellular host defenses. Several studies reported that alveolar macrophages are involved in the retention of deposited particles and in their removal, and clearly alveolar macrophages are capable of engulfing a wide variety of materials within hours after deposition [98]. Thus alveolar macrophages would actively uptake even particles loaded with drugs, such as our ASX microparticles.

In the upper airway, another type of clearance mechanism for exogenous materials, called mucociliary clearance, is present. The principle of the mucociliary escalator includes entrapment of foreign/inhalable particles in the mucus layer before the particles move to the lower respiratory regions. After that, the foreign particles are propelled along with mucus out of the trachea either by coughing or swallowing. The mucociliary escalator eliminates the majority of particles of size greater than 6 μm. [97]. In this case, the microparticles loaded with astaxanthin (2 μm mean diameter) might potentially escape the mucociliary clearance.

All these considerations suggest that pulmonary drug delivery is a potential way to treat lung fibrotic conditions. Several studies have indeed shown that microsphere drug delivery system is indeed useful for the treatment of asthma [99]. Overall, drug delivery through the lungs with astaxanthin microparticles might be feasible.

- Drug delivery for skin fibrosis

Cutaneous fibrosis is the accumulation of ECM components in the dermis, leading to compromised function and altered architecture of the dermis [100]. In its mildest form it may present only a minor aesthetic problem, but in the most severe cases can lead to debilitating pathologies of the skin, for example keloid and hypertrophic scars, and systemic sclerosis [101].

Autoimmunity and/or inflammation seem to play a central role because corticosteroids and/or immunosuppressants are effective for most of the skin fibrotic disorders. Immune cells, specifically macrophages, are key actors in inflammatory conditions of the skin. The mononuclear phagocyte system in the skin is composed of dendritic cells, monocytes and macrophages. In healthy dermal tissues, macrophages express a unique set of genes that support specific roles in scavenging the degradation intermediates of self macromolecules and in killing microorganisms, and have a slower turnover rate and a longer life than dendritic cells and monocytes [102].

Lakos *et al.* [103] reported that injections of bleomycin induced an early and transient inflammatory response in the dermis. The dermal infiltrate, composed predominantly of macrophages, preceded the development of fibrosis in a model of skin fibrosis [103]. Macrophages were markedly increased in lesional skin as well as in inflamed skin draining lymph nodes of inflamed skin in affected CD18 hypo mice [104].

Targeted therapy for skin fibrosis includes the administration of monoclonal antibodies and nano/micro drug delivery approaches.

In systemic sclerosis (SSc), promising clinical outcomes have been reported for the treatments with tocilizumab (an anti-IL-6 receptor antibody), Rituximab (an anti-CD20 antibody), and fresolimumab (an anti-TGF-β antibody) [105]. Asano Y. reported [105] that, in Ssc patients, the treatment with tocilizumab or fresolimumab commonly determines the inactivation of monocyte-macrophage lineage cells and the involvement of IL-6 and TGF-β in the activation of those cells during the fibrotic process of this disease.

Antioxidants have also been studied for their preventive and therapeutic effects in protecting healthy cells from radiation-induced DNA damage. Silymarin, an extract from milk thistle with antioxidant and anti-inflammatory effects, was shown to delay the onset of radiodermatitis in a randomized trial of forty breast cancer patients when applied topically as a gel for five weeks at the onset of radiotherapy [106]. In a prospective, nonrandomized study of 112 patients post-mastectomy, daily subcutaneous administration of the antioxidant amifostine through radiation treatment was associated with reduced erythema, edema, and moist skin desquamation compared with patients who did not receive antioxidant treatment [106]. Randomized control trials showed that the combination of oral pentoxifylline and vitamin E improved tissue compliance in breast cancer patients when taken daily for six months post-radiotherapy and reduced the RIF surface area when administered years after radiotherapy for breast cancer[106].

Oliveira dos Santos *et al.* showed that microparticles loaded with caffeine were homogeneously distributed through the subcutaneous space and were more retained in the hair follicle than free caffeine [107]. Gu *et al.* reported that vitamin C encapsulated into solid lipid microparticles exhibited an increased absorption than the vitamin C solution [108].

Overall, these observations indicate that topical administration of astaxanthin-loaded microparticles could be a potential and innovative way to deliver antioxidant drugs to skin phagocytes and modulate their inflammatory activity.

The present research shows that it is possible to encapsulate hydrophobic bioactive substances, specifically astaxanthin oleoresin, into micrometer-sized particles to target phagocytic cells and modulate their own functions. The results

support the thesis that ASX microparticles interfere with the positive feedback between ROS and TGF-β in phagocytic cells and protect them from radiation exposure, with a stronger protection effect if given in combination with pentoxifylline.

BIBLIOGRAPHY

[1] Wynn, T. A. Fibrotic disease and the TH1/TH2 paradigm. *Nat. Rev. Immunol.* **2004**, *4(8)*, 583-594. doi:10.1038/nri1412.

[2] Wynn, T. A. Common and unique mechanism regulate fibrosis in various fibroproliferative diseases. *J. Clin. Invest.* **2007**, *117 (3)*, 524-529. doi: 10.1172/JCI31487.

[3] Distler, J. H. W.; Györfi, A.; Ramanujam, M.; Whitfield, M. L; Königshoff, M.; Lafyatis, R. Shared and distinct mechanisms of fibrosis. *Nat. Rev. Rheumatol.* **2019**, *15(12)*, 705-730. doi: 10.1038/s41584-019-0322-7.

[4] Wynn, T. A. Cellular and molecular mechanisms of fibrosis. *J. Phatol.* **2008**, *214(2)*, 199-210. doi: 10.1002/path.2277.

[5] Richter, K.; Konzack, A.; Pihlajaniemi, T; Heljasvaara, R. Kietzmann, T; *Redox Biol.* **2015**, *6*, 344-352. doi: 10.1016/j.redox.2015.08.015.

[6] Friedman, S.; Sheppard, D.; Duffield, J. S.; Violette S. Therapy for fibrotic diseases: nearing the starting line. *Sci. Trans. Med.* **2013**, *5(167)*, 167sr1. doi: 10.1126/scitranslmed.3004700.

[7] Epelman, S.; Lavine, K. J.; Randolph, G. W. Origin and functions of tissue macrophages. *Immunity* **2014**, *41(1)*, 21-35. doi: 10.1016/j.immuni.2014.06.013.

[8] Zhao, Y.; Zou, W.; Du, J.; Zhao, Y. The origins and homeostasis of monocytes and tissue-resident macrophages in physiological situation. *J. Cell. Physiol.* **2018**, *233(10)*, 6425-6439. doi: 10.1002/jcp.26461.

[9] Sieweke, M. H.; Allen, J. E. Beyond stem cells: self-renewal of differentiated macrophages. *Science* **2013**, *342(6161)*, 1242974. doi: 10.1126/science.1242974.

[10] Italiani, P.; Boraschi, D. From monocytes to M1/M2 macrophages: phenotypical vs. functional differentiation. *Front. Immunol.* **2014**, *5*, 514. doi: 10.3389/fimmu.2014.00514.

[11] Dietert R. R. Macrophages as targets of developmental immunotoxicity. *OA Immunology* **2014,** *2(1)*, 2.

[12] Martinez, F. O.; Gordon, S. The M1 and M2 paradigm of macrophage activation: time for reassessment. *F1000Prime Rep.* **2014**, *6*, 13. doi 10.12703/P6-13.

[13] Mosser, D. M.; Edwards, J. P. Exploring the full spectrum of macrophage activation. *Nat. Rev. Immunol.* **2008**, *8(12)*, 958-969. doi: 10.1038/nri2448.

[14] Wu, T.; Chen, S., Wu, Y. Mucosal macrophage polarization role in the immune modulation. Chapter of *Cells of the immune system* **2019**. doi: http://dx.doi.org/10.5772/intechopen.86609.

[15] Quatromoni, J. G.; Eruslanov, E. Tumor-associated macrophages: function, phenotype, and link to prognosis in human lung cancer. *Am. J. Transl. Res.* **2012**, *4(4)*, 376-389. PMCID: PMC3493031.

[16] Rosales, C.; Uribe-Querol, E. Phagocytosis: a fundamental process in immunity. *Biomed. Res. Int.* **2017**, *2017*, 9042851. doi: 10.1155/2017/9042851. Epub 2017 Jun 12.

[17] Papadimitriou, J. M.; Ashman, R. B. Macrophages: current views on their differentiation, structure, and function. *Ultrastruct. Pathol.* **1989**, *13(4)*, 343-372. doi: 10.3109/01913128909048488.

[18] Rabinovitch, M. Professional and non-professional phagocytes: an introduction. *Trends Cell Biol.* **1995**, *5(3)*, 85-87. doi: 10.1016/s0962-8924(00)88955-2.

[19] Yong, S.; Song, Y.; Jin Kim, H.; Ul Ain, Q.; Kim, Y. Mononuclear phagocytes as a target, not a barrier, for drug delivery. *J. Control. Release* **2017**, *259*, 53-61. doi: 10.1016/j.jconrel.2017.01.024. Epub 2017 Jan 18.

[20] Janda, E.; Boi, L; Carta, A. Microglial Phagocytosis and its regulation: a therapeutic target in Parkinson's disease. *Front. Mol. Neurosci.* **2018**, *11*, 144. doi: 10.3389/fnmol.2018.00144. ECollection 2018.

[21] Lech, M.; Anders, H. Macrophages and fibrosis: how resident and infiltrating mononuclear phagocytes orchestrate all phases of tissue injury

and repair. *Biochim. Biophys. Acta* **2013**, *1832(7)*, 989-997. doi: 10.1016/j.bbadis.2012.12.001. Epub 2012 Dec 13.

[22] Laskin, D. L.; Sunil, V. R.; Gardner, C. R.; Laskin, J. D. Macrophages and tissue injury: agents of defense or destruction? *Annu. Rev. Pharmacol. Toxicol.* **2011**, *51*, 267-288. doi: 10.1146/annurev.pharmtox.010909.105812.

[23] Oishi, Y.; Manabe, I. Macrophages in inflammation, repai and regeneration. *Int. Immunol.* **2018**, *30(11)*, 511-528. doi: 10.1093/intimm/dxy054.

[24] Baskar, R.; Dai, J.; Wenlong, N.; Yeo, R.; Yeoh, K. Biological response of cancer cells to radiation treatment. *Front. Mol. Biosci.* **2014**, *1*, 24. doi: 10.3389/fmolb.2014.00024. eCollection 2014.

[25] Thun, M. J; DeLancey, J. O.; Center, M. M.; Jemal, A. Ward, E. M. The global burden of cancer: priorities for prevention. *Carcinogenesis*, **2010**, 31(1), *100-110*. doi: 10.1093/carcin/bgp263. Epub 2009 Nov 24.

[26] Baskar, R.; Lee, K. A.; Yeo, R.; Yeoh, K. Cancer and radiation therapy: current advances and fuure directions. *Int. J. Med. Sci.* **2012**, *9(3)*: 193-199. doi: 10.7150/ijms.3635. Epub 2012 Feb 27.

[27] Gong, L.; Zhang, Y.; Liu, C.; Zhang, M.; Han, S. Application of radiosensitizers in cancer radiotherapy. *Int. J. Nanomedicine* **2021**, *16*, 183-1102. doi: 10.2147/IJN.S290438. ECollection 2021.

[28] Azzam, E. I.; Gerin, J.; Pain, D. Ionizing radiation-induced metabolic oxidative stress and prolonged cell injury. *Cancer Lett.* **2012**, *327(1-2)*, 48-60. doi: 10.1016/j.canlet.2011.12.012. Epub 2011 Dec 17.

[29] Nikjoo, H. Radiation track and DNA damage. *Iran. J. Radiat. Res.* **2003**, *1(1)*, 3-16.

[30] Chiao, T.B.; Lee, A.J. Role of pentoxifylline and vitamin E in attenuation of radiation-induced fibrosis. *Ann. Pharmacother.* **2005**, *39*, 516-522. doi: 10.1345/aph.1E186.

[31] Straub, J. M.; New, J.; Hamilton, C. D.; Lomiska, C.; Shnayder, Y.; Thomas, S. M. Radiation-induced fibrosis: mechanisms and implications for therapy. *J. Cancer Res. Clin. Oncol.* **2015**, *141(11)*, 1985-1994. doi: 10.1007/s00432-015-1974-6. Epub 2015 Apr 25.

[32] Prasanna, P.; Stone, H. B.; Wong, R. S.; Capala, J.; Bernhard, E. J.; Vikram, B.; Coleman, C. N. Normal tissue protection for improving radiotherapy: where are the gaps? *Transl. Cancer Res.* **2012**, *1(1)*, 35-48.

[33] Jin, H.; Yoo, Y.; Kim, Y.; Kim, Y.; Cho, J.; Lee, Y. Radiation-induced lung fibrosi: preclinical animal models and therapeutic strategies. *Cancers (Basel)* **2020**; *12(6)*, 1561. doi: 10.3390/cancers12061561.

[34] Cheresh, P.; Kim, s.; Tulasiram, S.; Kamp, D. Oxidative stress and pulmonary fibrosis. *Biochim. Biophys. Acta* **2013**, *1832(7)*, 1028-1040. doi: 10.1016/j.bbadis.2012.11.021. Epub 2012 Dec 5.

[35] Reisz, J. A.; Bansal, N.; Qian, J.; Zhao, W.; Furdui, C. M. Effects of ionizing radiation on biological molecules – mechanisms of damage and emerging methods of detection. *Antioxid. Redox Signal.* **2014**, *21(2)*, 260-292. doi: 10.1089/ars.2013.5489. Epub 2014 Feb 21.

[36] Liu, R.; Desai, L. P. Reciprocal regulation of TGF-β and reactive oxygen species: a perverse cycle for fibrosis. *Redox Biol.* **2015**, *6*, 565-577. doi: 10.1016/j.redox.2015.09.009. Epub 2015 Oct 10.

[37] Ritcher, K.; Konzack, A.; Pihlajaniemi, T.; Heljasvaara, R.; Kietzmann, T. Redox-fibrosis: impact of TGF-β1 on ROS generators, mediators, and functional consequences. *Redox Biol.* **2015**, *6*, 344-352. doi: 10.1016/j.redox.2015.08.015. Epub 2015 Aug 28.

[38] Jiang, F.; Liu, G.; Dusting, G. J.; Chan, E. C. NADPH oxidase-dependent redox signaling in TGF-β mediated fibrotic responses. ***Redox Biol.*** **2014**, *2*, 267-272. doi: 10.1016/j.redox.2014.01.012. ECollection 2014.

[39] Roy, L.; Poirier, M.; Fortin, D. Transforming growth factor-beta and its implication in the malignancy of gliomas. *Target. Oncol.* **2015**, *10(1)*, 1-14. doi: 10.1007/s11523-014-0308-y. Epub 2014 Mar 5.

[40] Giri, S. N.; Hyde, D. M.; Hollinger, M.A. Effect of antibody to transforming growth factor beta on bleomycin induced accumulation of lung collagen in mice. *Thorax.* **1993**, *48(10)*, 959-966. doi: 10.1136/thx.48.10.959.

[41] Higashiyama, H. et al. Inhibition of activin receptor-like kinase 5 attenuates bleomycin-induced pulmonary fibrosis. *Exp. Mol. Pathol.* **2007**, *83(1)*, 39-46. doi: 10.1016/j.yexmp.2006.12.003. Epub 2006 Dec 24.

[42] Ishikawa, F. et al. A mitochondrial thioredoxin-sensitive mechanism regulats TGF-β-mediated gene expression associated with epithelial-mesenchymal transition. *Biochem. Biophys. Res. Commun.* **2014**, *443(3)*, 821-827. doi: 10.1016/j.bbrc.2013.12.050. Epub 2013 Dec 14.

[43] Jain, M. et al. Mitochondrial reactive oxygen species regulate transforming growth factor-β signaling. *J. Biol. Chem.* **2013**, *288(2)*, 770-777. doi: 10.1074/jbc.M112.431973. Epub 2012 Nov 30.

[44] Boureau, H. E.; Casterline, B. W.; Rada, B.; Korzeniowska, A.; Leto, T. L. Nox4 involvement in TGF-β and SMAD3-driven induction of the epithelial-to-mesenchymal transition and migration of breast epithelial cells. *Free Radic. Biol. Med.* **2012**, *53(7)*, 1489-1499. doi: 10.1016/j.freeradbiomed.2012.06.016. Epub 2012 Jun 19.

[45] Jarman, E. R. et al. An inhibitor of NADPH oxidase-4 attenuates enstablished pulmonary fibrosis in a rodent disease model. *Am. J. Respir. Cell Mol. Biol.* **2014**, *50(1)*, 158-169. doi: 10.1165/rcmb.2013-0174OC.

[46] Liu, R. et al. Transforming growth factor β suppresses glutamate-cysteine ligase gene expression and induces oxidative stress in a lung fibrosis model. *Free Radic. Biol. Med.* **2012**, *53(3)*, 554-563. doi: 10.1016/j.freeradbiomed.2012.05.016. Epub 2012 May 23.

[47] Tiitto et al. Cell-specific regulation of gamma-glutamylcysteine synthetase in human interstitial lung diseases. *Hum. Pathol.* **2004**, *35(7)*, 832-839. doi: 10.1016/j.humpath.2004.03.010.

[48] Cui Y., Robertson J., Maharaj S., Waldhauser L., Niu J., Wang J., Farkas L., Kolb M., Gauldie J. Oxidative stress contributes to the induction and

persistence of TGF-β1 induced pulmonary fibrosis. *Int. J. Biochem. Cell Biol.* **2011**, *43*,1122-1133. doi: 10.1016/j.biocel.2011.04.005. Epub 2011 Apr 14.

[49] Lee, C. G. et al. Early growth response gene1-mediated apoptosis is essential for transforming growth factor beta1-induced pulmonary fibrosis. *J. Exp. Med.* **2004**, *200(3)*, 377-389. doi: 10.1084/jem.20040104.

[50] Westbury, C. B.; Yarnold, J. R. Radiation fibrosis – current clinical and therapeutic perspectives. *Clin. Oncol. (R. Coll. Radiol.)* **2012**, *24(10)*, 657-672. doi: 10.1016/j.clon.2012.04.001. Epub 2012 May 18.

[51] Delanian, S.; Lefaix, J. Current management for late normal tissue injury: radiation-induced fibrosis and necrosis. *Semin. Radiat. Oncol.* **2007**, *17(2)*, 99-107. doi: 10.1016/j.semradonc.2006.11.006.

[52] Geraci, J. P.; Mariano M. S.; Jackson, K. L. Amelioration of radiation nephropathy in rats by dexamethasone treatment after irradiation. *Radiat. Res.* **1993**, *134(1)*, 86-93.

[53] Evans, M. L.; Graham, M. M.; Mahler, Rasey, J. S. Use of steroids to suppress vascular response to radiation. *Int. J. Radiat. Oncol. Biol. Phys.* **1987**, *13(4)*, 563-567. doi: 10.1016/0360-3016(87)90072-1.

[54] Moulder, J. E. Pharmacological intervention to prevent or ameliorate radiation injuries. *Semin. Radiat. Oncol.* **2003**, *13(1)*, 73-84. doi: 10.1053/srao.2003.50007.

[55] Wen, W. X.; Lee, S. Y.; Siang, R.; Koh, R. Y. Repurposing pentoxifylline for the treatment of fibrosis: an overview. *Adv. Ther.* **2017**, *34(6)*, 1245-1269. doi: 10.1007/s12325-017-0547-2. Epub 2017 May 8.

[56] Okunieff, P. et al. Pentoxifylline in the treatment of radiation-induced fibrosis. *J. Clin. Oncol.* **2004**, *22(11)*, 2207-2213. doi: 10.1200/JCO.2004.09.101.

[57] Delanian, S.; Porcher, R.; Mekias, S.; Lefaix, J. Randomized, placebo-controlled trial of combined pentoxifylline and tocopherol for regression

of superficial radiation-induced fibrosis. *J. Clin. Oncol.* **2003**, *21(13)*, 2545-2550. doi: 10.1200/JCO.2003.06.064.

[58] Hart, G. B.; Mainous, E. G. The treatment of radiation necrosis with hyperbaric oxygen (OHP). *Cancer* **1976,** *37(6)*, 2580-2585. doi: 10.1002/1097-0142(197606)37:6<2580::aid-cncr2820370603>3.0.co;2-h.

[59] Pasquier, D; Hoelscher, T.; Schmutz, J.; Dische, S.; Mathieu, D.; Baumann, M.; Lartigau, E. Hyperbaric oxygen therapy in the treatment of radio-induced lesions in normal tissues: a literature review. *Radiother. Oncol.* **2004**, *72(1)*, 1-13. doi: 10.1016/j.radonc.2004.04.005.

[60] Kohl, R. R.; Kolozsvary, A.; Brown S. L.; Zhu, G.; Kim, J. H. Differential radiation effect in tumor and normal tissue after treatment with ramipril, an angiotensin-converting enzyme inhibitor. *Radiat. Res.* **2007**, 168(4), 440-5. doi: 10.1667/RR0707.1.

[61] Haydont, V.; Mathé, D.; Bourgier, C.; Abdelali, J.; Aigueperse, J.; Bourhis, J.; Vozenin-Brotons, M. Induction of CTGF by TGF-β1 in normal and radiation enteritis human smooth muscle cells: Smad/Rho balance and therapeutic perspectives. *Radiother. Oncol.* **2005**, *76(2)*, 219-225. doi: 10.1016/j.radonc.2005.06.029.

[62] Hauer-Jensen, M.; Fort, C.; Mehta, J. L.; Fink, L. M. Influence of statins on postoperative wound complications after inguinal or ventral herniorrhaphy. *Hernia* **2006**, *10(1)*, 48-52. doi: 10.1007/s10029-005-0030-x. Epub 2005 Sep 8.

[63] Chiao, T. B.; Lee, A. J. Role of pentoxifylline and vitamin E in attenuation of radiation-induced fibrosis. *Ann. Pharmacother.* **2005**, *39(3)*, 516-522. doi: 10.1345/aph.1E186. Epub 2005 Feb 8.

[64] Anscher, M. S. et al. Small molecular inhibitor of transforming growth factor-beta protects against development of radiation-induced lung injury. *Int. J. Radiat. Oncol. Biol. Phys.* **2008**, *71(3)*, 829-837. doi: 10.1016/j.ijrobp.2008.02.046. Epub 2008 Apr 12.

[65] Fakhria, S.; Abbaszadehb, F.; Dargahic, L.; Jorjania, M. Astaxanthin: a mechanistic review on its biological activities and health benefits.

Pharmacol. Res. **2018**, *136*, 1-20. doi: 10.1016/j.phrs.2018.08.012. Epub 2018 Aug 17.

[66] Binatti, E.; Zoccatelli, G.; Zanoni, F.; Donà, G.; Mainente, F. Chignola, R. Phagocytosis of astaxanthin-loaded microparticles modulates TGF-β production and intracellular ROS levels in J774A.1 macrophages. *Mar. Drugs* **2021**, *19(3*), 163. doi: 10.3390/md19030163.

[67] Farooq, M. A.; Aquib, M.; Ghayas, S.; Bushra, R.; Khan, D. H.; Parveen, A.; Wang, B. Whey protein: a functional and promising material for drug delivery systems recent developments and future prospects. *Polym. Adv. Technol.* **2019**, *30*, 2183-2191.

[68] Patel, S. Emerging trends in nutraceutical applications of whey protein and its derivatives. *J. Food Sci. Technol.* **2015**, *52(11)*, 6847-6858.

[69] Zanoni, F.; Vakarelova, M.; Zoccatelli, G. Development and characterization of astaxanthin-containing whey protein-based nanoparticles. *Mar. Drugs* **2019**, 1*7(11)*, 627. doi: 10.3390/md17110627.

[70] Tesseur, I.; Zou, K.; Berber, E.; Zhang, H.; Wyss-Coray, T. Highly sensitive and specific bioassay for measuring bioactive TGF-β. *BMC Cell Biol.* **2006**, *7*, 15. doi: 10.1186/1471-2121-7-15.

[71] Souza, C.; Mônico, D.A.; Tedesco, A.C. Implications of dichlorofluorescein photoinstability for detection of UVA-induced oxidative stress in fibroblasts and keratinocyte cells. *Photochem. Photobiol. Sci.* **2020**, *19*, 40-48. doi: 10.1039/c9pp00415g.

[72] Chignola, R.; Sega, M.; Molesini, B.; Baruzzi, A.; Stella, S.; Milotti, E. Collective radioresistance of T47D breast carcinoma cells is mediated by a Syncytin-1 homologous protein. *PLoS ONE* **2019**, *14*, e0206713. doi: 10.1371/journal.pone.0206713. ECollection 2019.

[73] Lefkovits, I.; Waldmann, H. *Limiting Dilution Analysis of Cells in the Immune System*, 1st ed.; Cambridge University Press: Cambridge, UK, 1979; pp. 38-82.

[74] Mishra, K.; Ojha, H.; Chaudhury, N.K. Estimation of antiradical properties of antioxidants using DPPH assay: a critical review and results. *Food Chem.* **2012**, *130*, 1036-1043. https://doi.org/10.1016/j.foodchem.2011.07.127

[75] Aoi, W.; Maoka, T.; Abe, R.; Fujishita, M.; Tominaga, K. Comparison of the effect of non-esterified and esterified astaxanthins on endurance performance in mice. *J. Clin. Biochem. Nutr.* **2018**, *62(2)*, 161-166. doi: 10.3164/jcbn.17-89. Epub 2017 Dec 27.

[76] Champion, J.A.; Walker, A.; Mitragotri, S. Role of particle size in phagocytosis of polymeric microspheres. *Pharm. Res.* **2008**, *25*, 1815-1821. doi10.1007/s11095-008-9562-y.

[77] Hammer, C. T.; Wills, E. D. The effect of ionizing radiation on the fatty acid composition of natural fats and on lipid peroxide formation. *Int. J. Radiat. Biol. Relat. Stud. Phys. Chem. Med.* **1979**, *35(4)*, 323-332. doi: 10.1080/09553007914550391.

[78] Takahashi, T. Routine management of microalgae using autofluorescence from chlorophyll. *Molecules* **2019**, *24(24)*, 4441. doi: 10.3390/molecules24244441.

[79] Schroder K.; Hertzog, P.; Ravasi, T.; Hume, D. A. Interferon-gamma: an overview of signals, mechanisms and functions. *J. Leukoc. Biol.* **2004**, *75(2)*, 163-189. doi: 10.1189/jlb.0603252. Epub 2003 Oct 2.

[80] Ransy, C.; Vaz, C.; Lombès, A.; Bouillaud, F. Use of H_2O_2 to cause oxidative stress, the catalase issue. *Int. J. Mol. Sci.* **2020**, *21(23)*, 9149. doi: 10.3390/ijms21239149.

[81] Franken, N.A.P.; Rodermond, H.M.; Stap, J.; Haveman, J.; Van Bree, C. Clonogenic assay of cells in vitro. *Nat. Protoc.* **2006**, *1*, 2315–2319. doi: 10.1038/nprot.2006.339.

[82] Jakobse, S.S.; Larsen, A.; Stoltenberg, M.; Bruun, J.M.; Soballe, K. Hydroxyapatite coatings did not increase TGF-β and BMP-2 secretion in murine J774A.1 macrophages, but induced a pro-inflammatory cytokine

response. *J. Biomater. Sci. Polym. Ed.* **2009**, *20*, 455-465. doi: 10.1163/156856209X416476.

[83] Dubois, C.M.; Blanchette, F.; Laprise, M.H.; Leduc, R.; Grondin, F.; Seidah, N.G. Evidence that furin is an authentic transforming growth factor-β1-converting enzyme. *Am. J. Pathol.* **2001**, *158*, 305-316. doi: 10.1016/s0002-9440(10)63970-3.

[84] Basak, A. Inhibitors of proprotein convertases. *J. Mol. Med.* **2005**, *83*, 844-855. doi: 10.1007/s00109-005-0710-0. Epub 2005 Oct 8.

[85] Bessler, H.; Gilgal, R.; Djaldetti, M.; Zahavi, I. Effect of pentoxifylline on the phagocytic activity, cAMP levels, and superoxide anion production by monocytes and polymorphonuclear cells. *J. Leukoc Biol.* **1986**, *40*, 747-754. doi: 10.1002/jlb.40.6.747.

[86] Fan, H.; Kim, S.M.; Cho, Y.J.; Eo, M.Y.; Lee, S.K.; Woo, K.M. New approach for the treatment of osteoradionecrosis with pentoxifylline and tocopherol. *Biomater. Res.* **2014**, *18*, 13. doi: 10.1186/2055-7124-18-13. eCollection 2014.

[87] Slinker, B.K. The statistics of synergism. *J. Mol. Cell. Cardiol.* **1998**, *30*, 723-731. doi: 10.1006/jmcc.1998.0655.

[88] Kobayashi, M.; Takizono, T.; Nishio, N.; Nagai, S.; Kurimura, Y.; Tsuji, Y. Antioxidant role of astaxanthin in the green alga Haematococcus pluvialis. *Appl. Microbiol.* **1997**, *48*, 351-356.

[89] Shahidi, F.; Ambigaipalan, P. Phenolics and polyphenolics in foods, beverages and spices: Antioxidant activity and health effects–A review. *J. Funct. Foods* **2015**, *18*, 820-897. https://doi.org/10.1016/j.jff.2015.06.018.

[90] Rodríguez, M. L; Padellano, L. C. Toxicity associated to radiotherapy treatment in lung cancer patients. *Clin. Transl. Oncol.* **2007**, *9(8)*, 506-512. doi: 10.1007/s12094-007-0094-4.

[91] Jarzebska, N.; Karetnikova, E. S.; Markov, A. G.; Kasper, M.; Rodionov, R. N.; Spieth, P. M. Scarred lung. An update on radiation-induced pulmonary fibrosis. *Front. Med. (Lausanne)* **2021**, *7*, 585756. doi: 10.3389/fmed.2020.585756. ECollection 2020.

[92] Williams, N. R.; Williams, S.; Kanapathy, M.; Naderi, N.; Vavourakis, V.; Mosahebi, A. Radiation-induced fibrosis in breast cancer: a protocol for an observational cross-sectional pilot study for personalised risk estimation and objective assessment. *Int. J. Surg. Protoc.* **2019**, *14*, 9-13. doi: 10.1016/j.isjp.2019.02.002. ECollection 2019.

[93] Ranjbar, A.; Ghahremani, M.H.; Sharifzadeh, M.; Golestani, A.; Ghazi-Khansari, M.; Baeeri, M.; Abdollahi, M. Protection by pentoxifylline of malathion-induced toxic stress and mitochondrial damage in rat brain. *Hum. Exp. Toxicol.* **2010**, *29*, 851–864. doi: 10.1177/0960327110363836. Epub 2010 Mar 1.

[94] Jarzebska, N.; Karetnikova, E. S.; Markov, A. G.; Kasper, M.; Rodionov, R. N.; Spieth, P. M. Scarred lung. An update on radiation-induced pulmonary fibrosis. *Front. Med. (Lausanne)* **2021**, *15(7)*, 585756. doi: 10.3389/fmed.2020.585756. eCollection 2020.

[95] Ghumman, M.; Dhamecha, D.; Gonsalves, A.; Fortier, L.; Sorkhdini, P.; Zhou, Y.; Menon, J. U. Emerging drug delivery strategies for idiopathic pulmonary fibrosis treatment. *Eur. J. Pharm Biopharm.* **2021**, *164*, 1-12.

[96] Basavaraj, K. N. et al. Pulmonary drug delivery: novel pharmaceutical technologies breathe new life into the lungs. *PDA J. Pharm. Sci.* **2011**, *65(5)*, 513-534. doi: 10.1016/j.ejpb.2021.03.017. Epub 2021 Apr 18.

[97] El-Sherbiny, I. M.; El-Baz, N. M.; Yacoub, M. H. Inhaled nano- and miroparticles for drug delivery. *Glob. Cardiol. Sci. Pract.* **2015**, *2015*, 2. doi: 10.5339/gcsp.2015.2. eCollection 2015.

[98] Lehnert, B. E. Pulmonary and thoracic macrophage subpopulations and clearance of particles from the lung. *Environ. Health Perspect.* **1992**, *97*, 17-46. doi: 10.1289/ehp.929717.

[99] SreeHarsha, N. et al. An efficient, lung-targeted, drug-delivery system to treat asthma via microparticles. *Drug Des. Devel. Ther.* **2019**, *13*, 4389. doi: 10.2147/DDDT.S216660. ECollection 2019.

[100] Do, N. N.; Eming, S. A. Skin fibrosis: models and mechanisms. *Curr. Res. Transl. Med.* **2016**, *64(4)*, 185-193. doi: 10.1016/j.retram.2016.06.003. Epub 2016 Nov 3.

[101] Shaw, T. J.; Kishi, K.; Mori, R. Wound-associated skin fibrosis: mechanisms and treatments based on modulating the inflammatory response. *Endocr. Metab. Immune Disord. Drug Targets* **2010**, *10(4)*, 320-330. doi: 10.2174/1871530311006040320.

[102] Malissen, B.; Tamoutounour, S.; Henri, S. The origins and functions of dendritic cells and macrophages in the skin. *Nat. Rev. Immunol.* **2014**, *14(6)*, 417-428. doi: 10.1038/nri3683.

[103] Lakos, G. et al. Targeted disruption of TGF-β/Smad3 signaling modulates skin fibrosis in a mouse model of scleroderma. *Am. J. Pathol.* **2004**, *165(1)*, 203-217. doi: 10.1016/s0002-9440(10)63289-0.

[104] Wang, H. et al. Activated macrophages are essential in a murine model for T cell-mediated chronic psoriasiform skin inflammation. *J. Clin. Invest.* **2006**, *116(8)*, 2105-2114. doi: 10.1172/JCI27180.

[105] Asano, Y. Recent advances in the treatment of skin involvement in systemic sclerosis. *Inflamm. Regen.* **2017**, *37(12)*. doi:10.1186/s41232-017-0047-4.

[106] Borelli, M. R.; Shen, A. H.; Lee, G. K.; Momeni, A.; Longaker, M. T.; Wan, D. C. Radiation-induced skin fibrosis: pathogenesis, current treatment options, and emerging therapeutics. *Ann. Plast. Surg.* **2019**, *83(4S Suppl. 1)*, S59-S64. doi: 10.1097/SAP.0000000000002098.

[107] Dos Santos, L. C. O.; Spagnol, C. M.; Guillot, A. J.; Melero, A.; Corrêa, M. A. Caffeic acid skin absorption: delivery of microparticles to hair follicles. *Saudi Pharm. J.* **2019**, *27(6)*, 791-797. doi: 10.1016/j.jsps.2019.04.015. Epub 2019 Apr 29.

[108] Gu, C.; Hu, C.; Ma, C.; Fang, Q.; Xing, T.; Xia, Q. Development snd characterization of solid lipid microparticles containing vitamin C for topical and cosmetic use. *Eur. J. Lipid Sci.* **2016**, *118(7)*, 1093-1103. https://doi.org/10.1002/ejlt.201500373.

Index

to me,
to my parents for their support along the way,
and to Rusty, my faithful and lovely dog.